2014

Quantifying The Effectiveness of a Grout Curtain Using a Laboratory-Scale Physical Model

Elliot N. Magoto
University of Kentucky, elliot.magoto@gmail.com

STUDENT AGREEMENT:

I represent that my thesis or dissertation and abstract are my original work. Proper attribution has been given to all outside sources. I understand that I am solely responsible for obtaining any needed copyright permissions. I have obtained needed written permission statement(s) from the owner(s) of each third-party copyrighted matter to be included in my work, allowing electronic distribution (if such use is not permitted by the fair use doctrine) which will be submitted to UKnowledge as Additional File.

I hereby grant to The University of Kentucky and its agents the irrevocable, non-exclusive, and royalty-free license to archive and make accessible my work in whole or in part in all forms of media, now or hereafter known. I agree that the document mentioned above may be made available immediately for worldwide access unless an embargo applies.

I retain all other ownership rights to the copyright of my work. I also retain the right to use in future works (such as articles or books) all or part of my work. I understand that I am free to register the copyright to my work.

REVIEW, APPROVAL AND ACCEPTANCE

The document mentioned above has been reviewed and accepted by the student's advisor, on behalf of the advisory committee, and by the Director of Graduate Studies (DGS), on behalf of the program; we verify that this is the final, approved version of the student's thesis including all changes required by the advisory committee. The undersigned agree to abide by the statements above.

Elliot N. Magoto, Student

Dr. L. Sebastian Bryson, Major Professor

Dr. Ed Wang, Director of Graduate Studies

QUANTIFIYING THE EFFECTIVENESS OF A GROUT CURTAIN USING A LABORATORY-SCALE PHYSICAL MODEL

THESIS

A thesis submitted in partial fulfillment of the requirements for the degree of Master of Science in Civil Engineering in the College of Engineering at the University of Kentucky

By

Elliot Nicholas Magoto

Lexington, Kentucky

Director: Dr. L. Sebastian Bryson, Associate Professor of Civil Engineering

Lexington, Kentucky

2014

ABSTRACT

QUANTIFIYING THE EFFECTIVENESS OF A GROUT CURTAIN USING A LABORATORY-SCALE PHYSICAL MODEL

In the past decade, the grouting industry has made significant technological advancements in real-time monitoring of flow rate and pressure of pumped grout, stable grout mix design, and with grout curtain concepts dealing with placement and orientation. While these practices have resulted in improved construction practices in the grouting industry, current design guidelines for grout curtains are still predominately based on qualitative measures such as engineering judgment and experience or are based on proprietary methods. This research focused on the development of quantitative guidelines to evaluate the effectiveness of a grout curtain in porous media using piezometric and hydraulic flow data. In this study, a laboratory-scale physical seepage model was developed to aid in the understanding and development methodology to evaluate the effectiveness of a grout curtain. A new performance parameter was developed based on a normalization scheme that utilized the area of the grout curtain and the area of the improved media. The normalization scheme combined with model-based Lugeon values that correspond to pore pressure and flow rate measurements at different soil unit weights and grout curtain spacings, produced a mathematical equation that can be used to quantify the effectiveness of a grout curtain. This study found a relationship that takes into account soil unit weight, grout curtain spacing and a new performance parameter that can be used to help predict the effectiveness of a grout curtain.

KEYWORDS: Grout Curtain; Seepage Cutoff; Lugeon Value; Hydraulic Conductivity; Pore Pressure

Elliot Nicholas Magoto

3/10/2014

QUANTIFIYING THE EFFECTIVENESS OF A GROUT CURTAIN USING A LABORATORY-SCALE PHYSICAL MODEL

By

Elliot Nicholas Magoto

_ L. Sebastian Bryson, Ph.D., P.E. _

Director of Thesis

Ed Wang, Ph.D., P.E. _

Director of Graduate Studies

3/10/2014 __

To

My Parents: Nicholas and Jill Magoto

My Brother: Zach Magoto

My Grandparents: Pete and Helen Magoto, Purcell and Louise Grilliot

Girlfriend: Kelsey Peters

For all their love, support and guidance.

ACKNOWLEDGEMENTS

I first off would like to send my gratitude's to Dr. L. Sebastian Bryson for his unwavering support and guidance. His knowledge and guidance has given me the opportunity to learn the skills necessary to become a successful engineer. His relentlessness has taught me to never give up and to keep moving forward. I appreciate all the time and effort that he has given me throughout my graduate career here at the University of Kentucky.

I would also like to show my appreciation to all my professors who have given me the opportunity to learn under, specifically Dr. L Sebastian Bryson, Dr. Michael Kalinski and Dr. Edward Woolrey. Without their time and effort, I wouldn't be where I am today. They have provided me with a solid technical background that I will be able to take with me as a practicing engineer.

My colleagues Kirk Jenkins, Xu Zhang, Joshua Wells, Ryan Ortiz and Travis Greenwell have all been valuable assets to the completion of my research. Their assistance with testing and preparation played a major role in the successful completion of my research.

TABLE OF CONTENTS

ACKNOWLEDGEMENTS iii

LIST OF TABLES vii

LIST OF FIGURES viii

Chapter 1: Introduction 1

1.1 Proposed Concept 4

1.2 Objectives of Research 5

1.3 Relevance of Research 6

1.4 Contents of Thesis 7

Chapter 2: Literature Review 9

2.1 Introduction to Grout Curtains 9

2.2 Grout Installation Techniques 10

2.3 Current Methodologies to Assess Grout Curtain Effectiveness 14

2.3.1 Monitoring Lugeon Values 14

2.3.2 Measuring Hydraulic Conductivity 20

2.3.3 Monitoring Pore Pressures 21

2.3.4 Grout Mix Design 21

2.3.5 Willowstick 22

2.4 Associated Technology 23

2.5 Case History Studies 25

2.6 Summary 27

Chapter 3: Experimental Methods and Materials 28

3.1 Test Material – Index Testing and Material Characterization............................ 28

3.2 Physical Model 30

3.3 Pore Pressure Measurements.. 31

3.3.1 Pore Pressure Transducers 32

3.3.2 Pore Pressure Transducer Calibration.. 33

3.4 Flow Rate Measurements 35

3.5 Lugeon Value Determination 35

Chapter 4: Modeling the Grout Curtain 37

4.1 Linear Representation of Grout Curtain-Acrylic Slats Testing and Results 37

4.1.1 Initial Equilibrium Testing.. 38

4.1.2 Procedures Testing With Grout Curtain and Results................................. 40

4.2 Development of a New Performance Parameter–Linear Replacement Ratio 45

4.3 Area Representation of Grout Curtain-Polyvinyl Chloride Pipe Testing and Results.. 48

4.4 Development of a New Performance Parameter – Area Replacement Index 49

4.5 Nested Pore Pressure Transducers 54

4.6 Pore Pressure Transducers Located at Bottom of Test Box.............................. 56

4.7 Summary 76

Chapter 5: Relationship Verification 77

Chapter 6: Summary and Conclusions 82

Appendix A: 85

Appendix B: 90

Appendix C: 115

REFERENCES 136

VITA 142

LIST OF TABLES

Table 2.1: Site conditions and grouting properties of four case history studies (Hong et al. 2003). 26

Table 3.1: Ohio River Valley sand and Kentucky River sand soil properties. 29

Table 4.1: Grout curtain orientations for Tests 1 through 7 along with their corresponding hydraulic conductivity and pore pressure measurements. 41

Table 4.2: Grout curtain orientations for Tests 1, 8, 9 and 10 along with their corresponding hydraulic conductivity and pore pressure measurements. 43

Table 4.3: Grout curtain orientations for Tests 11 through 16 along with their corresponding hydraulic conductivity and pore pressure measurements. 44

Table 4.4: Raw data from corresponding to S/D=1 and dry unit weight= 12.56 kN/m^3. . 55

Table 4.5: Sigmoidal curve fitting constants from Table Curve. 63

Table 4.6: Unit weight, S/D ratio, slope, Y-intercept and R^2 values for linear best fit lines of normalized average pore pressure versus normalized average Lugeon value plots. 68

Table 4.7: Unit weight, S/D ratio, slope, Y-intercept and R^2 values for linear best fit lines of normalized q/L versus normalized average Lugeon value plots. 70

Table 4.8: Unit weight, S/D ratio, slope, Y-intercept and R^2 values for linear best fit lines of area replacement index versus normalized average Lugeon value plots. 72

Table 5.1: Site conditions and grouting properties of four case history studies (Hong et al. 2003). 78

Table 5.2: Calculated absolute percent errors for all case history studies. 81

LIST OF FIGURES

Figure 1.1: Schematic of general grout curtain wall (Weaver, K. and Bruce, D., 2007).... 1

Figure 2.1: Teton Earthen Dam Failure in 1976 (Arthur, 1977)....................................... 9

Figure 2.2: Installation of a soilcrete column using jet-grouting (Hayward Baker, 2014).

.... 11

Figure 2.3: Illustration of the high-mobility grouting technique (Hayward Baker, 2014).

.... 12

Figure 2.4: Compaction grouting technique (Hayward Baker, 2014). 14

Figure 2.5: Typical real time monitoring and equipment and data acquisition system

(Quinones-Rozo, 2010)... 16

Figure 2.6: Schematic Lugeon test set-up (Quinones- Rozo, 2010)............................... 17

Figure 2.7: Houlsby's (1976) grouting applicability flow chart..................................... 19

Figure 2.8: Magnetic field mapped using Willowstick technology (White Paper, 2012). 23

Figure 2.9: Relationship between area replacement ratio and ground improvement factor.

(Priebe, 1995)... 25

Figure 3.1: Site locations where the Kentucky River sand and Ohio River Valley sand

were collected. 28

Figure 3.2: The composition of the working physical model... 30

Figure 3.3: Three pore pressure transducers connected to the National Instruments data

acquisition system.. 32

Figure 3.4: Kulite's XCL-11-250-150SG sealed gauge pore pressure transducer model

used in this study.. 33

Figure 3.5: Calibration curve and equation associated with the three pore pressure transducers. 34

Figure 4.1: Effect of a simple grout curtain on pore pressure with respect to time.......... 39

Figure 4.2: Eight possible slat locations along the proposed grout curtain line. 40

Figure 4.3: Pore pressure versus distance from pore pressure transducer for Tests 1-7... 42

Figure 4.4: Hydraulic conductivity versus distance from pore pressure transducer for Tests 1 through 7.......... 42

Figure 4.5: Graphical representation of the linear replacement relationship.................... 46

Figure 4.6: Linear replacement ratio versus pore pressure graph with grout curtain on (A) left hand side, and (B) right hand side. 47

Figure 4.7: Geometric configurations used in the development of the area replacement index. (A) Tangent Planer, (B) Tangent Circular, (C) Tangent Primary-Secondary and (D) Discontinuous Primary-Secondary.......... 50

Figure 4.8: Components of grout region where $A_{TOT} = (b_{TOT})(L_{TOT})$, $b_{TOT} =$ width of the grout region and $L_{TOT} =$ length of the grout region. 51

Figure 4.9: Relationship between normalized grouted area versus pore pressure for various geometric configurations.......... 52

Figure 4.10: Relationship between area replacement index versus pore pressure grouped by geometric configuration. 53

Figure 4.11: Influence of the drain on the three pore pressure transducers...................... 57

Figure 4.12: Area replacement index versus normalized average pore pressure, grouped by S/D ratios for a dry unit weight of (A) 12.56 kN/m^3, (B) 13.03 kN/m^3, (C) 13.35 kN/m^3 and (D) 13.82 kN/m^3. 59

Figure 4.13: Area replacement index versus normalized q/L, grouped by S/D ratios for a dry unit weight of (A) 12.56 kN/m^3, (B) 13.03 kN/m^3, (C) 13.35 kN/m^3 and (D) 13.82 kN/m^3. 60

Figure 4.14: (A) Fitted curves showing the relationship between area replacement index versus normalized average pore pressure, grouped by S/D ratios for a dry unit weight of 12.56 kN/m^3. (B) Fitted curves showing the relationship between area replacement index versus normalized q/L, grouped by S/D ratios for a dry unit weight of 12.56 kN/m^3...... 61

Figure 4.15: Linear relationship between normalized average pore pressure and normalized q/L grouped by S/D ratios for a dry unit weight of (A) 12.56 kN/m^3, (B) 13.03 kN/m^3, (C) 13.35 kN/m^3 and (D) 13.82 kN/m^3........ 64

Figure 4.16: Relationship between average pore pressure and q/L grouped by S/D ratios for a dry unit weight of (A) 12.56 kN/m^3, (B) 13.03 kN/m^3, (C) 13.35 kN/m^3 and (D) 13.82 kN/m^3. 65

Figure 4.17: Relationship between normalized average pore pressure and normalized average Lugeon values grouped by S/D ratios for a dry unit weight of (A) 12.56 kN/m^3, (B) 13.03 kN/m^3, (C) 13.35 kN/m^3 and (D) 13.82 kN/m^3. 66

Figure 4.18: Relationship between normalized q/L and normalized average Lugeon values grouped by S/D ratios for a dry unit weight of (A) 12.56 kN/m^3, (B) 13.03 kN/m^3, (C) 13.35 kN/m^3 and (D) 13.82 kN/m^3. 69

Figure 4.19: Relationship between area replacement index and normalized average Lugeon values grouped by S/D ratios for a dry unit weight of (A) 12.56 kN/m^3, (B) 13.03 kN/m^3, (C) 13.35 kN/m^3 and (D) 13.82 kN/m^3........ 71

Figure 4.20: S/D ratio versus m_1, grouped by dry unit weight. 73

Figure 4.21: Dry unit weight versus b_2. 74

Figure 5.1: Case history data versus predicted values plotted at dry unit weights of (A) 22.77 kN/m^3 and (B) 23.56 kN/m^3.......... 79

Figure 5.2: Relationship between predicted normalized average Lugeon value versus actual normalized average Lugeon values. 80

Chapter 1: Introduction

Grout curtains, also known as cut-off walls are vertically drilled tangent shafts that are filled with cementatious material that create a barrier to help prevent excessive seepage under a dam. Grout curtains are intended to be impervious walls that typically exist below infrastructure to minimize water seepage. Along with seepage minimization under dams, grout curtains are also found in karst terrain to minimize groundwater infiltration and subsequent erosion of the geologic formation. A generalized depiction of a grout curtain wall can be seen in Figure 1.1.

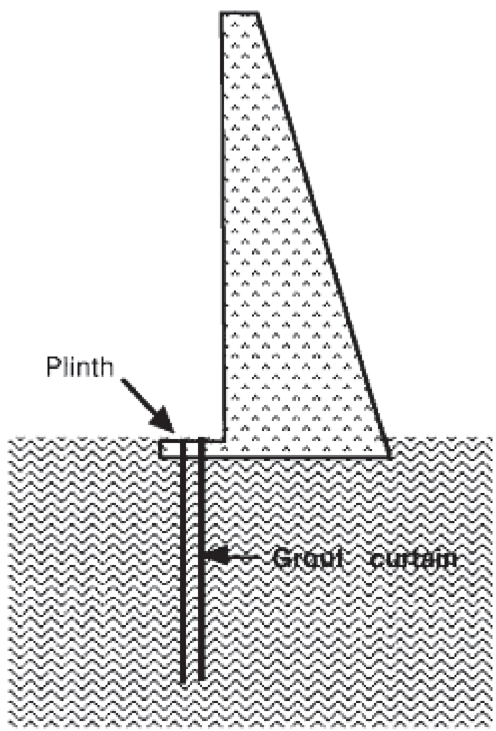

Figure 1.1: Schematic of general grout curtain wall (Weaver, K. and Bruce, D., 2007).

Dams dating back to the 1900's were predominately constructed in geologic areas consisting of karst terrain. Karst terrain is the resulting landform that is produced when groundwater dissolves and washes away existing rock material within the underlying soil structure. Cracks, voids, sinkholes and caves are a result of this dissolving behavior. The materials susceptible to dissolving include rock such as limestone, dolomite and gypsum according to research done by Veni et al. (2001). This dissolving behavior can cause significant problems with the structural integrity of various impoundments, specifically dams. Dams located in karst terrain often times deal with significant groundwater seepage issues. Given sufficient time, groundwater will eventually erode enough of the underlying soil structure to create conditions where dam failures can occur. To prevent dam failures from occurring in karst terrain, grout curtains are typically installed. As previously mentioned, grout curtains are installed to prevent excessive seepage under dams and to minimize groundwater infiltration.

In the past decade, the grouting industry has made significant technological advancements in real-time monitoring of flow rate and pressure of pumped grout, stable grout mix design, and with grout curtain concepts dealing with placement and orientation. While these practices have resulted in a renewed appreciation of the grouting industry, current design guidelines are still predominately based on qualitative measures such as engineering judgment, experience and rules-of-thumb. Not being able to use quantifiable means to assess the effectiveness of a grout curtain, has left many engineers spending lots of valuable time and money. Even though previous studies in the past few decades such as the studies conducted by Uromeihy and Farrokhi (2012) and Ajalloeian et al. (2012) both of which evaluate the groutability of Iranian dams have shown that qualitative based approaches have worked; being able to quantify the effectiveness of a grout curtain would seem to be more beneficial.

Today, most grout curtain designs and installations are performed based on local rules-of-thumb and experience combined with adequate engineering judgment. Even though using these qualitative approaches have shown to work in the past, many engineers and designers have questioned whether or not qualitative approaches are the most efficient way in determining the effectiveness of a grout curtain. According to Bruce (1992), the utilization of qualitative approaches previously discussed is not the most efficient approach when considering the effectiveness of a grout curtain. It is believed that lots of money, time and effort are lost when performing an extensive grouting program using qualitative approaches as the predominate basis. Qualitative based approaches have shown to work with the utilization of excessive materials and time. However, with today's society combined with the economical issues encountered, clients today do not have the unlimited resources at their disposal as they once did. Thus, it is important to develop a quantitative approach to predict the effectiveness of a grout curtain prior to installation. A quantitative approach would help engineers and designers optimize grout curtain performance while minimizing factors such as time, labor and cost.

Therefore, this research focused on the development of quantitative guidelines to evaluate the effectiveness of a grout curtain design in porous media using piezometric and hydraulic flow data. In this study, a laboratory-scale physical seepage model was developed to aid in the understanding and development methodology to evaluate the effectiveness of a grout curtain. A new performance parameter was developed based on a normalization scheme that utilized the area of the grout curtain and the area of the improved media. The normalization scheme combined with model-based Lugeon values that correspond to pore pressure and flow rate measurements at different soil unit weights and grout curtain spacings, produced a mathematical equation that can be used to quantify the effectiveness of a grout curtain. This study found a relationship that takes into account soil unit weight, grout curtain spacing and a new performance parameter that can be used to help predict the effectiveness of a grout curtain.

1.1 Proposed Concept

In order to develop a quantifiable relationship that assesses the effectiveness of a grout curtain, a new performance parameter had to be established as previously mentioned. Through much deliberation it was believed that a performance parameter similar to Priebes (1991) and Priebes (1995) area replacement ratio on vibro replacement columns for ground improvement could be utilized to help develop a new performance parameter that would aid in the quantification of a grout curtain. The area replacement ratio parameter presented in Priebes (1991) and Priebes (1995) research utilized various areas with respect to the improved and unimproved ground. This research uses an area replacement ratio combined with other parameters such as poisson's ratio and friction angle to help determine ground improvement effects on non-compactible cohesive soils utilizing load bearing columns of well compacted coarse grained backfill. Unfortunately, no data has been presented using the area replacement ratio as a parameter to help quantify the effectiveness of a grout curtain. However, since the installation of vibro replacement columns for ground improvement is similar to the installation of grout columns for a grout curtain, a new performance parameter based on the area replacement ratio seemed applicable. Therefore, this research utilized a new performance parameter similar to the area replacement ratio presented in Priebe (1991) and Priebe (1995) as a key component to quantifying the effectiveness of a grout curtain.

Along with the development of a new performance parameter, a laboratory-scale seepage model was an essential component to this research. The laboratory-scale seepage model will be used to investigate various piezometric and hydraulic flow data corresponding to various simulated grout curtain concepts. Previous research has been conducted using laboratory-scale models (Luofenga et al., 2012) to explore various seepage behaviors that develop with the presence of a highly permeable sand foundation. Similar to Luofenga et al., 2012 study, a research team explored seepage behavior with respect to slope stability upon failure of a dam (Awal et al., 2009). Additionally, another study (Liua et al., 2003) successfully utilized a laboratory-scale model to determine water flow patterns through foundations similar to seepage through a concrete dam. All three previous studies mentioned the difficulty in modeling highly complex geological insitu field conditions based on numerical modeling. Thus, it was concluded that laboratory-scale models were a necessity in the understanding and development of seepage behaviors with their corresponding situations. Since, it has been proven that laboratory-scale models can successfully aid in the understanding of seepage behavior, the use of a laboratory-scale seepage model seems applicable for quantifying the effectiveness of a grout curtain.

1.2 Objectives of Research

The goal of this research was to develop a laboratory-scale physical seepage model that would help elucidate general seepage behavior that could be used to establish a means of evaluating the effectiveness of grout curtain quantitatively rather than qualitatively. Therefore, the objectives of this research were as follows:

- Analyze current methods used to assess the effectiveness of a grout curtain
- Develop a laboratory-scale physical seepage model that would help investigate specific behavior related to seepage in porous media
- Develop a new performance parameter that would aid in the quantification of effectiveness of a grout curtain
- Develop a quantifiable relationship between the performance parameter and fundamental design parameters associated with the grout curtain
- Assess the general applicability of the new quantifiable relationship using case history studies to show that the quantifiable relationship can be scaled

1.3 Relevance of Research

As mentioned previously, lots of money and time are spent on developing and performing extensive grouting programs to improve the integrity of dams and impoundments based on qualitative measures. The current methods used to assess the effectiveness of a grout curtain, combined with today's current economical issues have created a need for a quantifiable relationship to assess the effectiveness of a grout curtain. Therefore, this research was established to develop a quantifiable relationship to assess the effectiveness of a grout curtain that could be used by engineers to help minimize factors such as time, cost and labor while providing an adequate solution. The quantifiable relationship that assesses the effectiveness of a grout curtain can be used to predict the behavior of simulated grout curtains prior to installation. This relationship allows engineers to have more control while optimizing the design of a grout curtain. This relationship avoids the use of rules-of-thumb and qualitative approaches currently used by industry to assess the effectiveness of a grout curtain. It is believed that this quantifiable relationship can also be used in ground improvement.

1.4 Contents of Thesis

Chapter 2 introduces the idea of grout curtains and current methodologies used to assess the effectiveness of grout curtains which entail Lugeon, hydraulic conductivity and pore pressure values. Accompanying this information, case histories are presented that are the primary bases for which the quantifiable relationship presented in this research is verified.

Chapter 3 describes the test materials used in this research. Along with test material descriptions, the development and description of the laboratory-scale physical seepage model is discussed herein.

Chapter 4 describes the associated test procedures that aided in the development of a quantifiable relationship. Test data and results associated with the testing procedures are presented as well. The development of a new performance parameter is described and addressed. Chapter 4 also presents the analysis that was performed during this research. This chapter describes and evaluates the trends observed during the experimentation portion of this research. These generalized trends were used in the development of a quantifiable relationship that can be used in assessing the effectiveness of a grout curtain.

Chapter 5 presents case history data that was used to verify the new quantifiable relationship. Case history studies will help assist in determining the accuracy of this relationship.

Chapter 6 recaps the discussion presented in this research in its entirety. Final conclusions brought forth by this research are summarized and discussed. A brief discussion of future research recommendations is presented.

Chapter 2: Literature Review

2.1 Introduction to Grout Curtains

Groundwater seepage under dams and other impoundments is a significant problem that geotechnical engineers are encountering more and more every day. As dams continue to age, groundwater seepage issues are becoming more prevalent. If groundwater seepage issues are left unaccounted for, significant problems can cultivate. Past history has shown that groundwater seepage under dams and other impoundments can cause significant problems not just for the owner, but to the surrounding communities. Problems associated with prolonged groundwater seepage under dams and impoundments have led to breaches. For example, the Teton Earthen Dam located in the eastern part of Idaho failed due to excessive seepage through the earth fill dam. The permeable loess core material combined with rock fissures along the abutments of the dam, allowed for significant seepage through and around the dam (Arthur, 1977). Figure 2.1, shows a picture of the Teton Earthen Dam failure.

Figure 2.1: Teton Earthen Dam Failure in 1976 (Arthur, 1977).

The seepage through the earthen dam caused structural degradation ultimately leading to the breach of the dam. Tremendous damage resulted in the breach of the Teton Earthen Dam. Significant flooding occurred in the communities just downstream of the dam. Damages were estimated to be nearly one billion dollars. Unfortunately, the flooding due to the breach of the dam claimed 14 lives. As can be seen, groundwater seepage under dams can introduce significant issues to the structural integrity of dams and other impoundments.

To avoid such horrific circumstances like the Teton Earthen Dam failure, the use of grout curtains has been proven to successfully mitigate groundwater seepage issues that are typically encountered at dams and other impoundments. Grout curtain walls are being incorporated in more dam construction designs since it is currently the most effective approach to mitigating seepage problems. Grout curtains are a cost effective way to diffuse seepage issues due to the low cost of the grout material. It is important to note that prior to the 1950's steel sheet piles were utilized to create impermeable walls similar to grout curtains as pointed out by Powers et al. (2007). However, literature (Powers et al., 2007) has shown that grout curtain walls outperform impermeable walls constructed of steel sheet piles with respect to factors such as cost and seepage mitigation. The mere cost of steel has precluded the use of steel sheet piles as a viable solution for seepage mitigation.

2.2 Grout Installation Techniques

There are three primary grout installation techniques that are widely used today in the civil engineering industry. The three grout curtain techniques that are commonly used today which are highlighted in the research done by Yong-Jiang and Xing-Wang (2012) include jet-grouting, high-mobility grouting, and compaction grouting. The goal of all three installation techniques is to simply prevent seepage from occurring under water-retaining structures, specifically dams.

Jet-grouting is a technique that uses high velocity and high pressure jets to hydraulically replace poor rock or in-situ soil material with a cementatious material known as grout. Specialized machinery connected to a grout monitoring system allow for the placement of grout. The process of jet-grouting is fairly simplistic. High velocity grout jets connected to a drill-stem allow for insitu soil to be eroded then mixed. The composition of insitu soil and grout is commonly referred as soilcrete (Hayward Baker, 2014). Figure 2.2 illustrates the installation of a soilcrete column using jet-grouting.

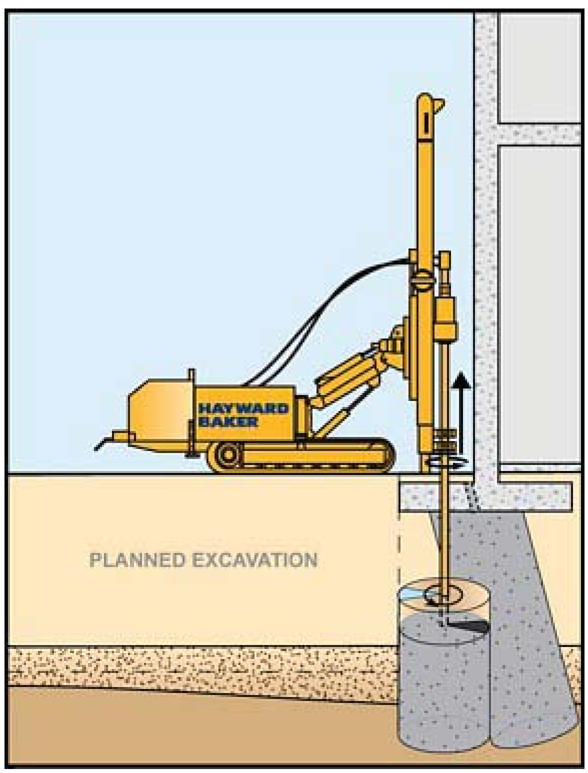

Figure 2.2: Installation of a soilcrete column using jet-grouting (Hayward Baker, 2014).

Given adequate time for set-up, the soilcrete columns cure and become high strength, low permeability material. Soilcrete columns are installed at predetermined locations where seepage issues are expected. Soilcrete columns are installed to help prevent groundwater seepage from occurring under dams and other impoundments. This technique is very versatile since grouting can take place above or below the ground water table and can be used in a wide range of soils from high plasticity clays to cohesionless sands.

High-mobility grouting uses the flow of a pressurized cementatious grout material. Over time, the grouting material enters into the crevices of the underlying soil causing the grout and soil to bind together. Figure 2.3 presents the high-mobility grouting technique.

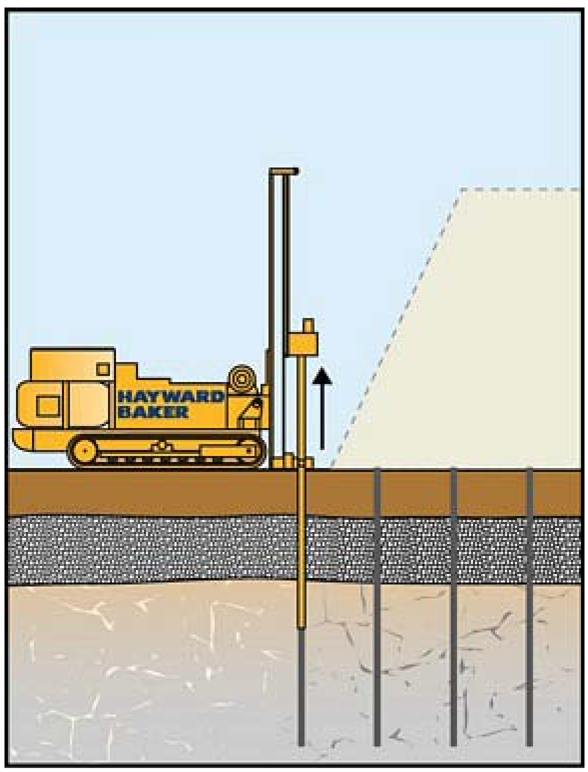

Figure 2.3: Illustration of the high-mobility grouting technique (Hayward Baker, 2014).

When performing high-mobility grouting for dams or other impoundments, it is imperative that the size of the pores or void spaces of the underlying soil material are matched to the particle size of the grout being applied. Having the appropriate grout with respect to particle size will allow for the grout material to enter the pore and void spaces of the underlying soil material. If the particle size of the grout is larger than the pore and void spaces of the underlying soil, grout will unable to enter the pore and void spaces. This type of grouting allows for increased strength properties such as cohesion, as well as decreased permeability.

Compaction grouting is another common technique used by industry today. Compaction grouting utilizes low viscosity grout to displace and densify loose soils. Also, compaction grouting is performed to stabilize large void spaces known as sinkholes by using a low-mobility grout mixture (Hayward Baker, 2014). The pressurized grout is injected into the ground by a pipe. As the grout is continuously injected, the pipe is slowly raised, forming a bulb like structure. For further clarity refer to Figure 2.4, which illustrates the compaction grouting technique.

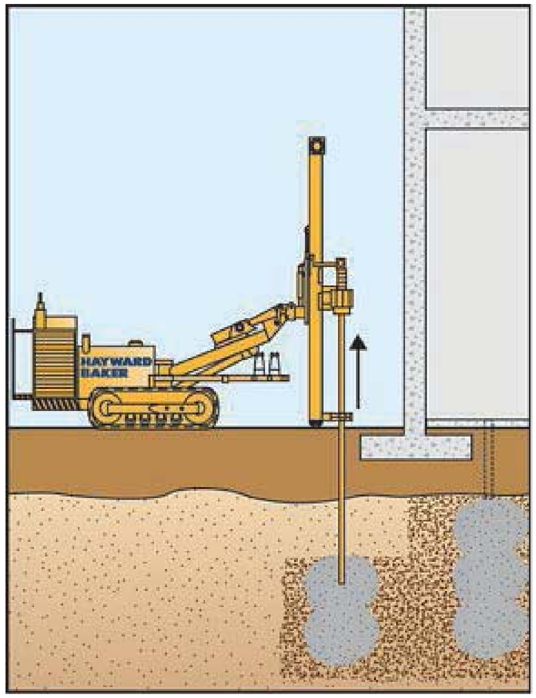

Figure 2.4: Compaction grouting technique (Hayward Baker, 2014).

The injected grout displaces the loose surrounding material. During the displacement and expansion of the grout material, geotechnical properties such as density, friction angle, and stiffness are increased. This technique reduces permeability while providing additional strength to existing underlying stratigraphy.

2.3 Current Methodologies to Assess Grout Curtain Effectiveness

2.3.1 Monitoring Lugeon Values

Monitoring Lugeon values during the installation of a grout curtain is the current state-of-the-practice for assessing grout curtain effectiveness. Lugeon values are defined as the injected volume of water in a length of time per length of rock beneath the reference elevation (Lugeon, 1933). The most common units attributed to the Lugeon value is 1 liter/minute per meter at a reference pressure of 1 MPa. Although the Lugeon value is similar to hydraulic conductivity, the Lugeon value is typically used in rock masses in which water travels through cracks in rocks, whereas hydraulic conductivity is used in conjunction with water traveling through soil pore space. Monitoring Lugeon values has many benefits. Benefits of ascertaining Lugeon values include the determination of flow characteristics, provide a sound basis for the selection of an appropriate grout mix, and most importantly for quality control purposes (Weaver, K. and Bruce, D., 2007). Lugeon values are used combined with qualitative measures such as engineering judgment and rules-of-thumb (Bruce, 1982; Quinn et al., 2011; Berhane and Walraevens, 2013) to address the effectiveness and structural integrity of grout curtain walls. Lugeon values have been increasingly used as a means to assess quality control of grouting operations due to technological advancements in data acquisition systems and real time monitoring equipment. According to Houlsby (1976), quality assurance of a grout curtain with the use of Lugeon values is a key component to assessing the effectiveness of a grout curtain. A typical real time monitoring equipment and data acquisition system currently used in industry can be seen in Figure 2.5. The combination of real time monitoring equipment and data acquisition systems have allowed researchers (Sasaki and Tosaka, 2012; Sadeghiyeh et al., 2013) to monitor Lugeon values during grout curtain installation procedures. As the costs for real time monitoring systems and data acquisition systems start to decline due to competitive markets, Lugeon values are going to become even more widely used.

Figure 2.5: Typical real time monitoring and equipment and data acquisition system (Quinones-Rozo, 2010).

2.3.1.1 Lugeon Test Procedures

The most common insitu testing procedure used to assess the need for foundation grouting at dams and other impoundments is the Lugeon test, also known as the packer test. The original Lugeon test was developed by Maurice Lugeon in 1933. With technological advancements in real time monitoring equipment, much research has been conducted on the applicability of the original Lugeon test over the years. Research done by Houlsby (1976) resulted in an updated Lugeon test that allows for tests to be conducted over a wider range of pressures, while using the same principles used in the development of the original Lugeon test. The updated Lugeon test, commonly referred to as the modified Lugeon test, is the current industry standard for ascertaining Lugeon values. Unlike the original Lugeon test developed by Maurice Lugeon, the modified Lugeon test consists of 5 consecutive stages. The first three stages are completed at increasing pressures while the last two stages are completed at decreasing pressures.

During each stage, water pressure is held constant, while pumping as much water through the test interval as possible. A schematic figure illustrating a Lugeon test configuration is presented in Figure 2.6.

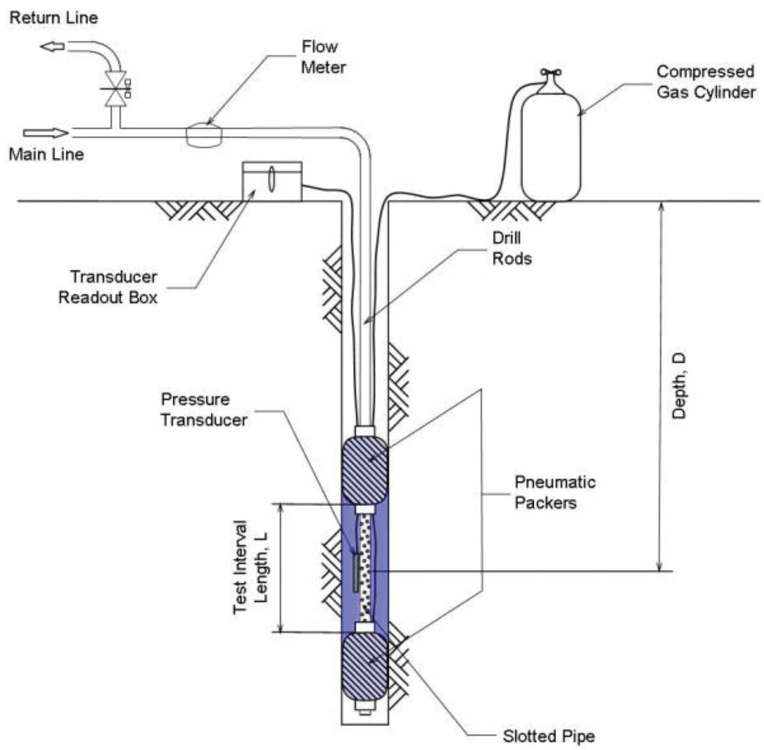

Figure 2.6: Schematic Lugeon test set-up (Quinones- Rozo, 2010).

During each stage, flow rate and pore pressure measurements are taken. These measurements are subsequently used to calculate a Lugeon value based on an equation presented in Houlsby (1976) and Quinones-Rozo (2010). The equation presented in Houlsby (1976) and Quinones-Rozo (2010) is the standard equation that is currently being used by industry to determine Lugeon test values, which can be seen in Equation 1.

$$LV = \alpha\left(\frac{q}{L}\right)\left(\frac{P_0}{P}\right) \tag{1}$$

where LV = Lugeon value, α = unit system coefficient, q = flow rate = Q/t where Q = total volume of water discharged and t = total time of test, L = test interval length of the representative test sample, P_0 = reference pressure = 1 MPa and P = water injection pressure.

The calculated Lugeon values are then assessed using Houlsby (1976) flow chart which can be seen in Figure 2.7 to determine whether or not grouting is warranted.

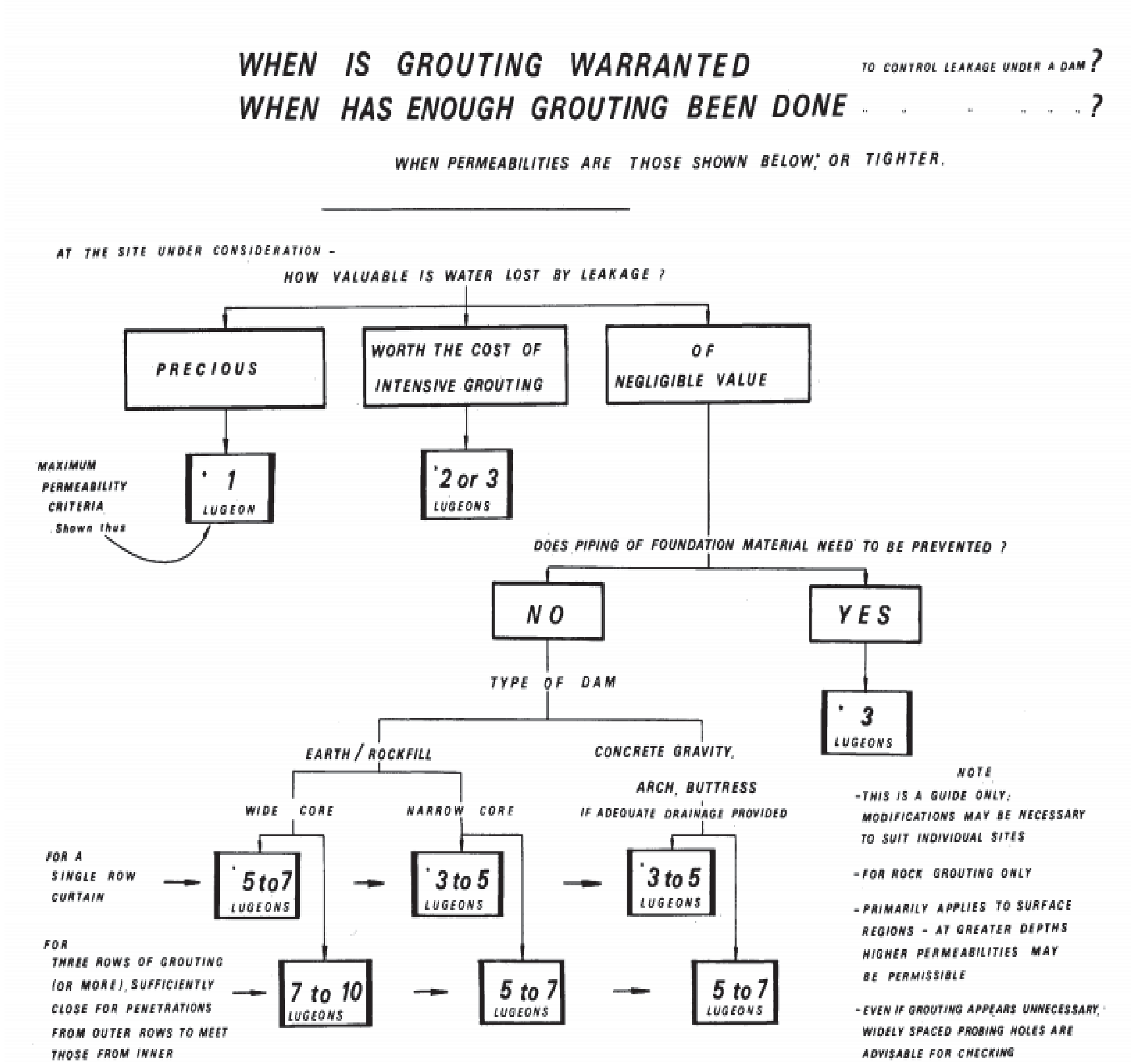

Figure 2.7: Houlsby's (1976) grouting applicability flow chart.

However, the use of Houlsby (1976) chart is more of a qualitative based approach or rule-of-thumb rather than a quantitative based approach. Lugeon values are not the only factor when determining if grouting is appropriate. Houlsby's (1976) research pointed out that other qualitative factors exist that should be taken in consideration, such as geological and other local factors. The grouting industry finds itself in an unfortunate situation where grout curtain effectiveness is determined by a qualitative based approach rather than a quantitative based approach.

2.3.1.2 Shortcoming of the Lugeon Test

Selecting an appropriate representative sample at a test site is a major drawback to the Lugeon test. The range of a single Lugeon test with a length interval of 10 feet is said to only encompass a 30 foot radius around the bore hole of interest (Bliss and Rushton, 1984). Since a Lugeon test only accurately depicts a limited area surrounding a bore hole, it is imperative to have a proper representative sample that takes into account the underlying soil material. However, if proper representative samples of the underlying soil material are obtained, Lugeon values are an appropriate measure to help aid in the quantification of the effectiveness of a grout curtain.

2.3.2 Measuring Hydraulic Conductivity

Grout curtain effectiveness is sometimes evaluated based on the degree of which in-situ hydraulic conductivity is reduced. In a previous study (Cotton and Matheson, 1990) conducted to evaluate the effectiveness of a grout curtain, hydraulic conductivity measurements were used to quantify effectiveness. In this study, effectiveness of a grout curtain was based on hydraulic conductivity measurements with varying grout curtain depths. This study found that an effective grout curtain is not achieved until the grout curtain hydraulic conductivity values is three to four orders of magnitude less than that of the surrounding material. However, the Cotton and Matheson (1990) study used hydraulic conductivity values through a homogenous soil mass as opposed to a fractured mass often times seen while grouting.

2.3.3 Monitoring Pore Pressures

Determining the effectiveness of a grout curtain using solely pore pressure measurements is uncommon. However, one researcher compared predicted and observed behavior of pore water pressure inside an Alavian earthfill dam in Iran (Aminfar et al., 2009). This study also investigated the effects pore water pressures had on the foundation of the dam by looking at the distribution of pore water pressures. Beyond this study, there is little data that has been presented using solely pore pressures to evaluate the effectiveness of a grout curtain.

2.3.4 Grout Mix Design

Early studies evaluating the effectiveness of a grout curtain were primarily based on the performance of the grout mix design. There were several researchers (Bodocsi and Bowers, 1991; Anagnostopoulos and Kadjispyrou, 2004; Ozgurel and Vipulanandam, 2005; Lirer et al., 2006) who investigated various grout mix design parameters, such as workability, strength, and durability of the grout material under different conditions, to help evaluate the performance of grout curtains. However, these researchers did not evaluate the influence of the installation sequence of grout curtains on the overall effectiveness.

2.3.5 Willowstick

Willowstick is a recently developed technology that attempts to define and model complex subsurface water systems using electromagnetic fields (White Paper, 2012). Willowstick technology utilizes the placement of strategically placed electrodes in conjunction with a power supply to help enhance magnetic fields that can assist in modeling preferential groundwater flow paths (White Paper, 2012). Figure 2.8 illustrates modeling done by Willowstick technology. Unlike typical electromagnetic and resistivity methods, the Willowstick technology understands that flow paths can be effectively modeled using electrode probes due to their thorough understanding of water content and subsurface electrical conductivity (White Paper, 2012). This technology was developed to be a cost effective method to modeling complex subsurface water systems. The traditional method of direct observation through the drilling of wells is too time consuming, labor intensive and expensive. The Willowstick technology capitalizes on low cost and increased safety factors. However, this may be considered state-of-the-art, it is not currently widely used by consultants. The research presented herein focused on readily available technologies currently used in industry. The Willowstick Technology was not used for this research. It is presented briefly herein for completeness. Further, future research using this technology is recommended.

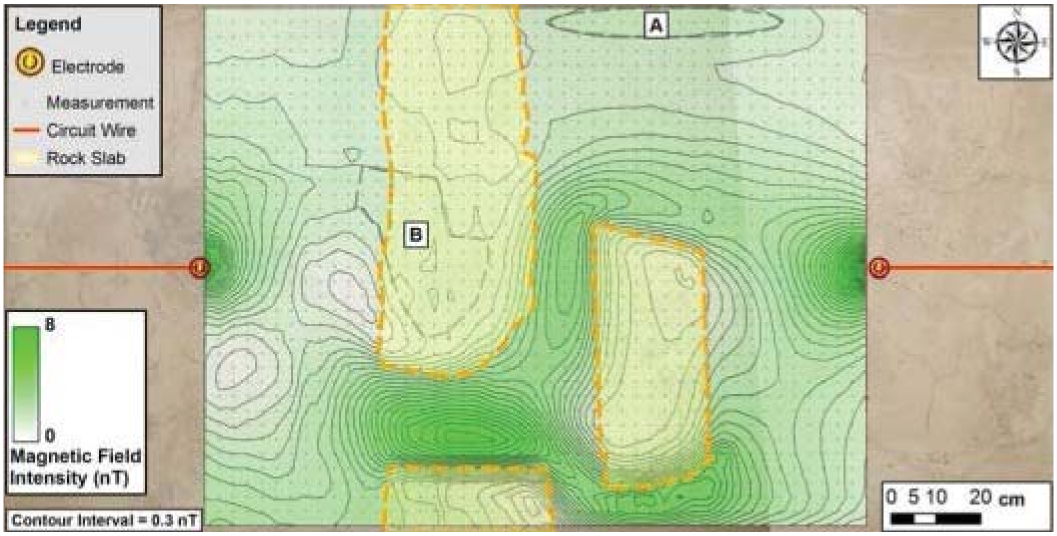

Figure 2.8: Magnetic field mapped using Willowstick technology (White Paper, 2012).

2.4 Associated Technology

As mentioned earlier in Chapter 1, the development of a new area performance parameter to assess the effectiveness of a grout curtain is essential to the success of this research. However, earlier studies (Bruce, D., 1982; Bruce, D., 1992; Uromeihy and Farrokhi, 2012; Gurocak and Alemdag, 2012) fail to use a performance parameter based on areas to assess the effectiveness of a grout curtain. These studies solely utilized Lugeon values to assess the effectiveness of a grout curtain. However, the studies conducted by Heinz Priebe in 1991 and 1995, utilized an area replacement ratio to determine an improvement factor which helps quantify the effectiveness with respect to ground improvement. Priebe (1991) and Priebe (1995) defined the area replacement ratio as the area of the improved ground divided by the total area of the unimproved ground. Equation 2 shows the area replacement ratio expression.

$$Area\ replacement\ ratio = \frac{A}{A_C} \quad (2)$$

where A = total area of the improved ground (area of the column(s)) and A_C = total area of the unimproved area.

The area replacement ratio is an expression that identifies the proportionality between the improved ground and unimproved ground. With further analysis, Priebe (1995) discovered a relationship that relates the area replacement ratio to an improvement factor (n) seen in Equation 3.

$$n = 1 + \left(\frac{A_C}{A}\right)\left(\frac{5 - A_C/A}{4\left(\tan^2\left(45 - \varphi_c/2\right)\right)\left(1 - A_C/A\right)} - 1\right) \quad (3)$$

where n = improvement factor, A = total area of the improved ground, A_C = total area of the unimproved area and φ_c = friction angle of the backfill material.

As can be seen by the relationship expressed in Equation 3, the ground improvement factor is a function of the reciprocal of the area replacement ratio and friction angle of the associated backfill material. Going a step further, Priebe discovered that the ground improvement factor was a function of poisson's ratio as well. Figure 2.9 illustrates the relationship from Equation 3 as a function of poisson's ratio.

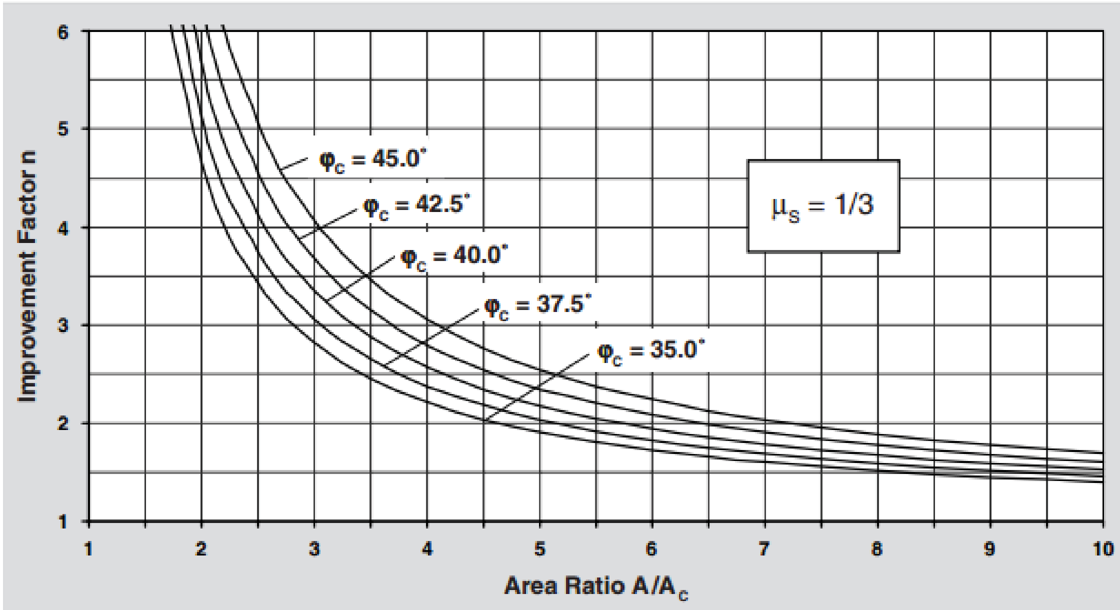

Figure 2.9: Relationship between area replacement ratio and ground improvement factor. (Priebe, 1995).

As seen in Figure 2.9, at a given area replacement ratio, friction angle and poisson's ratio, a ground improvement factor can be determined. This area replacement ratio provides a means to quantify the effectiveness of ground improvement. Little data has been presented using the area replacement ratio to evaluate the effectiveness of a grout curtain. However, it is believed that some type of area replacement ratio similar to the one Priebe (1991) and Priebe (1995) presented on ground improvement methods could be utilized in quantifying the effectiveness of a grout curtain.

2.5 Case History Studies

Four case history studies were investigated during this research. Case history data was obtained, to be used as the primary basis for which findings presented herein could be verified. Four separate dam structures were investigated in Hong et al. (2003)

research, which will later be used in thesis. The Hong et al. (2003) research investigated cut-off effects that are associated with rock grouting at various dam facilities using several parameters such as rock quality designation (RQD), injected cement volume, grout pressure and Lugeon values. The relationships that developed between these parameters were used in an attempt to develop a standard dam construction management program. Site properties, conditions and grouting properties can be seen in following table.

Table 2.1: Site conditions and grouting properties of four case history studies (Hong et al. 2003).

	Site 1	Site 2	Site 3	Site 4
Type of Dam	Concrete Face Rock Fill Dam	Gravity Concrete Dam	Concrete Face Rock Fill Dam	Concrete Face Rock Fill Dam
Type of Rock	Metamorphic	Sedimentary	Sedimentary	Sedimentary
Number of Holes	231	35	28	41
Depth of Holes (m)	40	20	20	40
Grout Spacing	1 column with 1.5 m spaced holes	2 columns at 3.0 m zigzag interval; 3.0 m spaced holes	1 column with 1.5 m spaced holes	2 columns at 3.0 m zigzag interval; 3.0 m spaced holes
Span of Grout Curtain (m)	347	105	42	123
Average Lugeon Value Before Grouting	3	3.9	11	2.37
Average Lugeon Value After Grouting	1	1.9	3	1
Injection Pressure (Mpa)	0.39-2.45	0.15-0.59	0.15-0.59	0.29-2.45
Assumed Grout Column Diameter (m)	1.016	1.016	1.016	1.016

However, the conclusions made in this research were predominately qualitatively based rather than quantitatively based. For research to be beneficial, relationships and behavior must be quantifiable. The research presented herein assessed the effectiveness of a grout curtain quantifiably.

2.6 Summary

As previously mentioned earlier in this thesis, monitoring Lugeon values during the installation of a grout curtain is the current state-of-practice when assessing the effectiveness of a grout curtain. It is believed that Lugeon values combined with a new performance parameter similar to the one presented by Priebe (1991) and Priebe (1995) could lead to a quantifiable relationship that helps predict the effectiveness of a grout curtain prior to installation. With very little data relating Lugeon values to a performance parameter that takes into account area, the need for further experimentation is proven necessary. However, this experimentation needs to be done using a laboratory-scale physical seepage model. The shear amount of equipment needed along with the associated costs, deemed a field monitoring program impractical.

Chapter 3: Experimental Methods and Materials

3.1 Test Material – Index Testing and Material Characterization

All testing during the study was performed on two natural sands that were taken from sites located in the state of Kentucky. The first test sand used came from the banks of the Ohio River, near Newport, Kentucky. The second test sand was found along the banks of the Kentucky River directly North of Frankfort, Kentucky. The test sands herein will be referenced as Ohio River Valley sand and Kentucky River sand. The exact site locations where the Ohio River Valley sand and Kentucky River sand was found can be seen in Figure 3.1.

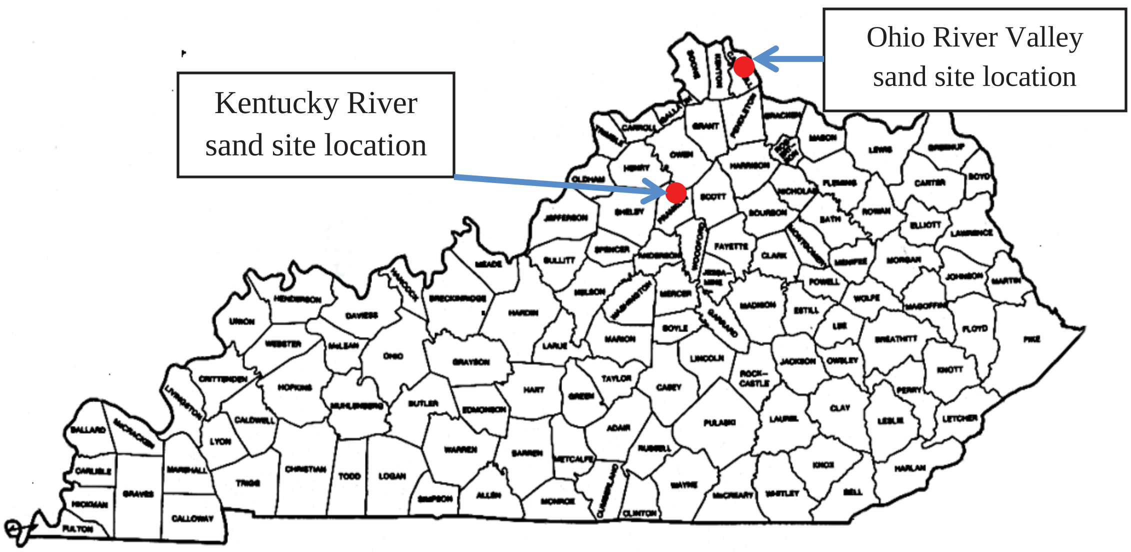

Figure 3.1: Site locations where the Kentucky River sand and Ohio River Valley sand were collected.

Initial index testing on the Ohio River Valley sand and Kentucky River sand consisted of four separate ASTM tests. The ASTM tests performed on the sand include particle-size distribution of soils using sieve analysis (ASTM D6913), specific gravity (ASTM D854), maximum index unit weight using a vibratory table (ASTM D4253) and minimum index unit weight (ASTM D4254). Both test sands were a coarse, poorly graded sand (SP) according to the Unified Soil Classification System (USCS). However, the particle grain sizes of the Kentucky River sand were much finer than the Ohio River Valley sand. The test results from the various ASTM tests performed on the Ohio River Valley sand and Kentucky River sand are populated in Table 3.1. To view recorded data from the particle-size distribution sieve analysis and specific gravity test refer to Appendix A.

Table 3.1: Ohio River Valley sand and Kentucky River sand soil properties.

Test Sand	Classification	Gs	D_{10} (mm)	D_{30} (mm)	D_{60} (mm)	Maximum Dry Unit Weight (kN/m^3)	Minimum Dry Unit Weight (kN/m^3)
Ohio River Valley Sand	SP	2.65	0.30	0.50	0.81	19.08	15.27
Kentucky River Sand	SP	2.67	0.11	0.17	0.21	18.42	12.01

Where D_{10} = the diameter in the particle-size distribution curve corresponding to 10 percent finer, D_{30} = the diameter in the particle-size distribution curve corresponding to 30 percent finer, D_{60} = the diameter in the particle-size distribution curve corresponding to 60 percent finer and Gs = specific gravity.

3.2 Physical Model

A laboratory-scale physical seepage model was developed to aid in the understanding and development of geotechnical trends that evaluate the effectiveness of a grout curtain. All testing during this study was performed in a non-conductive test box. The inside width, length and height dimensions are 595-mm, 595-mm and 610-mm respectively. The box was constructed using polycarbonate for the sides, fiberglass angles and shims and an acrylic base (Huff, 2010). A silicon based product was used to prevent water from leaking through the cracks in between the polycarbonate siding and acrylic base. Figure 3.2 shows the configuration of the physical model from plan view.

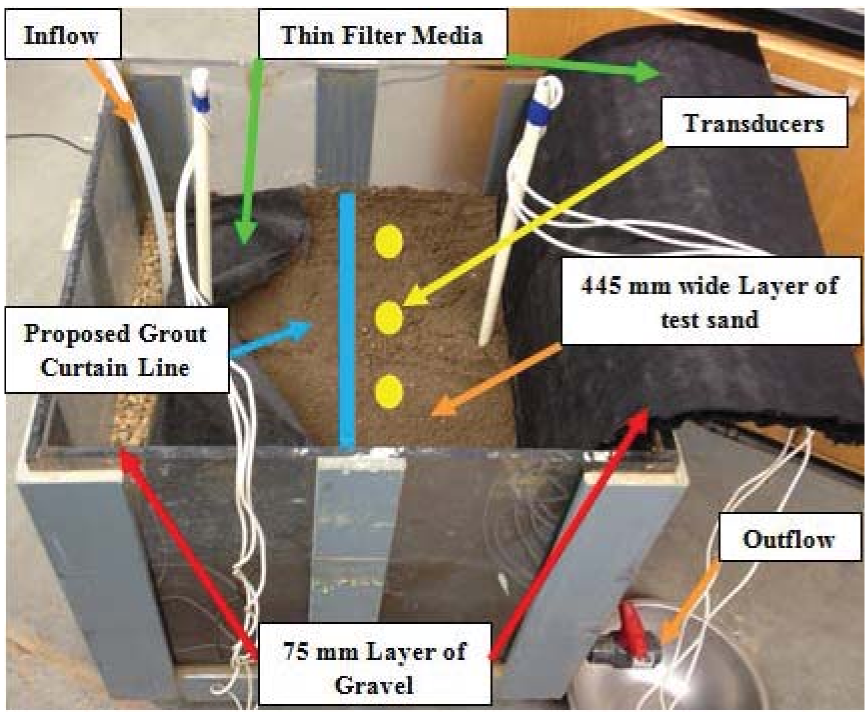

Figure 3.2: The composition of the working physical model.

The model consisted of upstream and downstream drainage media, with the test sand sandwiched in between. The drainage media consisted of vertical layers of gravel that were approximately 75-mm thick. The test sand section was approximately 445-mm thick. A thin piece of geosynthetic fabric was used between the sand and the gravel on both the upstream and downstream side to prevent infiltration of fines into the gravel. Seepage was achieved by pumping water into the physical model on the upstream side and being drained on the downstream side.

To reach a desired test unit weight, the weight of oven dry test sand was measured. The sand was oven dried for 24 hours. The test sand was placed in three separate layers. Each layer was approximately 17.3-cm thick. Upon placement of each layer, the test sand was compacted. A 22.68 kg weight dropped from half a meter high onto a flat surface was used to reach the necessary test unit weights. A flat surface was used to allow for equal force distribution across the entire area of the test media. This allowed for a uniform compaction effort.

3.3 Pore Pressure Measurements

To measure various pore pressures within the physical model for this study, three miniature pore pressure transducers were utilized as piezometers and installed at pre-determined locations in the test box. In this study, pore pressure values were measured using Kulite XCL-11-250-150SG sealed gauge miniature pore pressure transducers connected to a National Instruments data acquisition system. Figure 3.3 shows three transducers connected to the National Instruments data acquisition system.

Figure 3.3: Three pore pressure transducers connected to the National Instruments data acquisition system.

LabVIEW 2012 software was utilized to acquire and analyze the data. The data acquisition system combined with the development of a program within the LabVIEW 2012 software, made it possible to convert electrical readings to their corresponding pore pressure measurements. To further understand the step-by-step process of creating the program, refer to Appendix B.

3.3.1 Pore Pressure Transducers

The specific miniature pore pressure transducer model utilized in this study of the evaluation of the effectiveness of a grout curtain was a XCL-11-250-150SG sealed gauge pore pressure transducer manufactured by Kulite which can be seen in Figure 3.4. Each individual pore pressure transducer had a fully active four arm Wheatstone Bridge. The

XCL-11-250-150SG miniature sealed gauge pore pressure transducers were rated at 1.03 MPa well within the ranges of pressures that are expected in the physical model.

Figure 3.4: Kulite's XCL-11-250-150SG sealed gauge pore pressure transducer model used in this study.

3.3.2 Pore Pressure Transducer Calibration

Self-verification of the calibration of the XCl-11-250-150SG pore pressure transducers was essential in producing reliable data for this study. According to Kulite, the XCL-11-250-150SG was calibrated in a water-filled pressure tank. To verify that the XCL-11-250-150SG transducers would provide reliable data for this study, the pore pressure transducers were placed at various heights in a acrylic cylindrical tube that was filled with saturated test sand. Several readings were taken at different known pressure increments to verify that the pore pressure readings coming from the pore pressure transducers were indeed accurate. Known pressure increments were determined by multiplying the unit weight of water by the height. Pore pressure measurements taken by the pore pressure transducers were compared to various known pore pressures to develop a calibration equation. Pore pressure measurements were taken at the corresponding actual pressure readings of 0, 2.76, 4.14, 5.52 and 6.90 kPa. Figure 3.5 shows the calibration curves associated with the three pore pressure transducers used in this study.

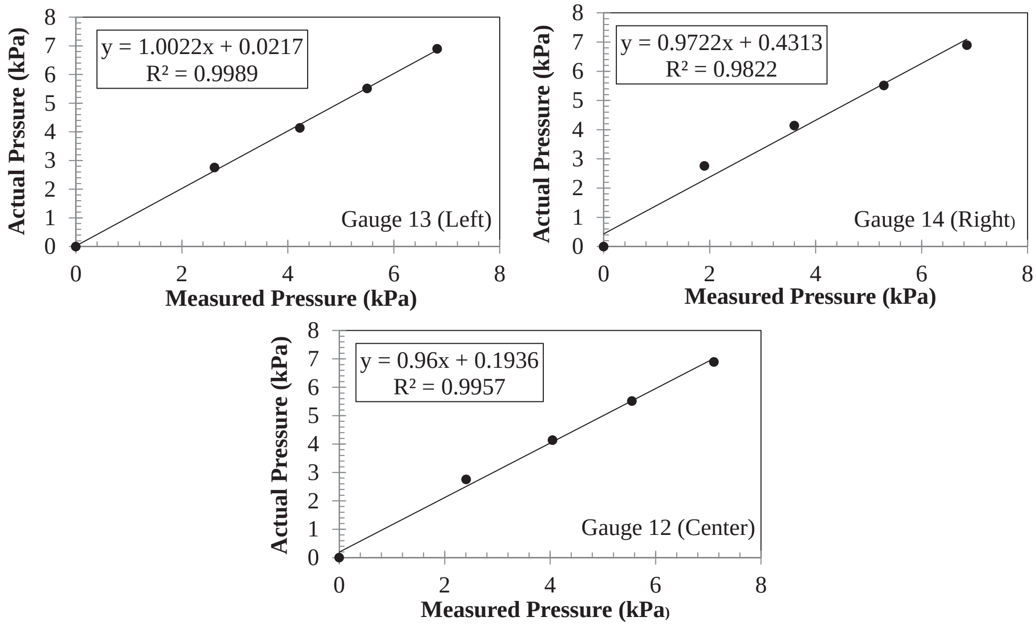

Figure 3.5: Calibration curve and equation associated with the three pore pressure transducers.

Each pore pressure transducer was calibrated individually, thus each pore pressure transducer has a corresponding calibration equation. The calibration equations used in this study are given as:

$$U_{ACT,13} = 1.022(U_{MEA,13}) + 0.0217 \tag{4}$$

$$U_{ACT,12} = 0.96(U_{MEA,12}) + 0.1936 \tag{5}$$

$$U_{ACT,14} = 0.9722(U_{MEA,14}) + 0.4313 \tag{6}$$

where U_{ACT} = actual pore pressure in kPa and U_{MEA} = measured pore pressure in kPa. Manually calibrating the three pore pressure transducers assured that the measured pore pressures in the test box were in fact accurate.

3.4 Flow Rate Measurements

Along with pore pressure measurements, flow rate measurements were also utilized to evaluate the effectiveness of a grout curtain. Measuring flow rates is a common measurement that is taken when trying to assess the efficiency of a grout curtain. Flow rate is an easy parameter to measure since there is no need for extensive equipment. Also, measurements can be taken in timely fashion. Several studies (Bruce, D., 1982; Nappi, M. et al., 2005; Saeidi, O. et al., 2013) used flow rate measurements to help assist in determining the effectiveness of a grout curtain, similar to this study. Flow rate values were determined using an approach similar to a constant head test. The water level on the upstream side of the box was held constant, while being drained on the downstream side. The volume of water coming out of the box was captured and measured over a specified time interval. A flow rate measurement is calculated using the following equation:

$$q = \frac{Q}{t} \tag{7}$$

where q = flow rate, Q = total volume of water discharged and t = total time interval of test.

The flow rate measurements were used as an input parameter in the Houlsby (1976) and Quinones-Rozo (2010) Lugeon value equation presented in Chapter 2, which helps in the quantification of the effectiveness of a grout curtain.

3.5 Lugeon Value Determination

Lugeon values were a key component to this study of quantifying the effectiveness of a grout curtain. Studies such as Hong (2003), Ajalloeian et al. (2012), and Parrock et al (2010) used Lugeon values as the primary factor in determining the effectiveness of a grout curtain under a dam. With this being said, Lugeon values were incorporated into this study to not only be consistent with the current state-of-the-practice, but also to allow for model verification which will be discussed later in this thesis. Since the study was conducted in a laboratory-scale physical seepage model as opposed to out in the field, slight modifications in the determination of Lugeon values were taken. This research measured flow rates similar to a standard Lugeon test. The volume of water flowing through the porous test media was measured over a specified time interval. However, the type of pressure measurements utilized in this research varied slightly from the pressure measurements of a standard Lugeon test. A standard Lugeon test measures a water injection pressure (P), which is the pressure at which water is pumped through a porous media. However, the equipment available for this research was unable to measure a water injection pressure. Pore pressure measurements were utilized to help determine corresponding Lugeon values instead. Since this research did not measure water injection pressures directly, “true” Lugeon values were unable to be obtained. However, allowing sufficient time for pore pressure measurements to reach a state of equilibrium, allowed for pore pressure measurements to be used as water injection pressures. Although this research did not strictly measure “true” Lugeon values, it is still a reasonable approximation.

Chapter 4: Modeling the Grout Curtain

Two separate test procedures were used to model the grout curtains for this study. The first test procedure utilized flat acrylic slats to simulate grout columns while using Ohio River Valley sand as the test media. The second test procedure used polyvinyl chloride (PVC) pipes and Kentucky River sand. Flat acrylic slats were used in an attempt to quantify the effectiveness of a grout curtain based on lengths. PVC pipes were used in a similar fashion as the flat acrylic slats. However, PVC pipes were utilized to address the effectiveness of grout curtain based on areas. Using PVC pipes allowed for an accurate geometric representation of a true grout curtain. The test media changed between the two test procedures due to quantity issues. Both these sands classified as a poorly graded sand (SP) according to Unified Soil Classification System (USCS). However, comparing the D_{10} values for both of the test samples, it is evident that particle grain size of the Kentucky River sand is much finer than the particle grain size of the Ohio River Valley sand. Both procedures measure pore pressures and volume of discharge as subsequent simulated grout columns are placed in the test media in various orientations.

4.1 Linear Representation of Grout Curtain-Acrylic Slats Testing and Results

For this study, only one of three calibrated pore pressure transducers was installed at a pre-determined location within the soil profile. The pore pressure transducer was placed directly in the center of the test media. Pore pressure measurements along with corresponding volume discharge measurements were subsequently taken during the various installation sequences of the simulated grout curtain under a constant head. The volume discharge measurements were taken to calculate corresponding hydraulic conductivity values based on constant head methodology. The combination of volume discharge measurements and several known dimensional parameters of the test media within the laboratory-scale physical seepage model allowed for the determination of hydraulic conductivity values based on the following equation.

$$K = \left(\frac{Q}{t}\right)\left(\frac{\Delta H}{L}\right)\left(\frac{1}{A}\right) \tag{8}$$

where K = hydraulic conductivity, Q = volume of water being discharged, t = time interval, ΔH = total head, L = length of the test media and A = cross-sectional area of test media.

Hydraulic conductivity values were determined in an attempt to identify different trends that could be used to help quantify the effectiveness of a grout curtain. Hydraulic conductivity values were believed to be a possible parameter to assess the effectiveness of a grout curtain similar to the research presented by Cotton and Matheson (1990).

4.1.1 Initial Equilibrium Testing

Before the grout curtain was placed, the test box was flooded by closing the drain and filling the box with water until the water level was 25-mm above the soil surface. After flooding the physical model with water, the drain was opened and the water was pumped into the physical model at a rate that kept the inflow rate equal to the outflow rate. In essence, the physical model was held at a constant head for 30 minutes before any initial testing was completed to provide adequate time for saturation. Running the initial test with no grout curtain present produced a hydraulic conductivity value of 0.0085 cm/s and a pore pressure value 3.17 kPa.

Another initial test that was conducted was a test that showed the change in pore pressure with respect to time with the presence of a simple grout curtain. The purpose of this test was to ascertain the amount of time required for pore pressures to reach equilibrium. The grout curtain consisted of two-acrylic slats, 76.2 mm-wide, inserted 25.4 mm upstream of the pore pressure transducer. Figure 4.1 shows the effects the simple grout curtain had on the pore pressure with respect to time. It also shows that approximately 20 minutes after the grout curtain was inserted 25.4 mm upstream of the pore pressure transducer, the pore pressure values began to level off and stay constant. This figure shows that pore pressure readings should be taken at least 20 minutes after the grout curtain is inserted into the Ohio River Valley sand to allow it to reach an equilibrium state.

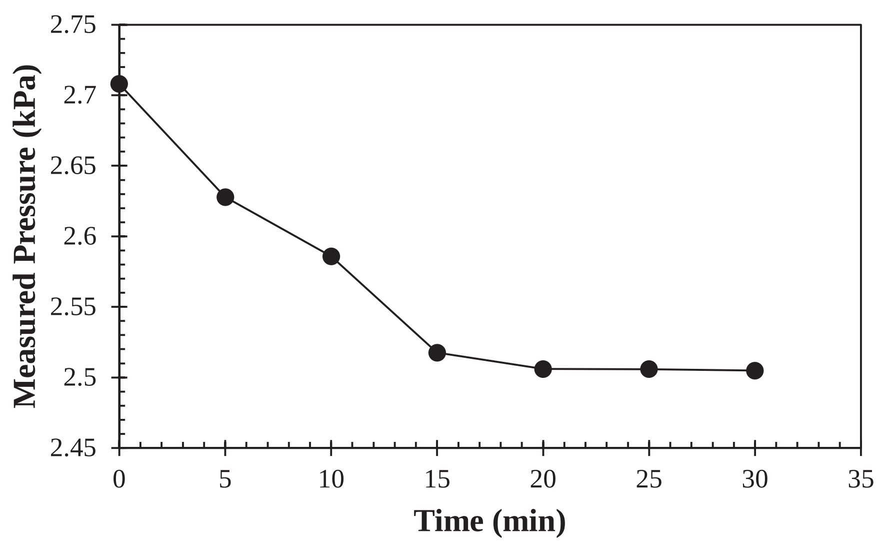

Figure 4.1: Effect of a simple grout curtain on pore pressure with respect to time.

It is important to note that the initial pressure at time zero in Figure 4.1 is not equal to the initial pressure without the presence of a simple grout curtain. Two separate tests were conducted using two different amounts of porous media.

4.1.2 Procedures Testing With Grout Curtain and Results

Experimentation was performed to ascertain the effect of installation sequence on the performance parameters. For this series of tests, pore pressure and hydraulic conductivity were used as performance parameters. The testing consisted of five sets of tests that used three orientation schemes. Each set of tests in this test series utilized two-acrylic slats, 76.2-mm wide, inserted 25.4-mm upstream of the transducer. Each set of tests had its own grout curtain placement scheme along the proposed grout curtain line. The proposed grout curtain line within the physical model can be seen in Figure 4.2. In the figure, the numbers represent possible slat locations. Pore pressure and hydraulic conductivity values were measured during each test set.

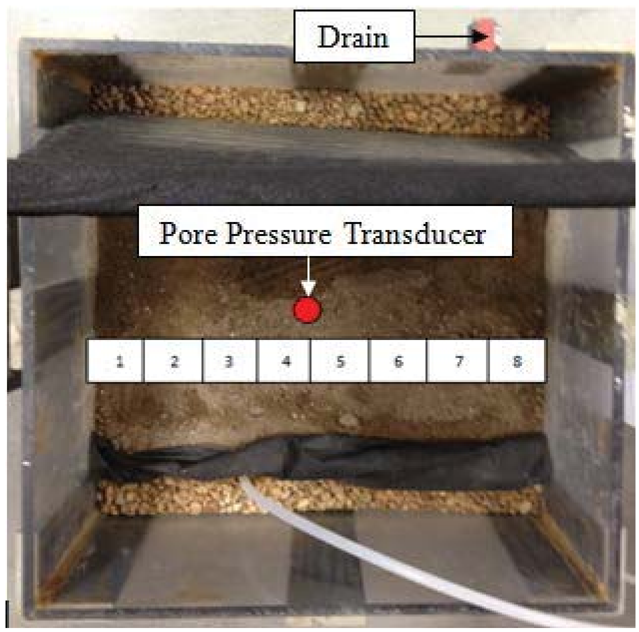

Figure 4.2: Eight possible slat locations along the proposed grout curtain line.

The first orientation scheme used in this test series was to move two 76.2-mm wide acrylic slats across the length of the proposed grout curtain line. Table 4.1 shows the various grout orientations associated with Tests 1 through 7, along with their corresponding pore pressure and hydraulic conductivity measurements.

Table 4.1: Grout curtain orientations for Tests 1 through 7 along with their corresponding hydraulic conductivity and pore pressure measurements.

Tests	Left Slat Location	Right Slat Location	Pore Pressure (kPa)	Hydraulic Conductivity (cm/s)
1	4	5	3.09	0.0078
2	2	3	2.79	0.0081
3	1	2	2.40	0.0074
4	3	4	3.03	0.0071
5	5	6	2.82	0.0065
6	6	7	2.51	0.0069
7	7	8	2.32	0.0067

During Tests 1 through 4, the two-76.2 mm wide acrylic slats started directly in the middle of the box and moved to the left. However, during Tests 1, 5, 6 and 7 the two-76.2 mm wide acrylic slats started directly in the middle of the box and moved to the right. By looking at Figure 4.3, the effects of the location of the drain can be seen. Tests 1 through 4, with the grout curtain on the left hand side, experienced higher pore pressures than Tests 1, 5, 6 and 7, with the grout curtain on the right hand side, because the flow of water had a more direct path to the drain. Plotting pore pressure versus distance from the pore pressure transducer, Tests 1 through 4 and Tests 1, 5, 6 and 7 both follow the same trend. As the two-76.2 mm wide acrylic slats get further and further away from the pore pressure transducer, the lower the pore pressure became. The assumption is that the lower the pore pressure, the more effective the grout curtain was.

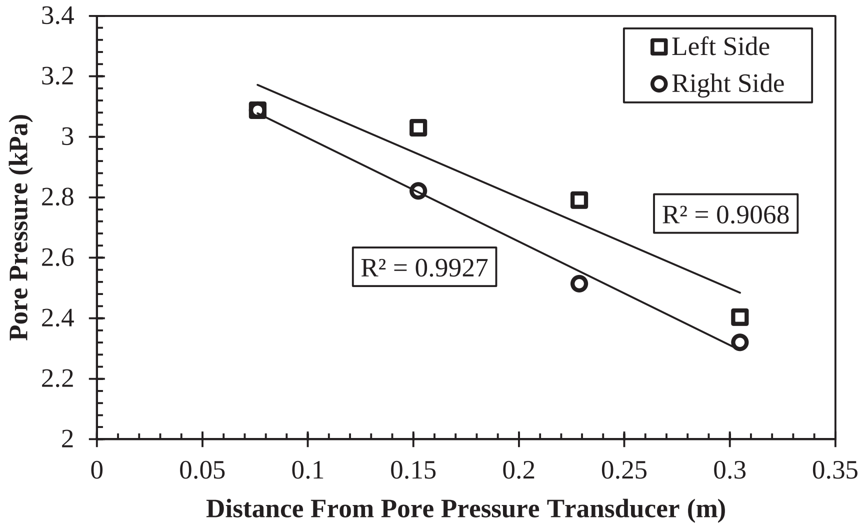

Figure 4.3: Pore pressure versus distance from pore pressure transducer for Tests 1-7.

The effect of the drain can also be seen in Figure 4.4 which plots hydraulic conductivity versus distance from the pore pressure transducer.

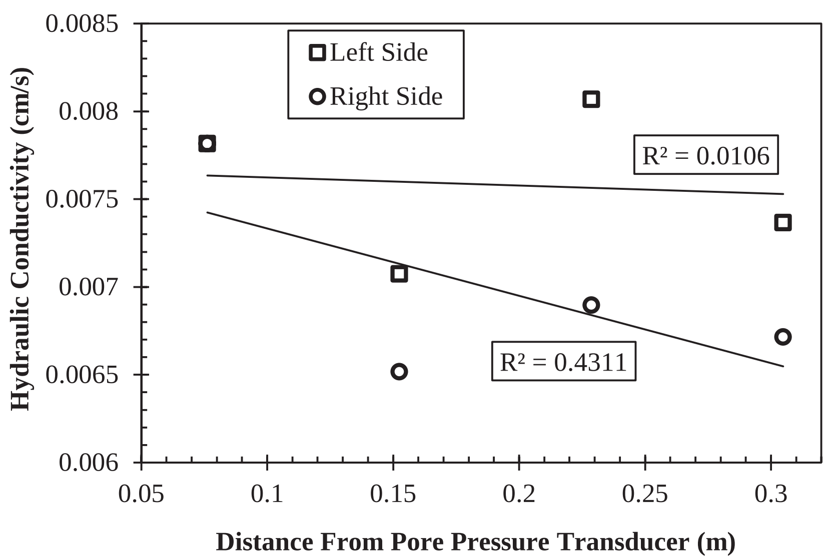

Figure 4.4: Hydraulic conductivity versus distance from pore pressure transducer for Tests 1 through 7.

Tests 1 through 4 with the grout curtain on the left hand side, experienced higher hydraulic conductivity values than Tests 1, 5, 6 and 7 with the grout curtain on the right hand side because the flow of water had a more direct path to the drain. Other than the observed behavior previously discussed, no further trends developed with respect to hydraulic conductivity in this study.

The second orientation scheme used in this study started out with one-76.2 mm wide acrylic slat on each end of the proposed grout curtain line. The slats then preceded inwards towards the pore pressure transducer. This orientation scheme was conducted to help determine whether or not changes in sequencing had any kind of effect on pore pressure and hydraulic conductivity. Table 4.2 shows the various grout curtain orientations for Tests 1, 8, 9 and 10 along with their corresponding pore pressure and hydraulic conductivity measurements. For further clarity on this specific grout curtain orientation scheme, refer to Table 4.2 and Figure 4.2.

Table 4.2: Grout curtain orientations for Tests 1, 8, 9 and 10 along with their corresponding hydraulic conductivity and pore pressure measurements.

Tests	Left Slat Location	Right Slat Location	Pore Pressure (kPa)	Hydraulic Conductivity (cm/s)
8	1	8	2.41	0.0065
9	2	7	2.63	0.0065
10	3	6	3.10	0.0063
1	4	5	3.09	0.0078

The results obtained from this series of tests, showed that sequencing does have an effect on pore pressure and hydraulic conductivity. As the acrylic slats propagated towards the pore pressure transducer, higher pore pressures resulted. Hydraulic conductivity stayed fairly constant as the acrylic slats preceded inward, with the exception of Test 1.

The third orientation scheme used in this study was holding one-76.2 mm-wide acrylic slat stationary in the middle next to the pore pressure transducer, while moving the other 76.2 mm wide acrylic slat outward along the proposed grout curtain line. This orientation scheme was conducted to help determine the effects on pore pressure and hydraulic conductivity with respect to which side the simulated grout curtain was placed. Table 4.3 shows the various grout curtain orientations for Tests 11-16 along with their corresponding pore pressure and hydraulic conductivity measurements.

Table 4.3: Grout curtain orientations for Tests 11 through 16 along with their corresponding hydraulic conductivity and pore pressure measurements.

Tests	Left Slat Location	Right Slat Location	Pore Pressure (kPa)	Hydraulic Conductivity (cm/s)
11	4	8	2.30	0.0064
12	4	7	2.69	0.0067
13	4	6	3.04	0.0071
14	1	5	2.39	0.0064
15	2	5	2.78	0.0067
16	3	5	3.13	0.0071

Test results associated with this test series showed that when the simple grout curtain was placed on the right hand side of box along the proposed grout curtain line, pore pressures were lower compared to when grout curtain was on the left hand side. Upon speculation it was believed that the observed pore pressure behavior was a result of the water flow path. Since the water had a more direct path to the drain when the simulated grout curtain was positioned on the left hand side, higher pore pressures resulted as compared to when the grout curtain was positioned on the right hand side. Hydraulic conductivity stayed constant, when comparing measurements with the grout curtain on the left and right hand sides.

4.2 Development of a New Performance Parameter–Linear Replacement Ratio

As was discussed earlier in Chapter 2, it was hypothesized that an area replacement ratio could be used to quantify effectiveness. However, the use of flat acrylic slats precluded the use of areas. Therefore, a linear replacement ratio was developed. The linear replacement ratio was equal to the width of the installed slats divided by the total width of the model. Unfortunately, this relationship was inadequate because it did not take into account the various installation sequences. In addition, initial testing showed the location of the pore pressure transducer and drain influenced the results.

To evaluate the effectiveness of a grout curtain, this study utilized a linear replacement ratio $\left(\bar{x}_2\right)$ based on a double normalization scheme. The linear replacement ratio takes into account the distance the centroids of the acrylic slats are from the pore pressure transducer and drain, respectively. This normalization scheme was conducted to understand the influence of the drain within the laboratory-scale physical model. The linear replacement ratio equation that was developed is given in Equation 9 and is graphically presented in Figure 4.5

$$\bar{x}_2 = \frac{\left(\dfrac{d_1 + d_2}{L_1 + L_2}\right)}{\left(\dfrac{d_1 + d_2}{D_1 + D_2}\right)} \qquad (9)$$

where $\bar{x}_2$ =double normalization value, d_1 =the distance between the centroid of the first slat and the midpoint of the pore pressure transducer, d_2 =the distance between the centroid of the second slat and the midpoint of the pore pressure transducer, L_1 =the length of the first slat, L_2 =the length of the second slat, D_1 =the distance from the centroid of the first slat to the midpoint of the drain, and D_2 =the distance from the centroid of the second slat to the midpoint of the drain.

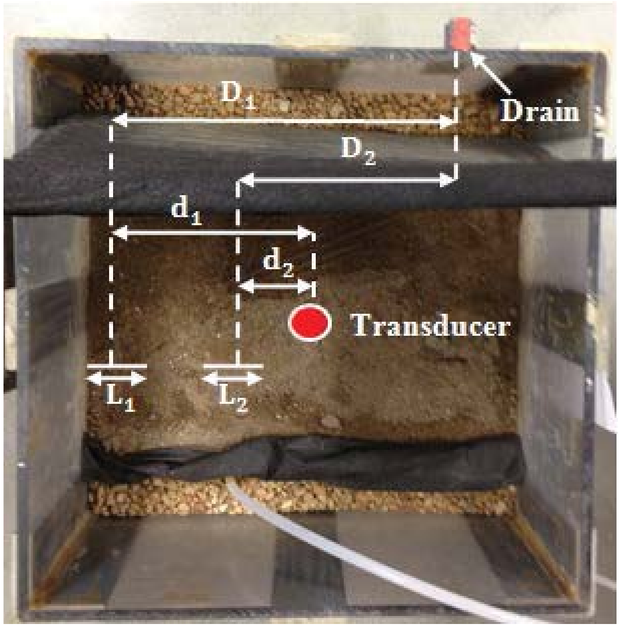

Figure 4.5: Graphical representation of the linear replacement relationship.

Figure 4.6 presents a plot of the linear replacement ratio versus pore pressure for all tests in this study. Refer back to Table 4.1, Table, 4.2 and Table 4.3 for further clarity on grout curtain orientations for all tests in this study. It can be seen in Figure 4.6 that the data produced well-defined curves. Figure 4.6 shows as the total length of the slats got further away from the pore pressure transducer the pore pressure decreased. The lower the pore pressure, the more effective was the grout curtain.

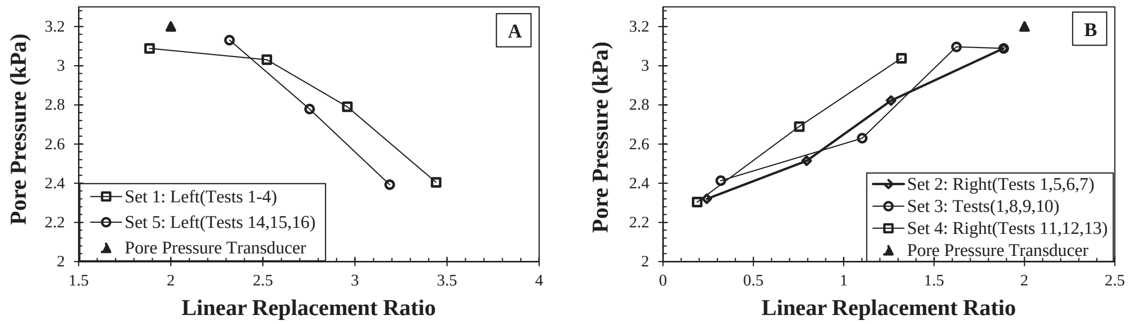

Figure 4.6: Linear replacement ratio versus pore pressure graph with grout curtain on (A) left hand side, and (B) right hand side.

The effects of the positioning of the drain within the laboratory-scale physical seepage model can be seen as well. Comparing tests with the same sequence, but on opposite sides of the physical model show the effects the drain position has on pore pressure measurements. When the grout curtain was placed on the left hand side of the physical model, pore pressure measurements tended to be higher than when the grout curtain was placed on the right hand side. This trend was consistent for all tests completed in this study since the flow of water had a more direct path to the drain when the grout curtain was on the left hand side of the physical model. The linear replacement ratio coupled with pore pressure measurements produced trends that will help contribute to quantification of the effectiveness of a grout curtain. However, the use of flat acrylic slats to represent a grout curtain wall does not encapsulate the true geometry of a grout curtain wall. Thus, the study used polyvinyl chloride (PVC) piping to take into account area as opposed to just length.

4.3 Area Representation of Grout Curtain-Polyvinyl Chloride Pipe Testing and Results

Similar to the acrylic slats testing, pore pressure transducers were utilized and installed at a pre-determined location within the test media. However, it is important to note that three pore pressure transducers were utilized, the test media used was the Kentucky River sand and the simulated grout columns were PVC pipes. Just like the acrylic slats testing, pore pressure measurements along with volume discharge measurements were subsequently performed during the various installation sequences of the simulated grout curtain. Measurements were taken every 25 minutes after the placement of PVC piping to allow for pore pressures to reach an equilibrium state. This time interval was determined from monitoring pore pressures and times in the manner presented in the “Initial Equilibrium Testing” section. However, it is noted that the time intervals were slightly different. Testing with the Kentucky River sand required measurements to be taken at 25 minutes instead of 20 minutes. The slight difference in time interval is due to a lower hydraulic conductivity.

Twenty sets of tests were performed during this test series. The twenty sets of tests were comprised of five spacing-to-diameter ratios (S/D) at four different dry unit weights. The spacing-to-diameter ratio is the ratio of the center-to-center spacing between grout columns along the proposed grout curtain line to the diameter of grout column itself. The diameter of all grout columns was 22 mm. The five different S/D ratios used in this study include 1, 1.18, 1.45, 1.62 and 2.17. These S/D ratios were selected to accommodate for equal spacing between grout columns. Not only did these S/D ratios accommodate for equal spacing, but they also allowed for the two grout columns at the ends of the proposed grout curtain line to touch the sides of the test box. The four dry unit weights that were tested were 12.56, 13.03, 13.35, and 13.82 kN/m^3. The dry unit weights were selected to fit within the maximum and minimum relative unit weights tabulated earlier in Table 3.1. But before PVC testing was performed, it was essential for this research that a new performance parameter utilizing areas be developed. By using the development of a new performance parameter combined with measured Lugeon values, it was believed that a grout curtain's effectiveness could be quantified prior to installation.

4.4 Development of a New Performance Parameter – Area Replacement Index

As mentioned earlier in Chapter 2, it was believed that an area replacement ratio similar to the one presented by Priebe (1991) and Priebe (1995) for ground improvement could be utilized to help in the quantification of the effectiveness of a grout curtain. Through experimentation with various proposed area replacement approaches, a new performance parameter was developed, which will be referenced throughout the remainder of this thesis as the area replacement index (λ).

To evaluate the effectiveness of a grout curtain, this study utilized a area replacement index value based on a double normalization scheme. The double normalization scheme was developed to take into account the amount of grout curtain placed within the area of improved ground and geometric configuration. The development of the area replacement index was based on four separate geometric configurations which are illustrated in Figure 4.7. Pore pressure measurements were subsequently taken as each additional grout column was installed following one of the geometric configurations.

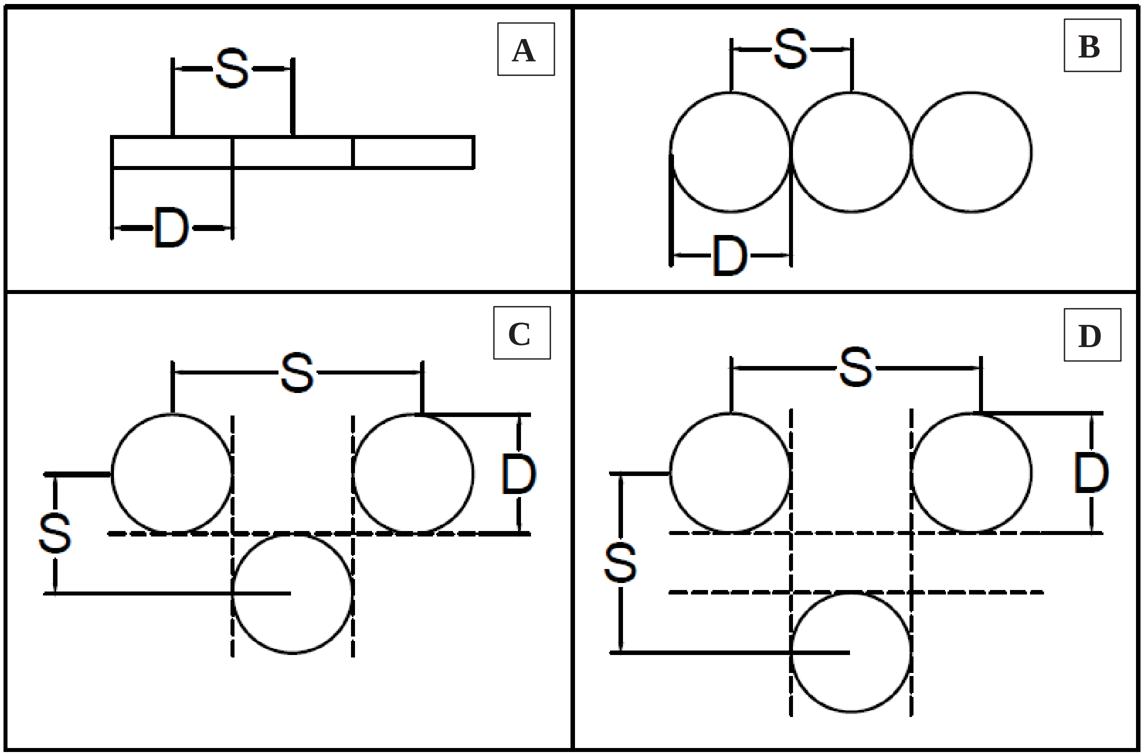

Figure 4.7: Geometric configurations used in the development of the area replacement index. (A) Tangent Planer, (B) Tangent Circular, (C) Tangent Primary-Secondary and (D) Discontinuous Primary-Secondary.

Seen in Figure 4.7, the tangent planer configuration is a rectangular trench section similar to a slurry wall panel. Testing was completed using flat acrylic slats, similar to the ones discussed earlier in this chapter. Tangent circular configuration is composed of a single row of circular grout columns placed tangent to one another. Both, tangent primary-secondary and discontinuous primary-secondary configurations are composed of two rows of circular grout columns. The only difference is the second row of grout columns for the discontinuous primary-secondary configuration is offset by a distance of half the diameter of a grout column. It is important to note that configurations identified in Figure 4.7 as B, C and D utilized the same 2.2-cm diameter PVC piping for grout columns.

The area replacement index utilizes a double normalization scheme. The first normalization scheme utilized is illustrated by the following:

$$\overline{A}_G = \left(\frac{\sum_{1}^{i} A_{GC}}{A_{TOTAL}} \right) \qquad (10)$$

where $\overline{A}_G$ = the normalized grouted area, A_{GC} = summation of the area of the grout columns, i = the number of grout columns installed at a specific time, A_{TOTAL} = total area of ground to be improved given the width of grout column by the total length of the grout region. For further clarification, Figure 4.8 shows a generalized graphical representation of the proposed grout curtain region and components.

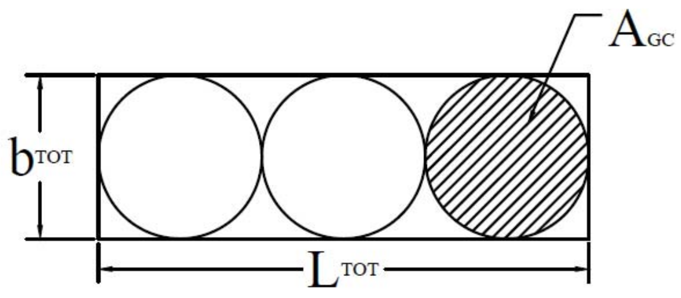

Figure 4.8: Components of grout region where $A_{TOTAL} = (b_{TOT})(L_{TOT})$, b_{TOT} = width of the grout region and L_{TOT} = length of the grout region.

Normalizing A_{GC} by A_{TOTAL}, allows for the evaluation of the effects of the area with respect to the area of improved ground. The relationship between normalized grouted area versus pore pressure for the four geometric configurations are shown in Figure 4.9.

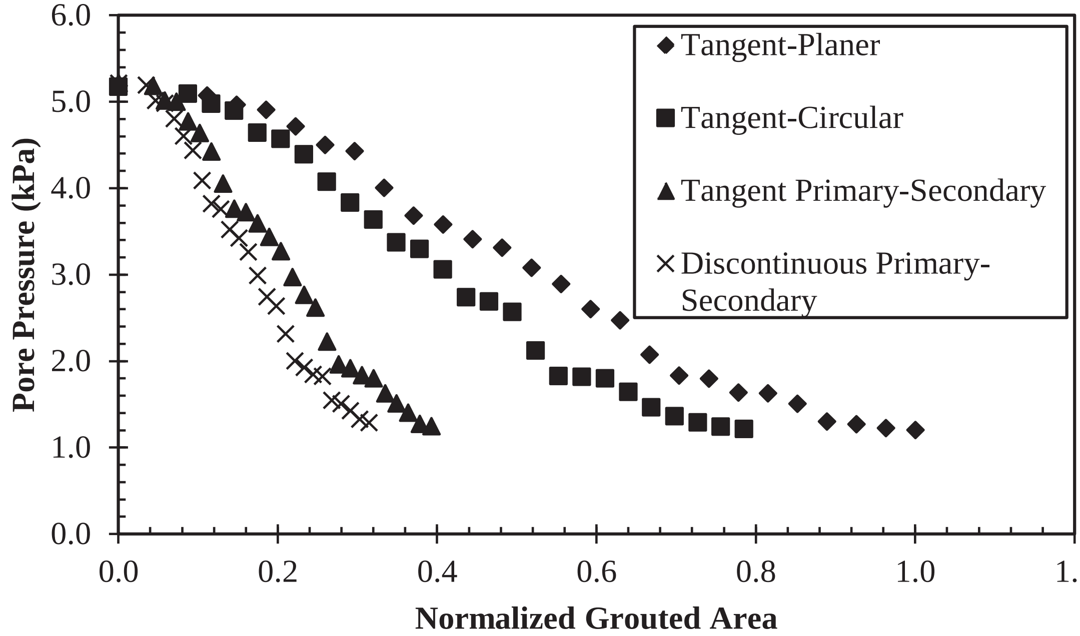

Figure 4.9: Relationship between normalized grouted area versus pore pressure for various geometric configurations.

As seen in Figure 4.9, in addition to varying with the normalized grouted area, pore pressure also varied consistently with respect to the geometric configuration. Thus, further normalization was done to take into account geometric configuration. The second normalization scheme takes into account geometric configuration and is given in the following form:

$$\lambda = \left[\frac{\left(\sum_{1}^{i} A_{GC} \Big/ A_{TOTAL} \right)}{\left(A_{GC(MAX)} \big/ A_{TOTAL} \right)} \right] \tag{11}$$

where $\lambda =$ area replacement index, $A_{GC(MAX)} =$ the maximum area of the grout columns that will fit within the grouted region at a specific S/D ratio.

Normalizing Equation 11 by $A_{GC(MAX)}/A_{TOTAL}$ takes into consideration geometric configuration. For example, if the geometric cross-section of the grout column is anything other than circular, this ratio will take this into consideration. Figure 4.10 shows the relationship between area replacement index versus pore pressure grouped by geometric configuration.

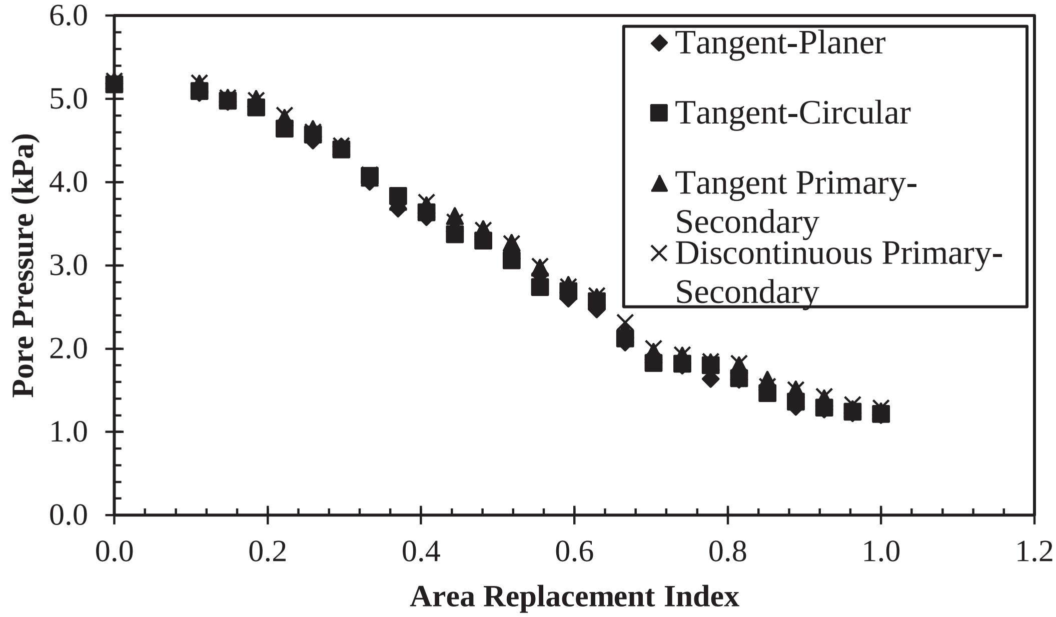

Figure 4.10: Relationship between area replacement index versus pore pressure grouped by geometric configuration.

As seen in Figure 4.10, the curves presented in Figure 4.9, collapsed to one curve after further normalization. At a constant area replacement index, pore pressure measurements at different geometric configurations seem to be equal. This is an indication that the area replacement index takes into consideration the amount of grout curtain placed within the area of improved ground and the geometric configuration. Thus, to simply testing procedures, all further testing was completed using the tangent circular geometric configuration only.

4.5 Nested Pore Pressure Transducers

Nested pore pressure testing with PVC pipes was similar to the acrylic slats testing. However, it is important to note that the test media used was the Kentucky River sand, the simulated grout columns were PVC pipes with a diameter of 22 mm, and three pore pressure transducers were utilized and positioned differently than when performing the acrylic slats testing. The pore pressure transducers were situated in a manner within the porous media, where all three transducers were within the same column at various known pressures, hence the word nested. The three pore pressure transducers were nested directly in the center of the box. Gauge 12, Gauge 13 and Gauge 14 were placed in a vertical column at known reference pressures of 2.29 kPa, 3.62 kPa and 5.17 kPa, respectively. Known reference pressures were determined by multiplying the unit weight of water by the height. This series of tests was performed to determine a pore pressure gradient with respect to depth. Having this data would help illustrate the effects on pore pressure with respect to depth at different S/D ratios and dry unit weights.

Pore pressure and volume discharge measurements were taken, as each additional PVC pipe was placed along the proposed grout curtain line within the test box. Upon completion of the initial test, three-22 mm diameter PVC pipes were placed into the center of the test box along the proposed grout curtain line at the desired S/D ratios. Pore pressure and volume discharge measurements were again taken 25 minutes after the placement of PVC pipes. With these two measurements, corresponding Lugeon values were calculated by utilizing Equation 1 presented in Chapter 2. This process was repeated adding one additional PVC pipe at the same desired S/D ratio, while alternating sides of the proposed grout curtain line until the grout curtain reached the sides of the test box. The entire process was repeated for all tests. Table 4.4 shows raw data corresponding to the test where the S/D ratio = 1 and a dry unit weight = 12.56 kN/m^3. For additional test data corresponding to nested pore pressure transducer testing see Appendix C.

Table 4.4: Raw data from corresponding to S/D=1 and dry unit weight= 12.56 kN/m^3.

Test	# of PVC Pipes	Pore Pressure-Gauge 12(kPa) Top	Pore Pressure-Gauge 13(kPa) Middle	Pore Pressure-Gauge 14(kPa) Bottom	Discharge Volume (mL)
Run 0	0	2.352	3.690	5.159	5520
Run 1	3	2.101	3.390	5.098	5423
Run2	4	2.167	3.515	5.075	5215
Run 3	5	1.937	3.287	4.952	5193
Run 4	6	1.841	3.127	4.683	4956
Run 5	7	1.840	3.222	4.652	4720
Run 6	8	1.831	3.262	4.503	4631
Run 7	9	1.512	3.087	4.213	4321
Run 8	10	1.343	3.058	4.243	3812
Run 9	11	0.905	2.335	3.975	3561
Run 10	12	0.425	1.857	3.721	3389
Run 11	13	Dry	1.471	3.521	3251
Run 12	14	Dry	1.052	3.275	3000
Run 13	15	Dry	0.845	2.875	2651
Run 14	16	Dry	0.642	2.683	2563
Run 15	17	Dry	0.411	2.596	2312
Run 16	18	Dry	0.213	2.318	2015
Run 17	19	Dry	Dry	2.136	1875
Run 18	20	Dry	Dry	2.006	1623
Run 19	21	Dry	Dry	1.945	1452
Run 20	22	Dry	Dry	1.842	1261
Run 21	23	Dry	Dry	1.812	1205
Run 22	24	Dry	Dry	1.625	1195
Run 23	25	Dry	Dry	1.425	1182
Run 24	26	Dry	Dry	1.358	1099
Run 25	27	Dry	Dry	1.309	1082

It is observed that Gauge's 12 and 13 were unable to record pore pressures for all tests. Gauge 12 and Gauge 13 were able to record data until Run 10 and Run 16, respectively. Two of the pore pressure transducers read "Dry" because the pore pressure transducers were located above the ground water table. This same problem was encountered for several tests at different S/D ratios and dry unit weights. Aware that this would present a problem, it was determined that pore pressure transducers be placed at the bottom of the test box as the research moved forward. Placing the pore pressure transducers at the bottom of the box prevented them from reading "Dry".

4.6 Pore Pressure Transducers Located at Bottom of Test Box

Due to pore pressure transducers drying out, it was determined that the three pore pressure transducers be placed at the bottom of the test box in a line parallel to the proposed grout curtain seen in Figure 3.2. They were placed 25.4-mm downstream of the proposed grout curtain, equal distant from one another. The test procedure outlined in the "Nested Pore Pressure Transducers" section was followed. The only difference was the placement of the three pore pressure transducers. Gauge 12, 13, and 14 were placed in the center, left and right hand sides of the box looking downstream, respectively. The pore pressure transducers were placed in such a fashion in hopes to see if there were any influences from the drain. However, it was determined through plotting pore pressure for all three transducers versus area replacement index, the drain had little influence on the readings of the pore pressure transducers. Figure 4.11 illustrates the influence of the drain from one test set (S/D =1 and dry unit weight = 12.56 kN/m^3).

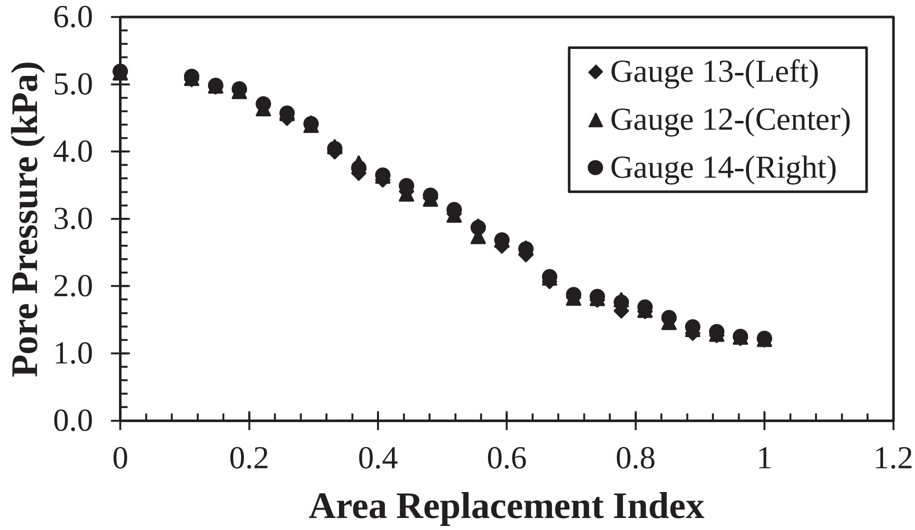

Figure 4.11: Influence of the drain on the three pore pressure transducers.

As observed in Figure 4.11, there was no significant variance in the pore pressure readings between the three transducers. Since this was consistent across all 20 tests, it was determined that an average pore pressure from the three transducers be used for further analysis.

Once test data was collected for all 20 test sets (five S/D ratios at four various unit weights), the data was analyzed for the intent of developing a quantifiable relationship between the area replacement index, Lugeon value, S/D ratio, and dry unit weight. To do so, various plots were developed to help in the understanding. The area replacement index was plotted versus several combinations and variations of parameters. It was determined through experimentation that combinations of average pore pressure, Lugeon values, and flow loss would provide the most correlation.

Flow loss is a typical parameter measured when calculating Lugeon values and can be seen in Equation 12:

$$Flow\ Loss = \frac{q}{L} \tag{12}$$

where $q =$ flow rate out of the test box = Q/t and $Q =$ volume of discharge, t = total time interval with which volume of discharge was collected and $L =$ test interval length of the representative test sample.

In order to scale the results from the test box, average pore pressure, flow loss and Lugeon values were normalized as:

$$Normalized\ Average\ Pore\ Pressure = \frac{P}{P_0} \tag{13}$$

$$Normalized\ Flow\ Loss = \left[\frac{\left(\frac{q}{L}\right)}{\left(\frac{q_0}{L_0}\right)}\right] \tag{14}$$

$$Normalized\ Lugeon\ Value = \frac{LV}{LV_0} \tag{15}$$

where P_0, q_0/L_0, $LV_0 =$ initial test measurements with no PVC pipes.

The normalization factors utilized in this research where from the initial test measurements described earlier in this chapter, when no PVC pipes were present, just the test media itself. Plots using these parameters are shown throughout the remainder of this chapter.

Figure 4.12 shows the relationship between area replacement index and normalized average pore pressure and shows how that relationship varies as the S/D ratio varies.

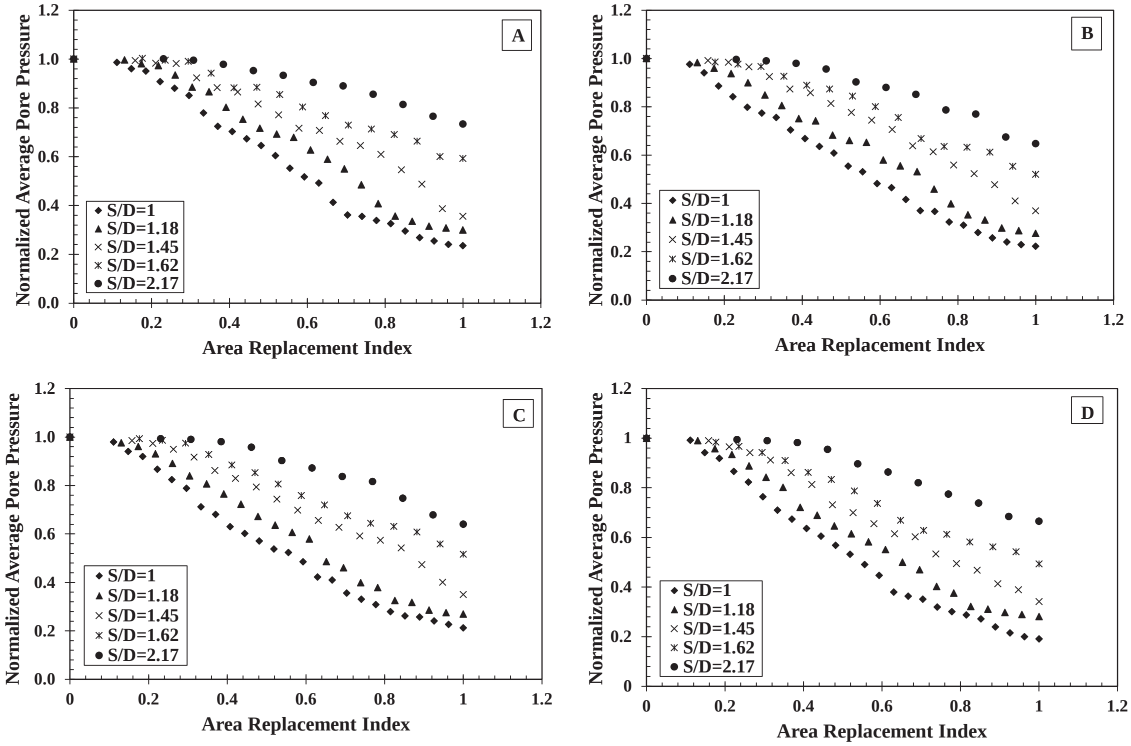

Figure 4.12: Area replacement index versus normalized average pore pressure, grouped by S/D ratios for a dry unit weight of (A) 12.56 kN/m^3, (B) 13.03 kN/m^3, (C) 13.35 kN/m^3 and (D) 13.82 kN/m^3.

For all 20 tests, as the area replacement index increases, the normalized average pore pressure decreases. Furthermore, at a constant area replacement index, the S/D ratio has a large effect on the normalized average pore pressure. For a given area replacement index, the relationship between the change in normalized average pore pressure and the change in S/D ratio do not appear to be proportional. However, there does seem to be some correlation between the shapes of the curves. All tests performed, display a similarly shaped curve.

Figure 4.13 illustrates the relationship between area replacement index and normalized q/L and shows how that relationship varies as the S/D ratio varies.

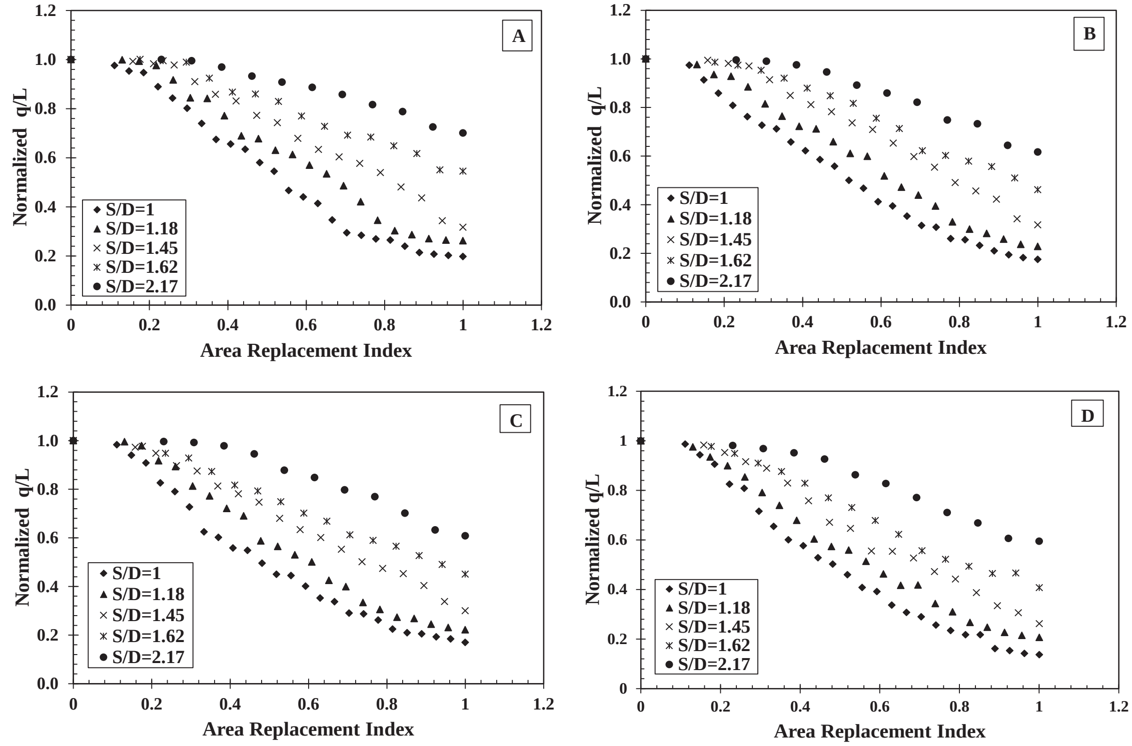

Figure 4.13: Area replacement index versus normalized q/L, grouped by S/D ratios for a dry unit weight of (A) 12.56 kN/m^3, (B) 13.03 kN/m^3, (C) 13.35 kN/m^3 and (D) 13.82 kN/m^3.

At a constant area replacement index, the S/D ratio has an effect on normalized q/L seen in Figure 4.13. Also, at a constant S/D ratio, as the area replacement index increases, the normalized q/L decreases. Looking at Figure 4.12 and Figure 4.13, the relationship between area replacement index and normalized q/L and the relationship between area replacement index and normalized average pore pressures are quite similar. The behavior of these curves presented seem to be consistent crossed all S/D ratios and dry unit weights.

The curves presented in Figure 4.12 and Figure 4.13, were curve fitted using a fitting program, Table Curve (SYSTAT, Chicago, IL). The curves presented in these figures, were curve fit to identify the general equation form that describes the behavior of these curves. Figure 4.14 illustrates fitted curves showing the relationship between area replacement index and normalized average pore pressure, and area replacement index versus normalized q/L at a dry unit weight of 12.56 kN/m^3. It should be noted that similar behavior was witnessed across all dry unit weights. However, for simplicity only results for a dry unit weight of 12.56 kN/m^3 were presented.

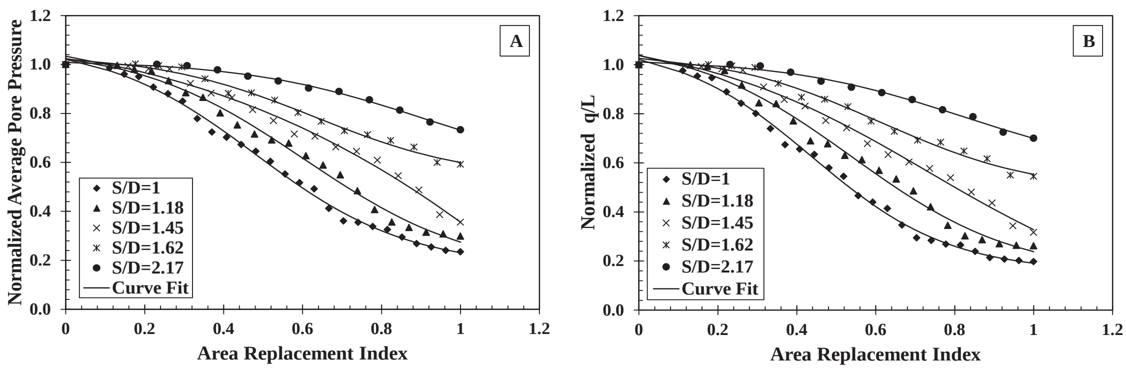

Figure 4.14: (A) Fitted curves showing the relationship between area replacement index versus normalized average pore pressure, grouped by S/D ratios for a dry unit weight of 12.56 kN/m^3. (B) Fitted curves showing the relationship between area replacement index versus normalized q/L, grouped by S/D ratios for a dry unit weight of 12.56 kN/m^3.

The general equation describing the behavior of the curves presented in Figure 4.14 were identified as a sigmoid. The specific equation that was identified having the highest R^2 values across all S/D ratios and dry unit weights can be seen in following equation:

$$y = a + \left(\frac{b}{1 + \exp\left(-\left(\frac{x-c}{d} \right) \right)} \right) \quad (16)$$

where y = normalized average pore pressure or normalized q/L, x = area replacement index, and a, b, c, d = constants.

Constants a, b, c and d were unable to be identified as specific properties of the curve through further analysis. However, for completeness constants a, b, c, d and R^2 values corresponding to the curve-fit plots of area replacement index versus normalized average pore pressure, and area replacement index versus normalized q/L are tabulated in Table 4.5. The constants and R^2 values are tabulated for all four dry unit weights.

Table 4.5: Sigmoidal curve fitting constants from Table Curve.

	Dry Unit Weights (kN/m^3)	S/D Ratio	a	b	c	d	R^2
Area Replacement Index vs Normalized Average Pore Pressure	12.56	1	0.17	0.92	0.48	-0.19	1.00
		1.18	0.14	0.93	0.61	-0.22	0.99
		1.45	-1.37	2.55	1.36	-0.48	0.99
		1.62	0.53	0.52	0.63	-0.20	0.99
		2.17	0.54	0.48	0.91	-0.23	0.99
	13.03	1	0.10	1.10	0.43	-0.26	1.00
		1.18	0.07	1.06	0.59	-0.27	0.99
		1.45	0.07	1.01	0.77	-0.28	1.00
		1.62	0.47	0.55	0.65	-0.17	0.99
		2.17	0.48	0.54	0.84	-0.20	0.99
	13.35	1	0.14	1.04	0.40	-0.23	1.00
		1.18	0.17	0.90	0.53	-0.20	1.00
		1.45	-0.12	1.28	0.82	-0.37	0.99
		1.62	0.49	0.55	0.59	-0.18	0.99
		2.17	0.44	0.58	0.87	-0.21	0.99
	13.82	1	0.14	1.04	0.40	-0.22	1.00
		1.18	0.19	0.92	0.49	-0.21	0.99
		1.45	0.25	0.83	0.58	-0.22	0.99
		1.62	0.48	0.54	0.56	-0.16	1.00
		2.17	0.62	0.39	0.70	-0.15	1.00
Area Replacement Index vs. Normalized q/L	12.56	1	0.15	0.94	0.44	-0.17	1.00
		1.18	0.14	0.96	0.54	-0.21	0.99
		1.45	0.00	1.13	0.73	-0.30	0.99
		1.62	0.48	0.57	0.61	-0.20	0.99
		2.17	0.55	0.47	0.82	-0.23	0.99
	13.03	1	0.08	1.15	0.38	-0.25	1.00
		1.18	0.10	1.00	0.53	-0.23	1.00
		1.45	0.09	1.00	0.69	-0.26	0.99
		1.62	0.42	0.60	0.63	-0.17	0.99
		2.17	0.51	0.51	0.76	-0.18	0.99
	13.35	1	0.13	1.10	0.33	-0.21	0.99
		1.18	0.17	0.93	0.47	-0.18	1.00
		1.45	0.11	1.01	0.61	-0.28	1.00
		1.62	0.37	0.70	0.57	-0.23	1.00
		2.17	0.51	0.51	0.75	-0.18	0.99
	13.82	1	0.09	1.14	0.35	-0.21	0.99
		1.18	0.12	1.04	0.44	-0.23	0.99
		1.45	0.18	0.92	0.54	-0.22	0.99
		1.62	0.38	0.65	0.55	-0.17	1.00
		2.17	0.53	0.48	0.69	-0.16	1.00

Figure 4.15 shows the relationship between normalized average pore pressure and normalized q/L. The normalized average pore pressure and normalized q/L values that

are were shown seem to be proportional. Normalized average pore pressure was plotted versus normalized q/L to determine whether or not the two parameters were indeed proportional. This proportionality seems to occur over all five S/D ratios and four unit weights.

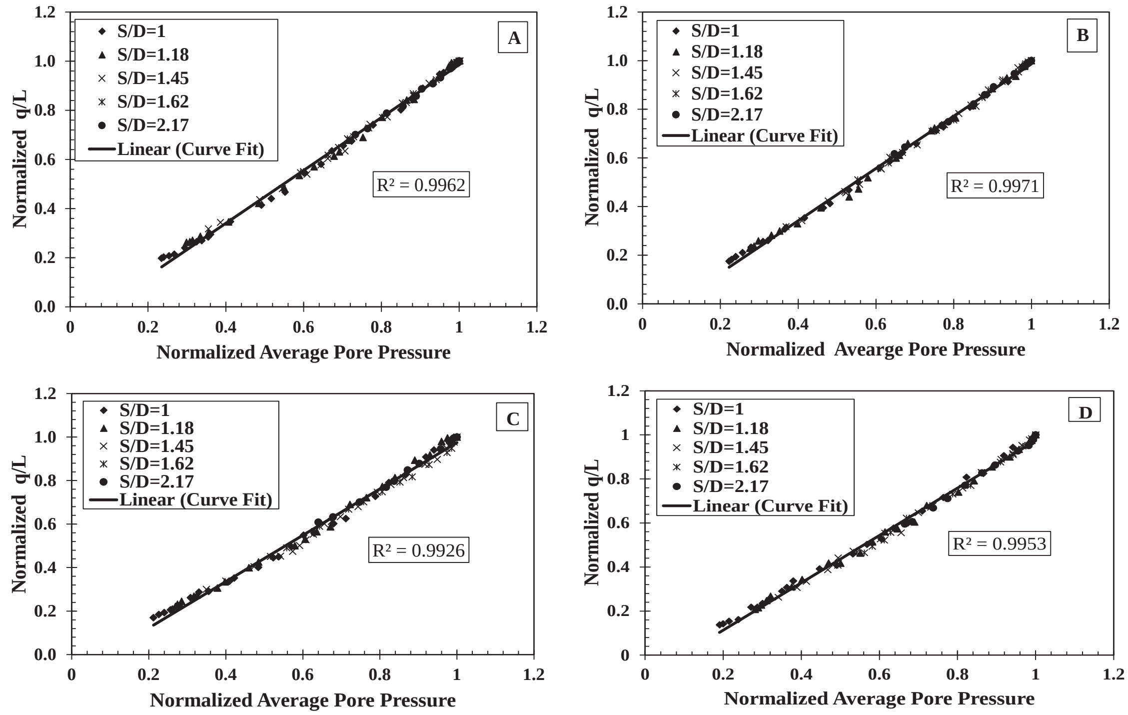

Figure 4.15: Linear relationship between normalized average pore pressure and normalized q/L grouped by S/D ratios for a dry unit weight of (A) 12.56 kN/m^3, (B) 13.03 kN/m^3, (C) 13.35 kN/m^3 and (D) 13.82 kN/m^3.

Looking at Figure 4.15, the proportionality between normalized average pore pressure and normalized q/L seems to occur over all five S/D ratios and four dry unit weights. The R^2 values presented in Figure 4.15, suggest that the relationship between normalized pore pressure and normalized q/L is highly linear for all S/D ratios and dry unit weights. For all five S/D ratios at all four dry unit weights, R^2 values were greater than 0.99. As the normalized pore pressure decreases, the normalized q/L decreases. According to Quinones-Rozo (2010) research, a linear relationship between pore pressure and q/L describes laminar flow. Laminar flow occurs when fluid is moving at low velocity. When fluids move at low velocities, no lateral mixing takes place. Also, Quinones-Rozo (2010) research found out that Lugeon values are approximately equal regardless of pore pressure during laminar flow. Figure 4.16 was developed to verify that the flow within the laboratory-scale physical seepage model was indeed laminar.

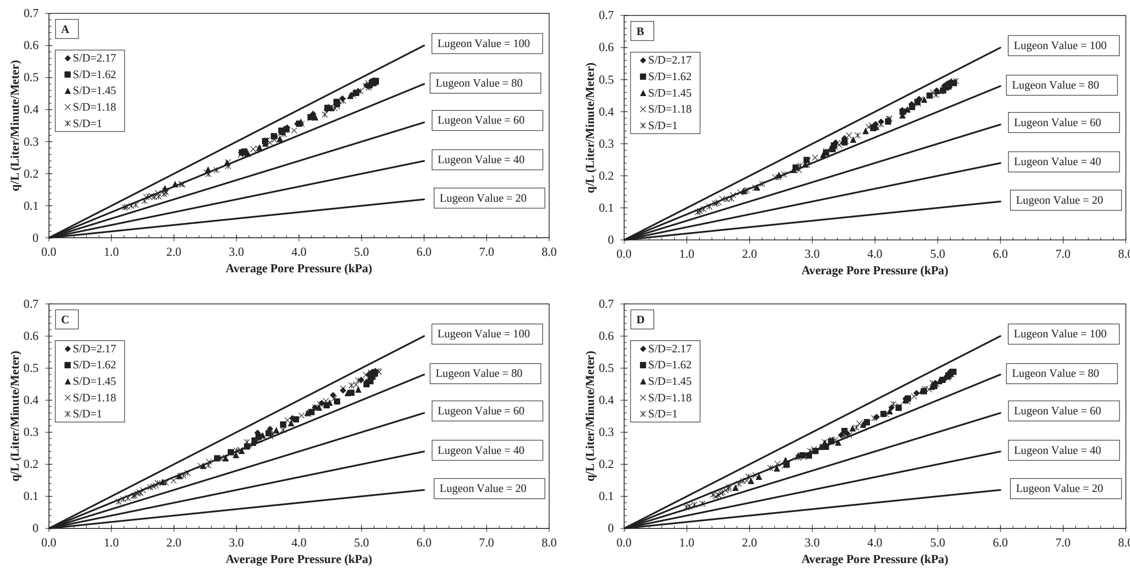

Figure 4.16: Relationship between average pore pressure and q/L grouped by S/D ratios for a dry unit weight of (A) 12.56 kN/m^3, (B) 13.03 kN/m^3, (C) 13.35 kN/m^3 and (D) 13.82 kN/m^3.

As seen in Figure 4.16, most data points across all S/D ratios and dry unit weights fell within the boundaries corresponding to a Lugeon value of 80 and 100. This figure illustrates that Lugeon values seen within the laboratory-scale psychical seepage model were fairly constant at various average pore pressures. This behavior is consistent with the characterization of laminar flow described in Quinones-Rozo (2010) research.

Now that the flow behavior within the test box has been characterized, normalized pore pressure and normalized q/L were plotted versus normalized Lugeon values. As stated earlier in this thesis, Lugeon values are used in this study to help quantify the effectiveness of a grout curtain. Utilizing Lugeon values in this study allows implementation of the proposed efficiency parameters using current field techniques. Figure 4.17 illustrates the relationship between normalized average pore pressure versus normalized average Lugeon value grouped by S/D ratio at various dry unit weights.

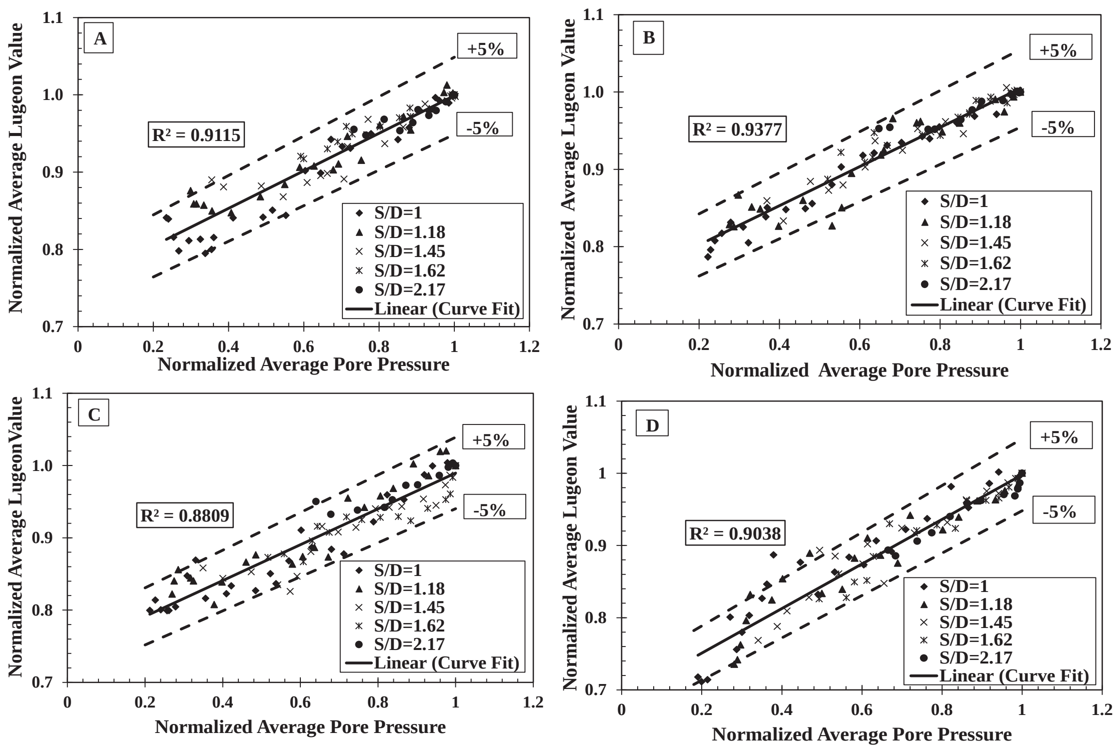

Figure 4.17: Relationship between normalized average pore pressure and normalized average Lugeon values grouped by S/D ratios for a dry unit weight of (A) 12.56 kN/m^3, (B) 13.03 kN/m^3, (C) 13.35 kN/m^3 and (D) 13.82 kN/m^3.

As seen in Figure 4.17, it appears that there is a linear relationship between normalized average pore pressure and normalized average Lugeon value. However, the figure does show some variability with respect to normalized Lugeon values. The normalized Lugeon values for all S/D ratios at various different dry unit weights do have some scatter. The scatter in these plots deal with the pressure range that was observed in the box. The maximum pore pressure that was observed in the box was 5.30 kPa. Looking back at the equation that was utilized to calculate Lugeon values for this study presented in Chapter 2, the equation uses a reference pressure of 1 MPa. Since, the test box is operating at such small pressures compared to the reference pressure; small changes in pore pressure can result in much larger changes in Lugeon values. Even though test data appears to scatter a little, a consistent trend has developed for all S/D ratios at all dry unit weights. As the normalized average pore pressure decreases, so does the normalized average Lugeon values. Linear curve fitting for the individual test data shown in Figure 4.17, produced high R^2 values. R^2 values for all S/D ratios at all dry unit weights were greater than 0.82 and can be seen in Table 4.6. These high R^2 values imply that a linear relationship between normalized average pore pressure and normalized average Lugeon value exists. Further analysis shows that at constant unit weight, as the S/D ratio increases, the slope of the linear best fit line decreases.

Table 4.6: Unit weight, S/D ratio, slope, Y-intercept and R^2 values for linear best fit lines of normalized average pore pressure versus normalized average Lugeon value plots.

Dry Unit Weight (kN/m^3)	S/D Ratio	Slope	Y-Intercept	R^2
12.56	1	0.26	0.73	0.92
	1.18	0.22	0.78	0.92
	1.45	0.21	0.78	0.84
	1.62	0.19	0.81	0.96
	2.17	0.18	0.81	0.82
13.03	1	0.26	0.74	0.97
	1.18	0.24	0.76	0.87
	1.45	0.25	0.75	0.95
	1.62	0.21	0.79	0.92
	2.17	0.15	0.84	0.88
13.35	1	0.26	0.79	0.90
	1.18	0.25	0.74	0.90
	1.45	0.25	0.73	0.85
	1.62	0.21	0.76	0.84
	2.17	0.19	0.80	0.83
13.82	1	0.34	0.68	0.89
	1.18	0.33	0.67	0.93
	1.45	0.31	0.69	0.91
	1.62	0.30	0.69	0.96
	2.17	0.29	0.70	0.89

A similar relationship was developed between normalized q/L and normalized average Lugeon value. Looking back at an earlier relationship developed between normalized average pore pressures versus normalized q/L seen in Figure 4.15, it appears that the relationship is highly linear. Knowing this relationship, a plot comparing normalized q/L versus normalized average Lugeon value should produce a plot that has a similar relationship to the normalized average pore pressure versus normalized average Lugeon value plot seen in Figure 4.17. Figure 4.18 shows the relationship between normalized q/L versus normalized average Lugeon value grouped by S/D ratio at various dry unit weights.

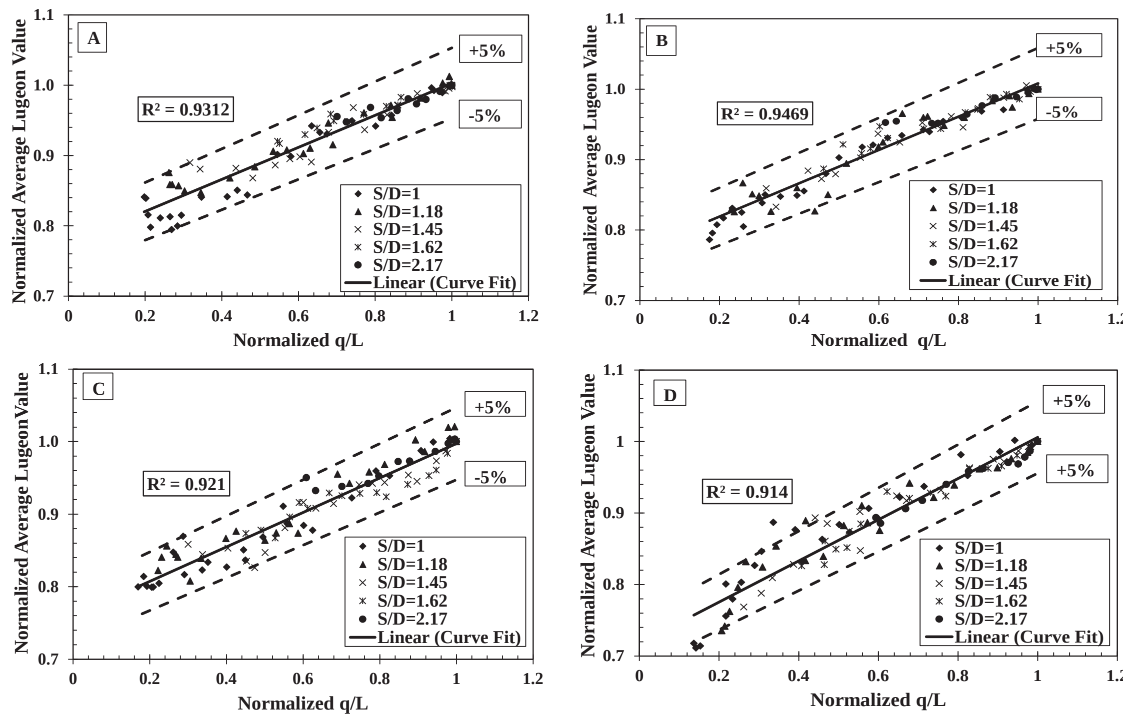

Figure 4.18: Relationship between normalized q/L and normalized average Lugeon values grouped by S/D ratios for a dry unit weight of (A) 12.56 kN/m^3, (B) 13.03 kN/m^3, (C) 13.35 kN/m^3 and (D) 13.82 kN/m^3.

As seen in Figure 4.18, a linear relationship between normalized q/L and normalized average Lugeon value developed. The behavior of this relationship was quite similar to the relationship illustrated in Figure 4.17, as expected. As normalized q/L decreases, the normalized average Lugeon value decreases. This trend was consistent across all S/D ratios and dry unit weights. Linear curve fitting produced best fit lines with high R^2 values which can be seen in Table 3.10. All R^2 values were greater than 0.87.

Table 4.7: Unit weight, S/D ratio, slope, Y-intercept and R^2 values for linear best fit lines of normalized q/L versus normalized average Lugeon value plots.

Dry Unit Weight (kN/m^3)	S/D Ratio	Slope	Y-Intercept	R^2
12.56	1	0.25	0.75	0.94
	1.18	0.21	0.79	0.95
	1.45	0.20	0.79	0.89
	1.62	0.17	0.83	0.97
	2.17	0.17	0.83	0.87
13.03	1	0.25	0.76	0.97
	1.18	0.23	0.77	0.91
	1.45	0.23	0.78	0.96
	1.62	0.19	0.81	0.94
	2.17	0.14	0.86	0.91
13.35	1	0.25	0.75	0.94
	1.18	0.25	0.76	0.94
	1.45	0.23	0.75	0.90
	1.62	0.19	0.78	0.89
	2.17	0.18	0.82	0.88
13.82	1	0.32	0.70	0.89
	1.18	0.28	0.72	0.90
	1.45	0.28	0.72	0.93
	1.62	0.28	0.72	0.95
	2.17	0.25	0.74	0.97

Plotting normalized average pore pressure and normalized q/L versus area replacement index and normalized average Lugeon value produced two distinct shapes. Normalized average pore pressure and normalized q/L plotted against area replacement index established non-linear sigmoidal shaped curves. While normalized average pore pressure and normalized q/L plotted against normalized average Lugeon value produced linear relationships.

Trends and relationships between normalized average pore pressure, normalized q/L, area replacement index and normalized average Lugeon values have been observed. To aid in the quantification in the effectiveness of a grout curtain, area replacement index was plotted versus normalized average Lugeon value for all S/D ratios at all dry unit weights. Figure 4.19 illustrates this relationship. Linear best fit lines forced through a normalized average Lugeon value of one are also seen in Figure 4.19. Equations for the linear best fit lines along with their corresponding R^2 values are tabulated in Table 4.8. Linear best fit lines were forced through a Lugeon value of one to allow for proper scaling and comparison to various case history data which will be discussed later.

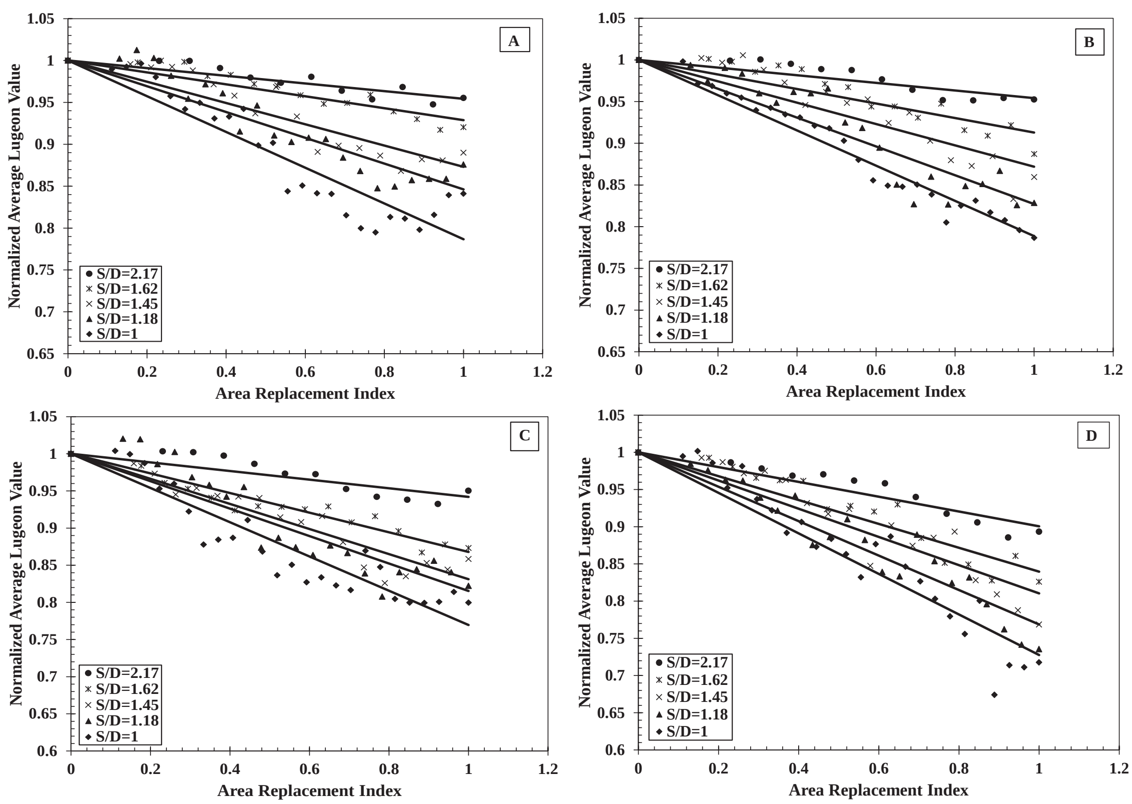

Figure 4.19: Relationship between area replacement index and normalized average Lugeon values grouped by S/D ratios for a dry unit weight of (A) 12.56 kN/m^3, (B) 13.03 kN/m^3, (C) 13.35 kN/m^3 and (D) 13.82 kN/m^3.

Table 4.8: Unit weight, S/D ratio, slope, Y-intercept and R^2 values for linear best fit lines of area replacement index versus normalized average Lugeon value plots.

Dry Unit Weight (kN/m^3)	S/D Ratio	Slope	Y-Intercept	R^2
12.56	1	-0.21	1.00	0.86
	1.18	-0.15	1.00	0.87
	1.45	-0.13	1.00	0.85
	1.62	-0.07	1.00	0.86
	2.17	-0.05	1.00	0.81
13.03	1	-0.21	1.00	0.96
	1.18	-0.17	1.00	0.84
	1.45	-0.13	1.00	0.82
	1.62	-0.09	1.00	0.82
	2.17	-0.05	1.00	0.78
13.35	1	-0.23	1.00	0.86
	1.18	-0.18	1.00	0.83
	1.45	-0.17	1.00	0.90
	1.62	-0.13	1.00	0.92
	2.17	-0.06	1.00	0.75
13.82	1	-0.27	1.00	0.90
	1.18	-0.23	1.00	0.91
	1.45	-0.19	1.00	0.86
	1.62	-0.16	1.00	0.89
	2.17	-0.10	1.00	0.88

R^2 values for all linear best fit lines were greater than 0.81, with the exception of two tests, S/D = 2.17 at a dry unit weight of 13.03 kN/m^3 and S/D = 2.17 at a dry unit weight of 13.35 kN/m^3. High R^2 values imply that a linear correlation between area replacement index and normalized average pore pressure as a function of S/D ratio exists. At this point, at a given S/D ratio, the relationship between area replacement index and normalized average Lugeon value can be described as shown in Equation 17.

$$LV_n = m_1(ARI) + 1 \tag{17}$$

where LV_n = normalized average Lugeon value, m_1 = slope of linear best fit line from the area replacement index versus normalized average Lugeon value plot and ARI = area replacement index.

Looking at the slopes of the linear best fit lines in Figure 4.19, at a constant S/D ratio, it appears that the slopes increase, as dry unit weight increases. Upon speculation, it is believed that as the dry unit weight increased, the void space between soil particles decreased resulting in less volume discharge, hence a decreased Lugeon value. This relationship is evident for all S/D ratios. Plotting S/D ratio versus m_1 as a function of dry unit weight shows another linear correlation seen in Figure 4.20.

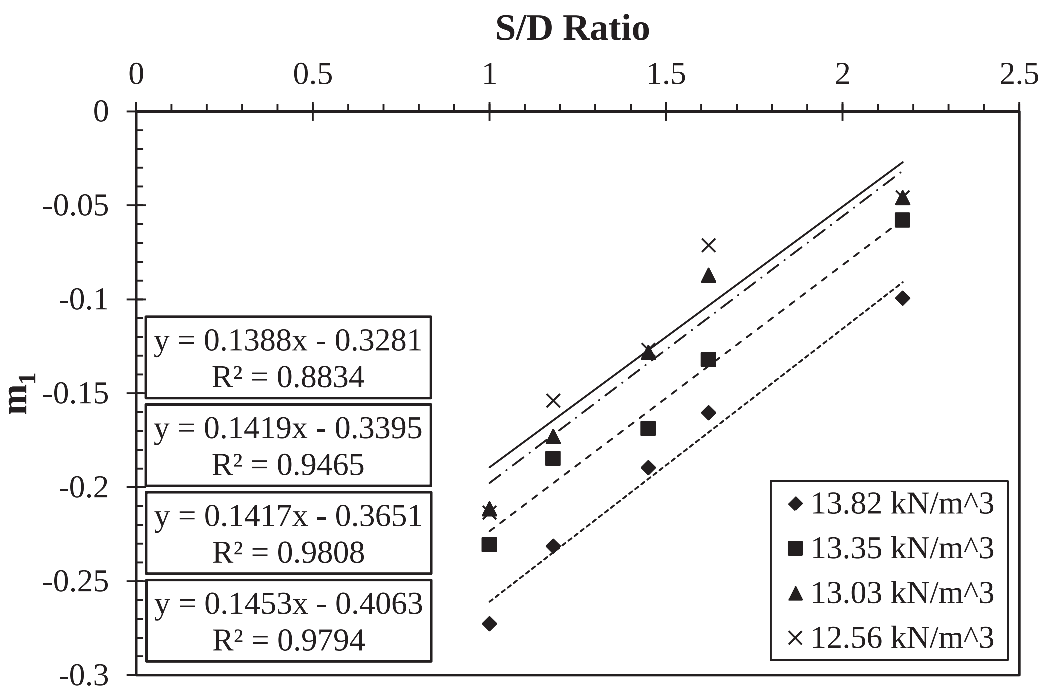

Figure 4.20: S/D ratio versus m_1, grouped by dry unit weight.

As seen in Figure 4.20, R_2 values for all 4 dry unit weights showed high linear correlation. Also, the slopes of the S/D ratio versus m_1 as a function of dry unit weight were approximately equal. Since the slopes of the best fit lines were approximately equal, an average slope value was obtained. The average slope obtained from the S/D ratio versus m_1 plot will be referred to as m_{2avg} which is equal to 0.1419. Equation 18 shows the linear relationship between S/D ratio versus m_1 as a function of dry unit weight.

$$m_1 = m_{2avg}\left(\frac{S}{D}\right) + b_2 \tag{18}$$

where S/D = spacing-to-diameter ratio and b_2 = y-intercept as a function of dry density. Now, substitute Equation 18 into Equation 17 to get Equation 19 which takes into account S/D ratio and area replacement index.

$$LV_n = \left(m_{2avg}\left(\frac{S}{D}\right) + b_2\right)ARI + 1 \tag{19}$$

The next step to this analysis was plotting dry unit weight versus b_2. This relationship can be seen in Figure 4.21.

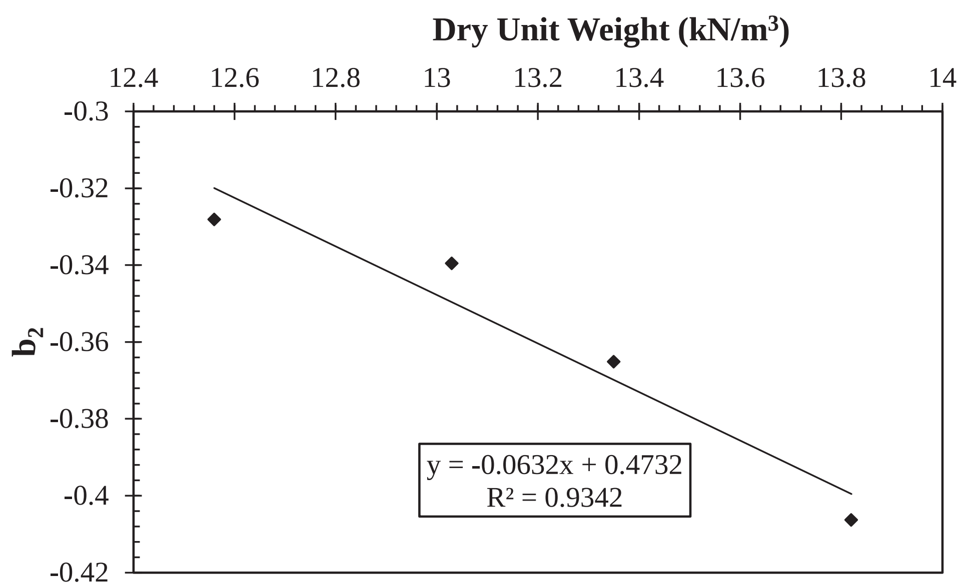

Figure 4.21: Dry unit weight versus b_2.

Once again, a highly linear correlation between dry unit weight and b_2 resulted. The equation for the best fit line through the test data is shown in Figure 4.21, which displays a relationship where dry unit weight increases as b_2 decreases. The slope and y-intercept presented in Figure 4.21 were assumed to be material constants of the test media used in this research and will be referred to as m_3 and b_3, respectively. For this research m_3 = -0.0632 and b_3 = 0.4732. However, further research should be focused on determining m_3 and b_3 material constants for various materials. Equation 20 shows the linear relationship between dry unit weight and b_2.

$$b_2 = m_3\left(\gamma_{dry}\right) + b_3 \tag{20}$$

where m_3 = material constant, b_3= material constant and γ_{dry} =dry unit weight.

At this point substitute Equation 20 into Equation 19 to get Equation 21 which gives the final relationship that calculates a normalized average Lugeon value.

$$LV_n = \left(m_{2avg}\left(\frac{S}{D}\right) + m_3\left(\gamma_{dry}\right) + b_3\right)ARI + 1 \tag{21}$$

where LV_n = normalized average Lugeon value, ARI = area replacement index, m_3 = material constant = -0.0632, b_3 = material constant = 0.4732, m_{2avg} = 0.1419, S/D = spacing-to-diameter ratio and γ_{dry} = dry unit weight.

Equation 21 is a function of S/D ratio, dry unit weight and area replacement index. This relationship quantifies the effectiveness of a grout curtain as a function of three parameters which include S/D ratio, dry unit weight and area replacement index.

4.7 Summary

It is possible to quantifiably predict the effectiveness of a grout curtain using a physical model knowing a few properties of the underlying soil material and grout curtain. Several trends and relationships developed when comparing normalized average pore pressure, normalized q/L, area replacement index and normalized average Lugeon values to one another at various S/D ratios and dry unit weights. These relationships along with further analysis, assisted in the creation of a new mathematical equation that helps predict the effectiveness of a grout curtain in a physical model. However, this new relationship has yet to be proven accurate using data from real life structures. To show that this relationship can be scaled up to real life structures, case history data needed to be obtained to assess the validity of this proposed relationship.

Chapter 5: Relationship Verification

To verify the accuracy of the newly developed relationship, case history data was collected and analyzed. The use of actual field data from different case history studies will further validate the relationship. Using case history data presented in Chapter 2 will help demonstrate that it is possible to predict the effectiveness of a grout curtain using additional data that was not used in the creation of this quantifiable relationship.

All four case history studies that were analyzed to assess the applicability of the proposed relationship (Equation 21) are dam structures located in South Korea. The specific names of the dams were not identified in the Hong et al. (2003) research, but rather identified as Site 1, Site 2, Site 3 and Site 4. Site 1, Site 3 and Site 4 are all concrete-faced rock fill dams while Site 2 is a gravity concrete dam. Metamorphic and sedimentary rock formations underlie all four dam structures. Table 2.1 presented in Chapter 2 provided pertinent information about the case history dams. This table is presented again here as Table 5.1 for continuity.

Table 5.1: Site conditions and grouting properties of four case history studies (Hong et al. 2003).

	Site 1	Site 2	Site 3	Site 4
Type of Dam	Concrete Face Rock Fill Dam	Gravity Concrete Dam	Concrete Face Rock Fill Dam	Concrete Face Rock Fill Dam
Type of Rock	Metamorphic	Sedimentary	Sedimentary	Sedimentary
Number of Holes	231	35	28	41
Depth of Holes (m)	40	20	20	40
Grout Spacing	1 column with 1.5 m spaced holes	2 columns at 3.0 m zigzag interval; 3.0 m spaced holes	1 column with 1.5 m spaced holes	2 columns at 3.0 m zigzag interval; 3.0 m spaced holes
Span of Grout Curtain (m)	347	105	42	123
Average Lugeon Value Before Grouting	3	3.9	11	2.37
Average Lugeon Value After Grouting	1	1.9	3	1
Injection Pressure (Mpa)	0.39-2.45	0.15-0.59	0.15-0.59	0.29-2.45
Assumed Grout Column Diameter (m)	1.016	1.016	1.016	1.016

Four separate parameters for each site had to be identified, which included normalized average Lugeon value, S/D ratio, area replacement index and dry unit weight. S/D ratios and area replacement index values were calculated for all four sites based on the geometry of the individual grout curtains which was presented in Chapter 2. The diameters of the grout columns include allowances for horizontal spread of the grout material. Horizontal spread is the maximum distance the grout material can penetrate the soil media. Typical grout curtain designs account for 1.016 m of horizontal spread (Hacker, 2014). Thus, the diameters of the grout columns for the case histories were assumed to be 1.016 m. Normalized average Lugeon values were calculated by dividing the average Lugeon value after grouting by the average Lugeon value before grouting. Dry unit weights of the underlying material were not presented. However, underlying rock types were given. With this knowledge, average dry unit weights for these underlying rock formations were assumed based on research done by Magner (1963) and

Akeinyemi et al. (2012). Metamorphic and sedimentary rocks were assumed to have unit weights of 23.56 kN/m^3 and 22.77 kN/m^3, respectively. These unit weights are well outside the unit weights tested in this research. To accommodate the assumed unit weights of the metamorphic and sedimentary rock formations, predicted curves were developed holding the S/D ratio and ARI constant in Equation 21. Predicted curves matching the unit weights of the underlying rock material allowed for easy comparison. Figure 5.1 illustrates the case history data plotted against predicted values.

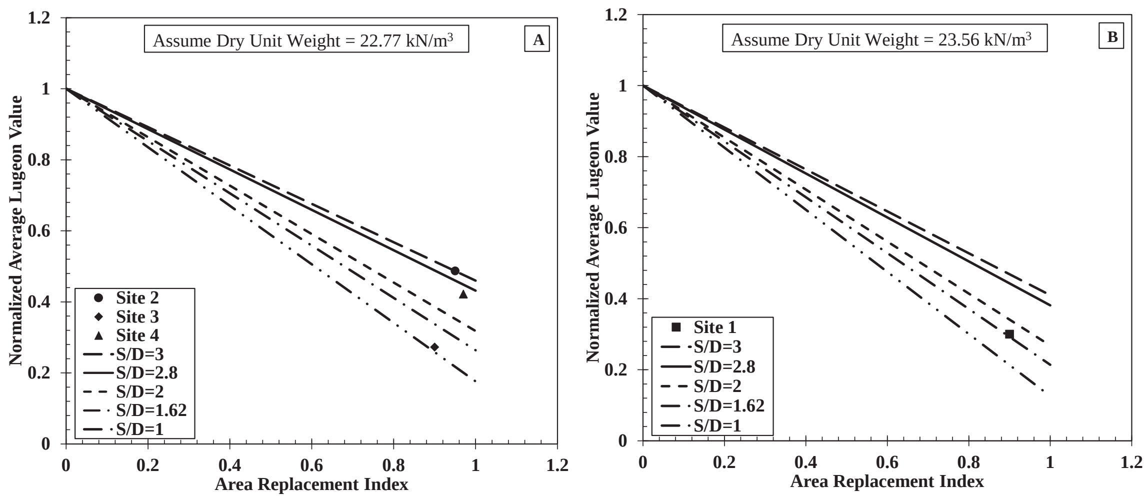

Figure 5.1: Case history data versus predicted values plotted at dry unit weights of (A) 22.77 kN/m^3 and (B) 23.56 kN/m^3.

As seen in Figure 5.1, all case history studies have S/D ratios between 1 and 3. Since the underlying rock material seen at Site 2, Site 3 and Site 4 were similar; these sites were plotted together, seen in Figure 5.1A. Site 1 composed of metamorphic rock, was plotted by itself seen in Figure 5.1B. To truly assess the applicability of the proposed relationship, predicted normalized average Lugeon values were plotted versus actual normalized average Lugeon values for all four case histories. Predicted values are compared to actual values in Figure 5.2.

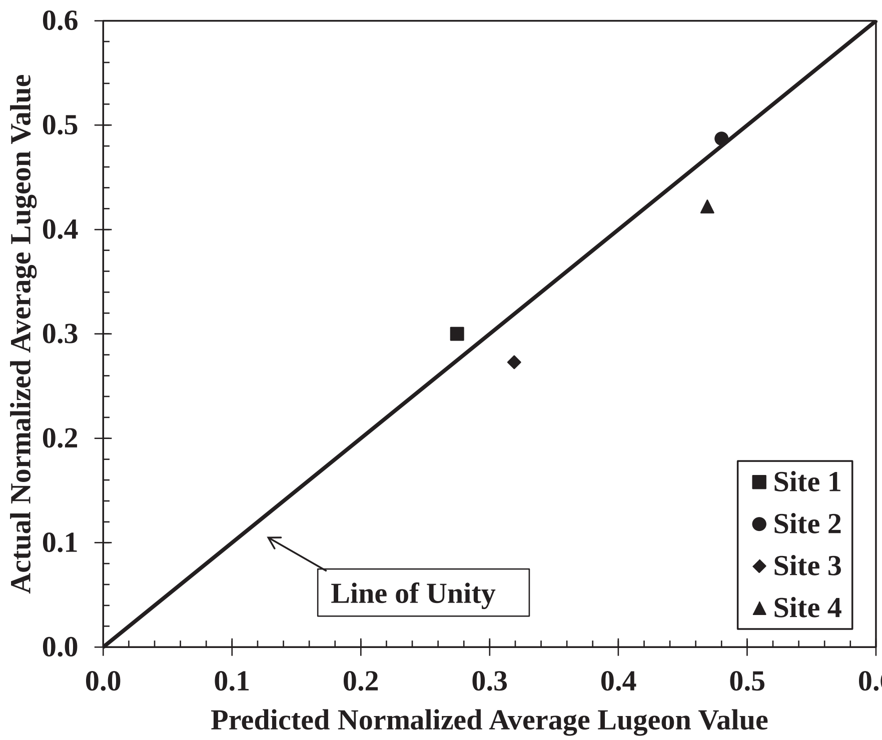

Figure 5.2: Relationship between predicted normalized average Lugeon value versus actual normalized average Lugeon values.

Figure 5.2 illustrates the applicability of the relationship presented in Equation 21 using data from four separate case histories. As is seen in the figure, all four points plot near the line of unity. The absolute percent error was calculated for all four case histories using Equation 22.

$$Absolute\ \%\ Error = \left| \frac{Actual\ \ Value - Expected\ \ Value}{Actual\ \ Value} \right| \times 100 \qquad (22)$$

Table 5.2, tabulates absolute percent error for each of the 4 case histories.

Table 5.2: Calculated absolute percent errors for all case history studies.

	Predicted Normalized average Lugeon value	Actual Normalized average Lugeon value	Absolute percent error (%)
Site 1	0.27	0.30	8.40
Site 2	0.48	0.49	1.42
Site 3	0.32	0.27	17.07
Site 4	0.47	0.42	11.20

Evaluating the absolute percent error values tabulated in Table 5.2, it is evident that the relationship presented in Equation 21 is reliable when predicting normalized average Lugeon values. Site 3 shows the highest absolute percent error of 17.1 percent. Site 2 on the other hand shows the lowest absolute percent error of 1.42 percent. Site 1 and Site 4 have absolute percent error values that fall in between the absolute percent errors of Site 2 and Site 3.

Normalized average Lugeon values can be predicted as a function of three parameters, S/D ratio, dry unit weight and area replacement index to assess the effectiveness of a grout curtain. Case history data further validates that the relationship that developed while testing in a box, can be scaled up to real life structures. Being able to reliably predict Lugeon values will prove very beneficial when designing grout curtain structures in the future.

Chapter 6: Summary and Conclusions

This thesis presented the results of a laboratory study that quantified the effectiveness of a grout curtain using a laboratory-scale physical seepage model. This study investigated changes in pore pressures and discharge volumes to determine corresponding Lugeon values at various unit weights and spacings. The development of a new performance parameter similar to the area replacement ratio used in ground improvement methods was utilized to help develop a quantifiable relationship. This research discovered a linear relationship that takes into account soil unit weight, grout curtain spacing and a new performance parameter that can be used to help predict the effectiveness of a grout curtain. Verification of this relationship was done by using various case history studies.

The information presented in Chapter 2, discussed the current methodologies in which grout curtains are assessed. However, it is pointed out that most of the prior research was predominately based on qualitative means such as prior experience and rules of thumb rather than quantitative means. Quantifying the effectiveness of a grout curtain prior to installation would prove very beneficial. It would help engineers minimize factors such as time, cost and labor.

Chapter 3 presented the development of a physical model. This physical model was used to help determine and illustrate various geotechnical trends that exist within the test media with various grout curtain configurations. Measurements of pore pressure and discharge volume for various S/D ratios at different dry unit weights were taken. These measurements were subsequently used to calculate Lugeon values, which were the primary basis for quantification.

It was presented in Chapter 2, that an area replacement parameter similar to Priebes (1991) and Priebes (1995) area replacement ratio for ground improvement, could be used as a means to quantify the effectiveness of a grout curtain. Therefore, a new performance parameter known as the area replacement index was developed and presented in Chapter 4.

The main goal of this research was to generate a new quantifiable relationship to predict the effectiveness of a grout curtain based on Lugeon values and area replacement index values. This research illustrated a linear relationship that is a function of three parameters S/D ratio, dry unit weight and area replacement index. Knowing these three parameters allows for the prediction of the effectiveness of a grout curtain.

Case history data was obtained and analyzed for four various sites to assess the accuracy of the newly developed quantifiable relationship. Plotting actual data from four various case histories versus predicted data utilizing the newly developed quantifiable relationship exemplified a fairly accurate relationship. This comparison provided the necessary evidence to show the relationship can be scaled.

Thus, it is possible to accurately predict the effectiveness of a grout curtain knowing three parameters S/D ratio, dry unit weight and area replacement index. Quantifying the effectiveness of a grout curtain gives engineers the ability to optimize their design, while providing an adequate solution.

The research that was presented in this thesis only covered five S/D ratios at five dry unit weights for one test media. This does not cover a wide enough spectrum to consider this a relationship to be used by industry for design. However, there is evidence presented in this thesis that supports the use of this newly developed quantifiable relationship to assess the effectiveness of a grout curtain. This is a significant step forward in the direction of assessing the effectiveness of a grout curtain quantifiably rather than qualitatively. The time and money that would be saved, further justify more research to be completed for this quantifiable relationship.

Future research should be aimed at further understanding the relationship between normalized Lugeon values with respects to S/D ratio and dry unit weight. This research showed that normalized average Lugeon values vary linearly as a function of S/D ratio, dry unit weight and area replacement index. However, the ranges of S/D ratios and dry unit weights were limited. Having a wider range of tests will allow for a better understanding of this relationship. Along the same lines, more test medias should be tested following the same procedures outlined in this research. As mentioned earlier, the quantifiable relationship that predicts the effectiveness of a grout curtain takes into account two material constants b_3 and m_3. Using different test medias will help determine these material constants and will provide further understanding of this quantifiable relationship. This proposed research could ultimately lead to a more accurate and useful relationship.

Appendix A:

Index Testing on Test Sand

Table A.1: Particle grain size analysis data (ASTM D6913) for Kentucky River sand.

Sieve Number	Opening (mm)	Weight Retained Each Sieve (g)	Weight of Soil Retained (g)	Weight of Soil Passed (g)	Percent Finer
3/8"	9.500	0.00	0	1471	100.000
No. 4	4.750	0.00	0	1471	100.000
No. 10	2.000	0.00	0	1471	100.000
No. 20	0.850	11.80	11.8	1459.2	99.198
No. 40	0.425	18.10	29.9	1441.1	97.967
No. 60	0.250	183.20	213.1	1257.9	85.513
No. 100	0.150	997.10	1210.2	260.8	17.729
No. 140	0.106	127.60	1337.8	133.2	9.055
No. 200	0.075	66.30	1404.1	66.9	4.548
Pan	0.000	66.90	1471	0	0.000
	Total	1471			

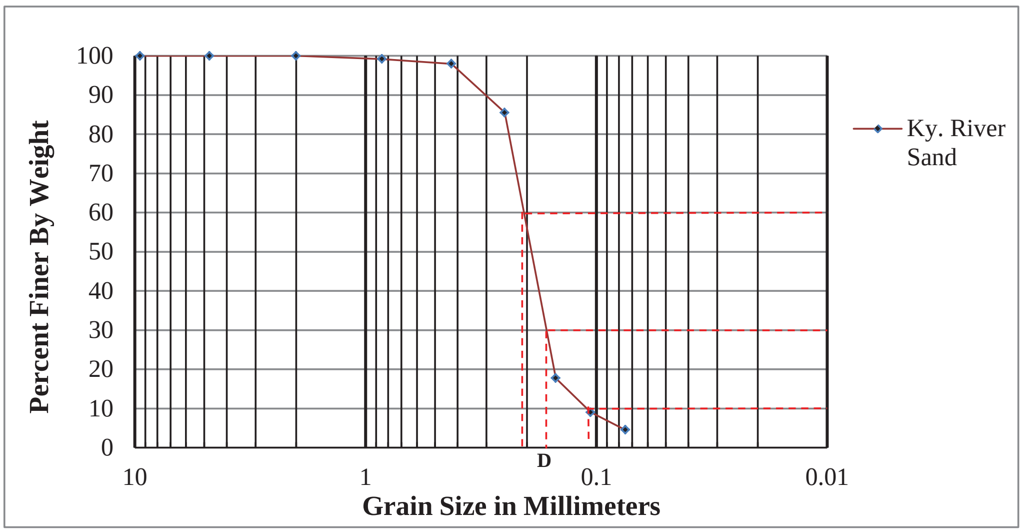

Figure A.1: Graphical representation of the particle grain size analysis test for Kentucky River sand.

Table A.2: Specific gravity data (ASTM D854) for Kentucky River sand.

Specific Gravity						
Soil Description	Ky. River Sand		Ky. River Sand		Ky. River Sand	
Test number	1		2		3	
Nominal Pycometer Volume	500	ml	500	ml	500	ml
Oven Dry Weight of Soil	100	g	96.3	g	89.2	g
Weight of Pycometer+ Water	665	g	660.7	g	662.6	g
Weight of Pycometer+ Water+Soil	727.4	g	721.1	g	718.4	g
Temperature	20	deg. Cels	20	deg. Cels	20	deg. Cels
Correction Factor K	1		1		1	
Specific Gravity	2.66		2.68		2.67	

Table A.3: Particle grain size analysis data (ASTM D6913) for Ohio River Valley Sand.

Sieve Number	Opening (mm)	Weight Retained Each Sieve (g)	Weight of Soil Retained (g)	Weight of Soil Passed (g)	Percent Finer
3/8"	9.500	0.00	0	1073.58	100.000
No. 4	4.750	38.92	38.92	1034.66	96.375
No. 10	2.000	139.27	178.19	895.39	83.402
No. 20	0.850	228.65	406.84	666.74	62.104
No. 40	0.425	451.43	858.27	215.31	20.055
No. 60	0.250	179.37	1037.64	35.94	3.348
No. 100	0.150	32.46	1070.1	3.48	0.324
No. 140	0.106	1.35	1071.45	2.13	0.198
No. 200	0.075	0.33	1071.78	1.8	0.168
Pan	0.000	1.80	1073.58	0	0.000
	Total	1073.58			

Figure A.2: Graphical representation of the particle grain size analysis test for Ohio River Valley sand.

Table A.4: Specific gravity data (ASTM D854) for Ohio River Valley sand.

Specific Gravity						
Soil Description	Ohio River Valley Sand		Ohio River Valley Sand		Ohio River Valley Sand	
Test number	1		2		3	
Nominal Pycometer Volume	500	ml	500	ml	500	ml
Oven Dry Weight of Soil	103.2	g	112.3	g	110.8	g
Weight of Pycometer+ Water	678	g	683	g	664	g
Weight of Pycometer+ Water+Soil	742.3	g	753.1	g	732.6	g
Temperature	20	deg. Cels	20	deg. Cels	20	deg. Cels
Correction Factor K	1		1		1	
Specific Gravity	2.65		2.66		2.63	

Appendix B:

Step-by-step Manual for Program Development in LabVIEW 2012

The pore pressure transducers used in this research were the Kulite XCL-11-250-150SG sealed gauge pore pressure transducers rated at 150 pounds per square inch. The three pore pressure transducers used in this research all contained calibration certificates provided by the manufacturer Kulite. The various information Kulite provided on these certificates will be essential data for the verification of Kulites calibration.

Wiring Modules

The first step in the calibration process of the Kulite XCL-11-250-150SG sealed gauge pore pressure transducers is to correctly assemble the module in the chaise from National Instruments(NI). The module that was used in the proper calibration of the Kulite XCL-11-250-150SG sealed gauge pore pressure transducers was the NI 9237 module. The NI 9237 module is a 4-channel, 24-Bit Half/Full-Bridge Analog Input Module. Figure B.1 shows the proper location within the NI chaise for the NI 9237 module.

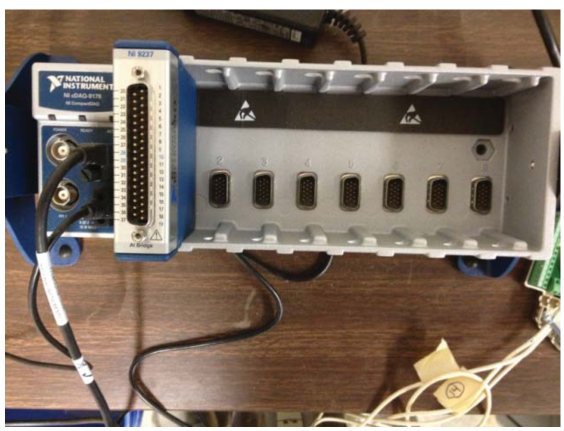

Figure B.1: Proper Location for the NI 9237 Module in the NI chaise

The second step is to properly wire the three Kulite XCL-11-250-150SG sealed gauge pore pressure transducers to the sub-connector that will eventually be inserted into the NI 9237 module. The three Kulite pore pressure transducers were wired in a fully active four arm wheatstone bridge. Each pore pressure transducer has five individual wires running from the pore pressure head with their own distinct color. Figure B.2 is showing the five different wires running from the Kulite XCL-11-250-150SG sealed gauge pore pressure transducer.

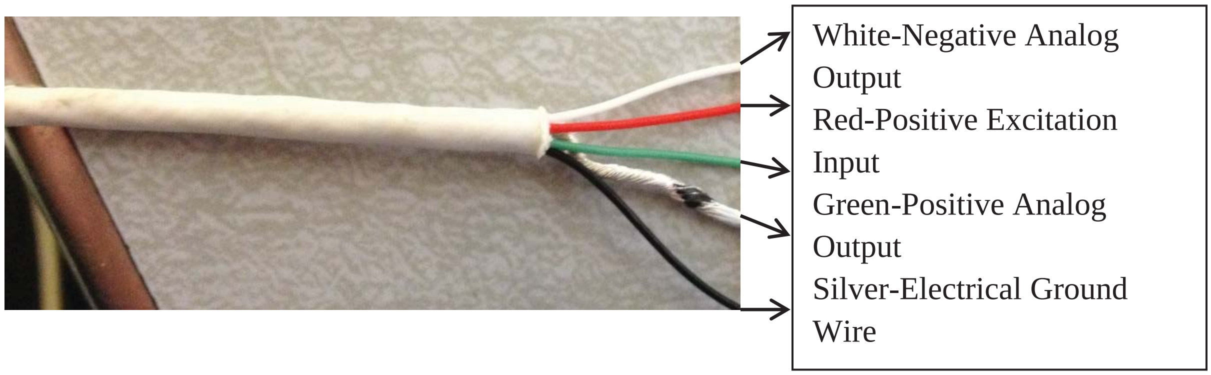

Figure B.2: Wires within each Kulite XCL-11-250-150SG sealed gauge pore pressure transducer

The red wire corresponds to the positive excitation input, the black wire corresponds to the negative excitation input, the green wire corresponds to the positive analog output, the white wire corresponds to the negative analog output, and the thick silver wire is the electrical ground wire.

Once one is familiar with the different types of wires that are within each Kulite XCL-11-250-150SG sealed gauge pore pressure transducer, it is time to wire all three pore pressure transducers to the NI sub-connector. Figure B.3 shows the proper way to wire each of the three Kulite XCL-11-250-150SG sealed gauge pore pressure transducers in a fully active four arm wheatstone bridge configuration.

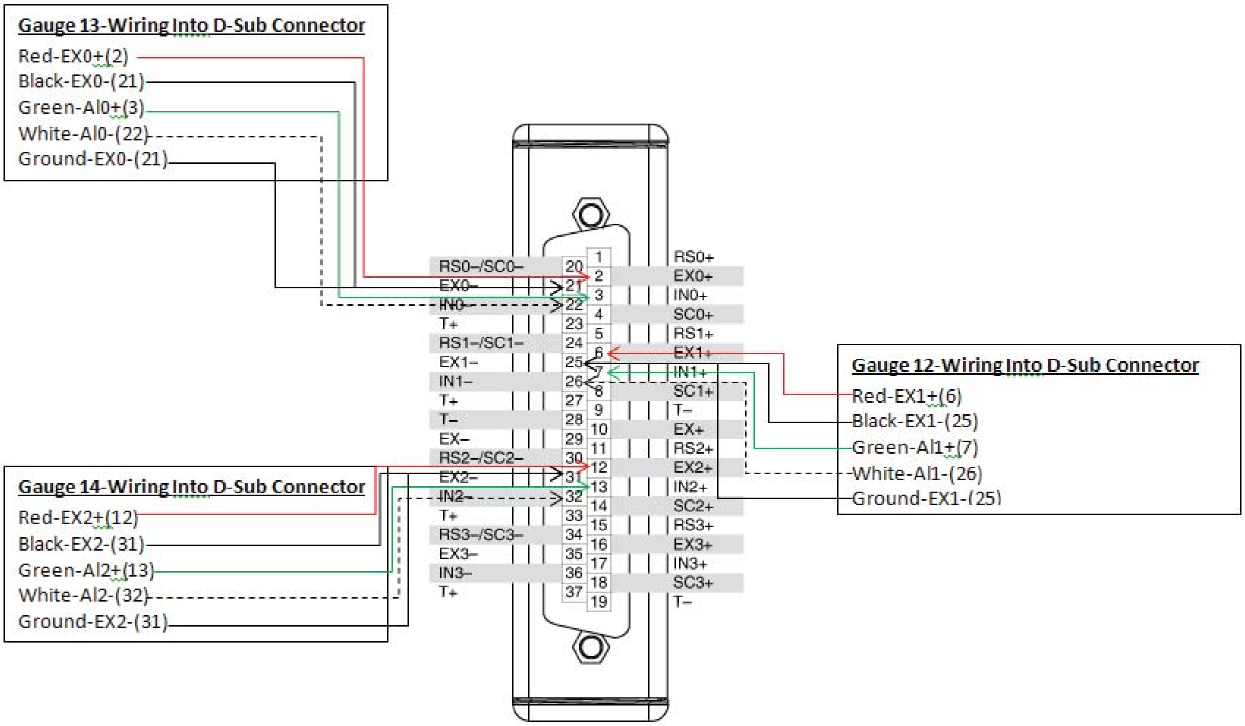

Figure B.3: Wiring diagram for pore pressure transducers in a fully active four arm Wheatstone bridge configuration

It is important to note that the ground wires for each of the three Kulite XCL-11-250-150SG sealed gauge pore pressure transducers were connected to the negative excitation input pin due to grounding issues. A voltmeter was used to check that there was no significant voltage difference between the ground wire and the negative excitation input pin.

Once the wires are correctly connected to the NI sub-connector, insert the NI Sub-connector into the NI 9237 Module as seen in Figures B.4 and B.5.

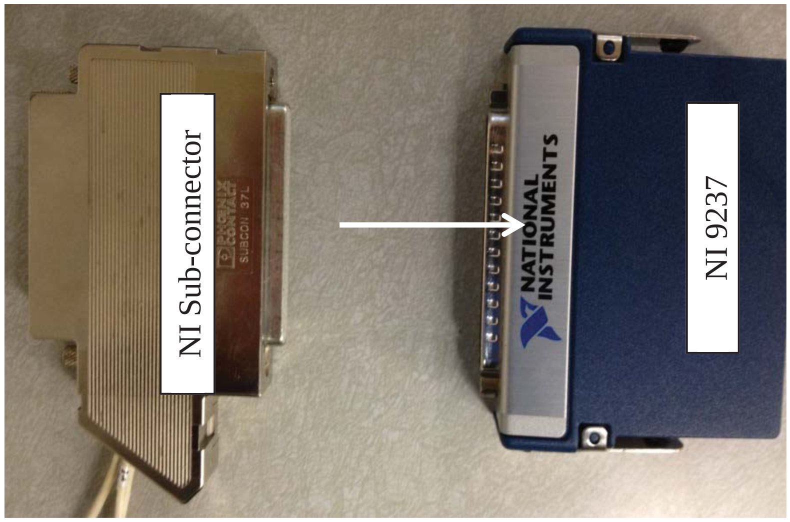

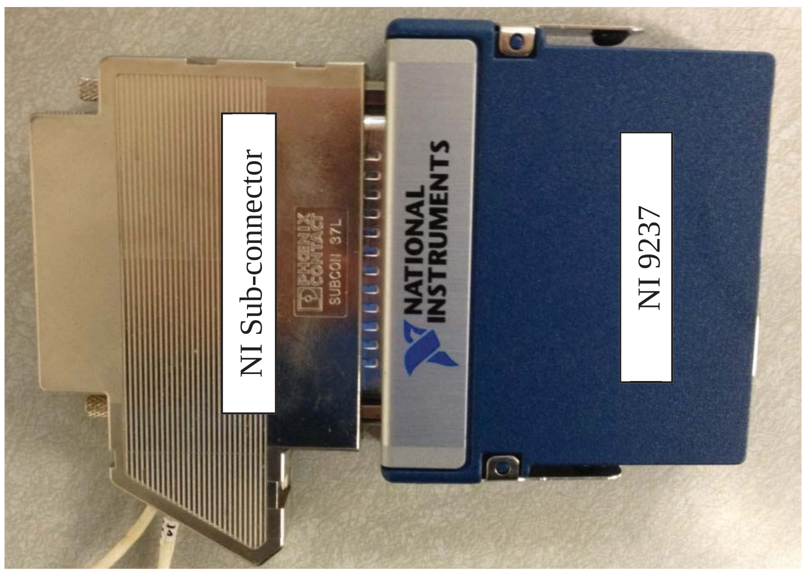

Figures B.4 (Top) and B.5 (Bottom): Show the connection of the NI sub-connector to the NI 9237 Module

Once the NI sub-connector is inserted into the NI 9237 Module which is then inserted into the NI chaise like Figure 1 shows, it is time to start acquiring data through National Instruments LabVIEW 2012 software.

LabVIEW Program Set-Up

Now it is time to install National Instruments LabVIEW 2012 software into the computer. The LabVIEW 2012 software comes with two cd-ROMs, both of which need to be installed for full use of the software. Once both cd-ROMs are installed, open up NI MAX to make sure that the modules are being read by the LabVIEW 2012 software, after being connected through the USB port. Once the NI MAX user menu opens up, there will be a box along the left hand side of the window. Now click on Devices and Interfaces. The following window should look like the Figure B.6 if the LabVIEW 2012 software is recognizing the NI chaise and NI 9237 Module correctly.

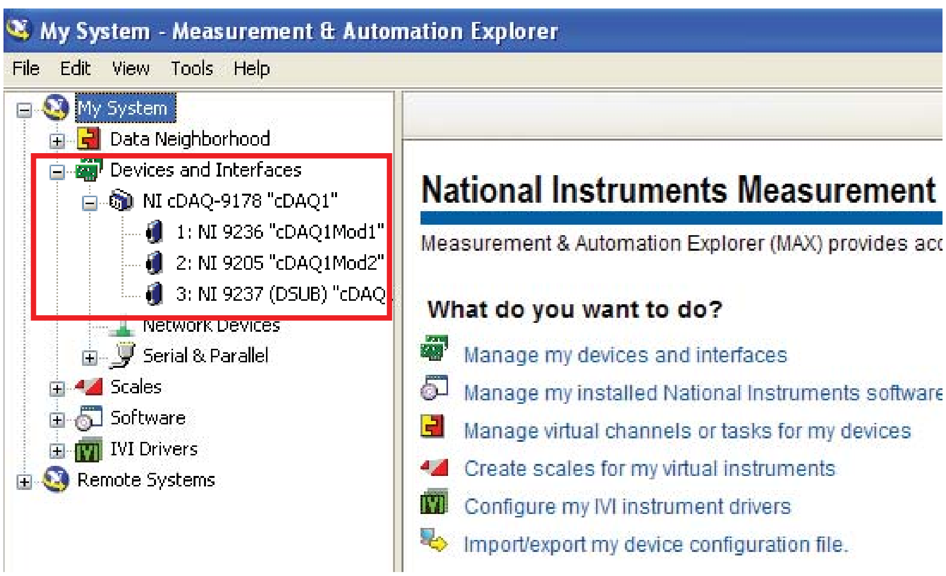

Figure B.6: NI Max user window showing the NI chaise and NI 9237 Module being recognized by LabVIEW 2012.

The next step in getting the data aquistion system working is to open up a brand new VI page in LabVIEW 2012 software. Once you open up a new VI work page, two windows should appear; the first being the Block Diagram, and the second being the

Front Panel. The Block Diagram is where the actually computer code is written and the Front Panel is where all the data is displayed. The figure below shows the two windows that appear when you open up a new VI work page.

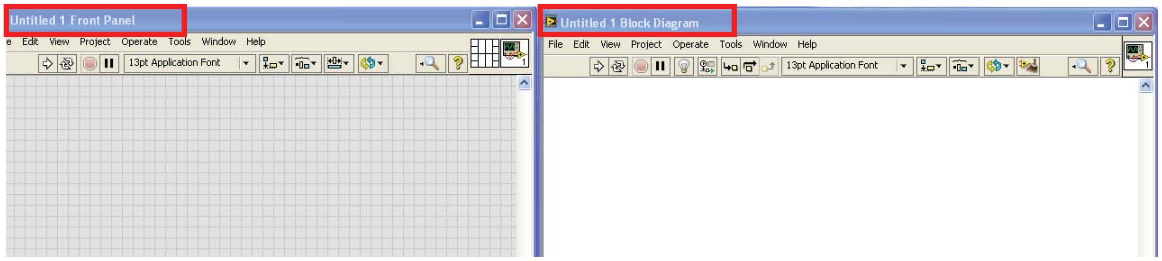

Figure B.7: Shows the Front Panel and the Block Diagram windows once opening up a new VI work page in LabVIEW 2012.

To begin writing code for the data aqusition system, the functions window must be opened in the Block Diagram window. To open the functions window, right click anywhere in the Block Diagram window and click on the push pin in the upper left hand corner of the functions window. Now the functions window should appear and look like the Figure B.8

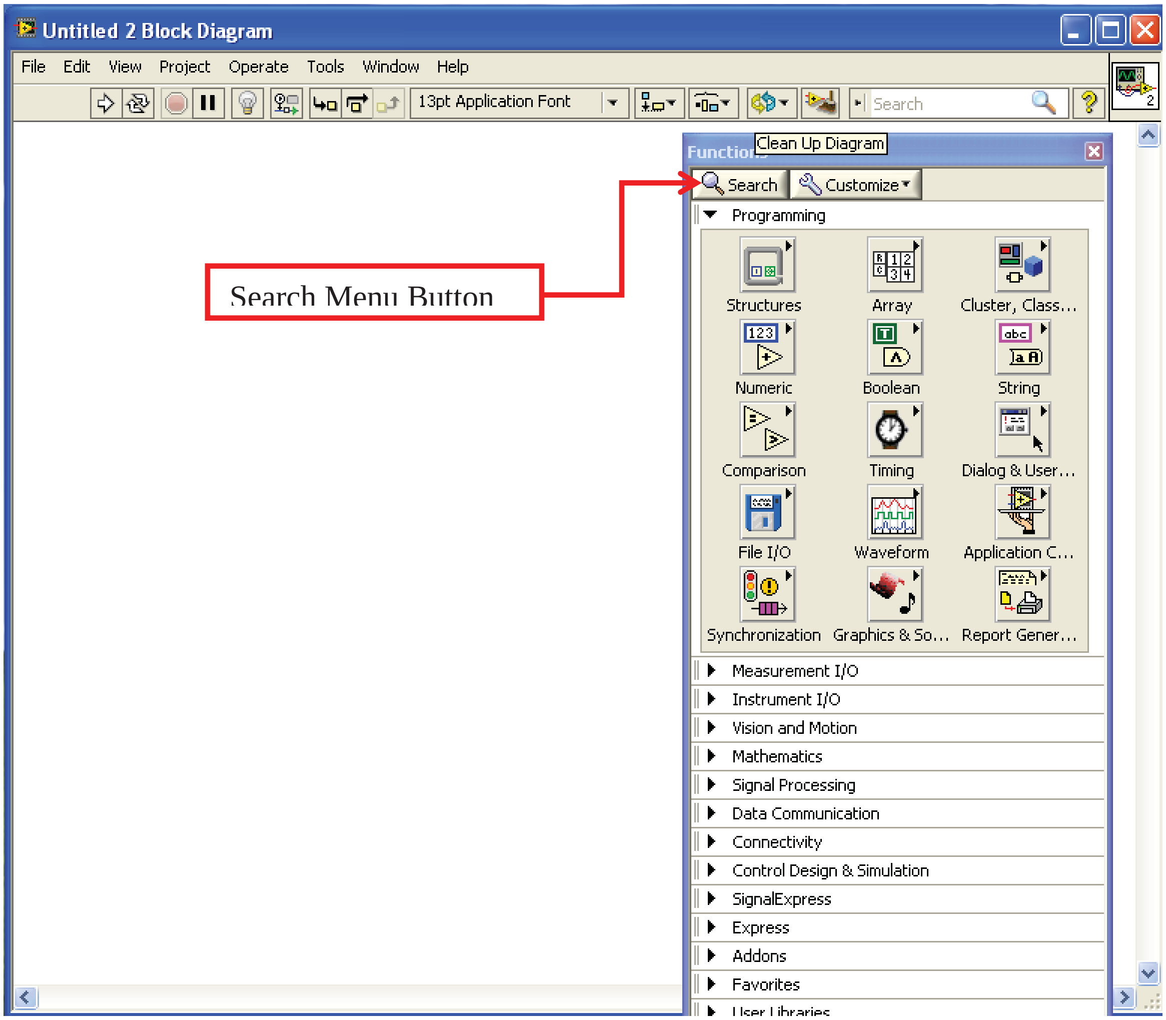

Figure B.8: Shows the functions window opened in the Block Diagram. Also shows the location of the search menu button.

Now that the function window is opened in the Block Diagram, it is time to start configuring functions to acquire pressure data from our three pore pressure transducers. The first function needed is the DAQ Assistant. To find the DAQ Assistant function, click on the "Search" button in the top left corner of the functions and type in "DAQ Assistant". This can be seen in Figure 8 above. Click and drag the DAQ Assistant Input Icon anywhere on the Block Diagram. A window will appear asking what type of signal it is. Click on Acquire Signals. More options will appear under Acquire Signals. Click on Analog Input. Once again more options will appear under Analog Input. Click on Pressure then Pressure(Bridge). Now a new window will appear asking for what channels are going to be used. Click on the plus sign to the left of where it shows the NI 9237 Module. This will allow you to see all the different channels within the NI 9237 Module. Since we will only be using three pore pressure transducers, we only need to select channels ai0, ai1, and ai2. Then click the finish button in the bottom of the window. The window for selecting the channels should look like Figure B.9.

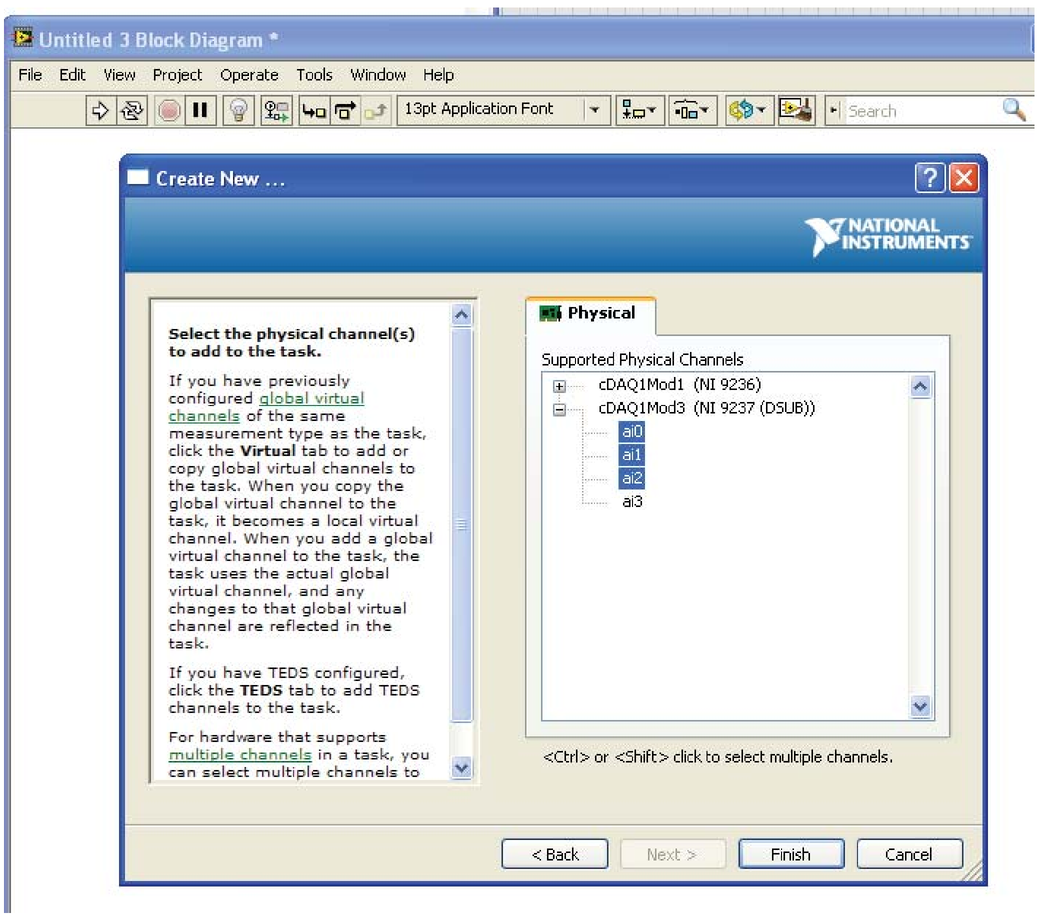

Figure B.9: This figure is showing the three channels that need to be selected to acquire data from the three different pore pressure transducers.

After clicking the finish button, the DAQ Assistant window will appear. On the left hand side of the DAQ Assistant Window, a little box titled “Channel Settings” should appear.

Make sure to highlight all three channels named Pressure_0, Pressure_1, and Pressure_2 so that all three channels can be set up the exact same way. Under the tab "Settings" there are many boxes for user input. Under "Signal Input Range", the maximum input is 150, the minimum input is 0 and the scaled units are pounds per square inch(psi). The bridge type selected should be Full Bridge and the Vex Source selected should be Internal. The Vex Value is 10 volts and the bridge resistance is 1000 ohms(1k ohms). Select <No Scale> for Custom Scaling. Under "Time Settings" the acquisition mode selected should be Continuous Samples, the Samples to Read should be 1613(1.613k) and the Rate should be 1613 hertz(1.613k). Figure B.10 below shows all the user input under the settings tab in the DAQ Assistant window.

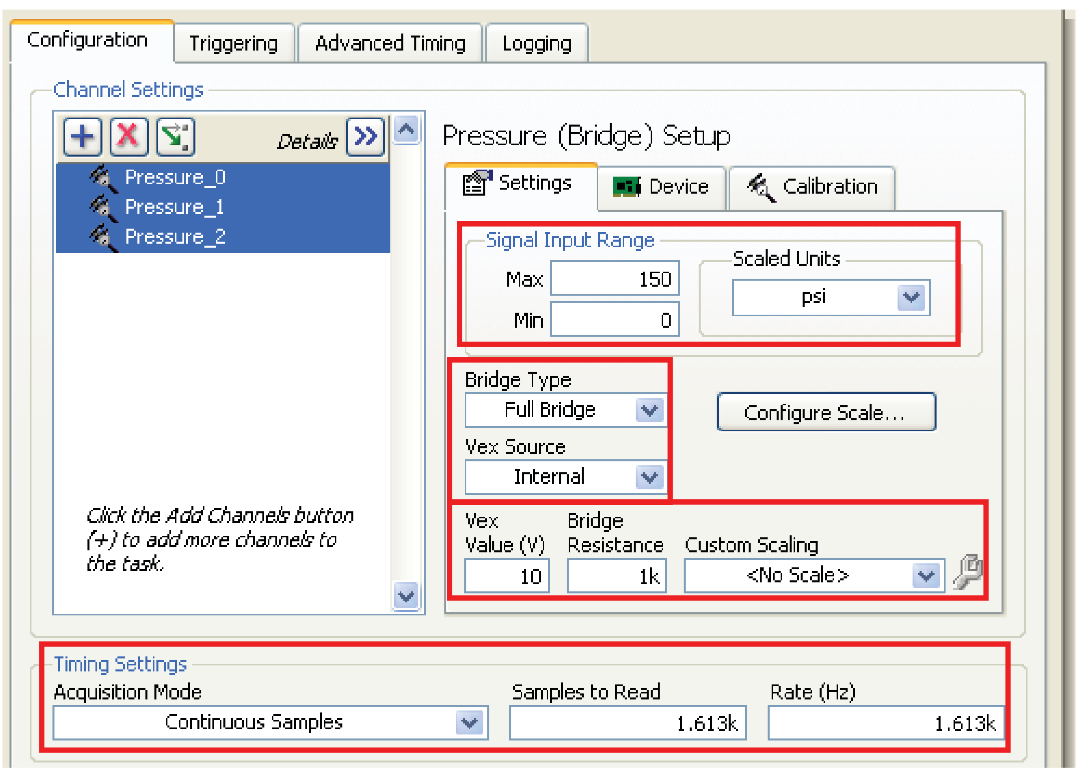

Figure B.10: Shows all the user input that are required for all three channels. By highlighting all three channels at once all the user inputs for all channels will be changed.

After inputing all the user inputs under the settings tab, highlight the first pore pressure transducer (Pressure_0) and click on the “Configure Scale” button which can be seen in Figure B.11.

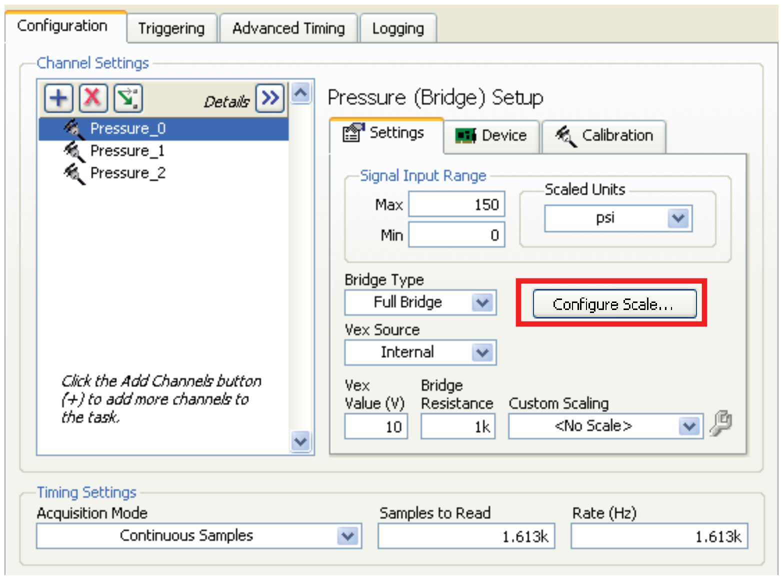

Figure B.11: Shows the location of the configure scale button for pore pressure transducer Pressure_0.

Upon clicking the “Configure Scale” button for the first pore pressure transducer, a new window will appear asking for more user input. Under scale type select “Two-Point Linear”. Under electrical, type in 0 for the “First Value” box and 0.0737 for the “Second Value” box. The 0.0737 value is the sensitivity value that comes from the calibration sheet provided by the pore pressure transducer manufactureer divided by 10. Under physical, type in 0 for the “First Value” box and 1 for the “Second Value” box. Make sure the units under the electrical section is mV/V and units under the physical section are psi. Then click the “OK” button. Figure B.12 shows the exact user input for the first pore pressure transducer.

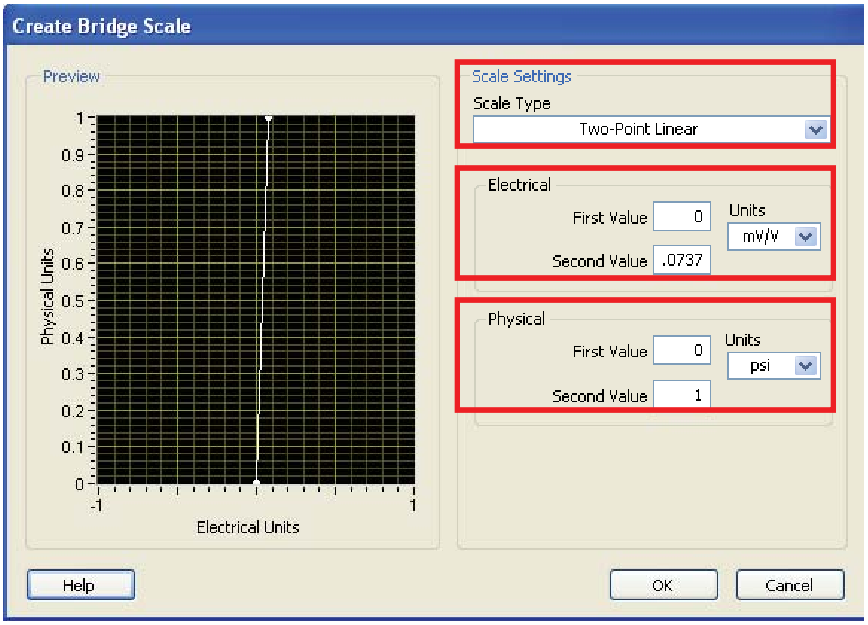

Figure B.12: Shows the user inputs for the first pore pressure transducer(Pressure_0).

Now repeat the same process to configure the scale for the second pore pressure transducer (Pressure_1). Highlight the second pore pressure transducer (Pressure_1) and click on the "Configure Scale" button which can be seen in Figure B.13.

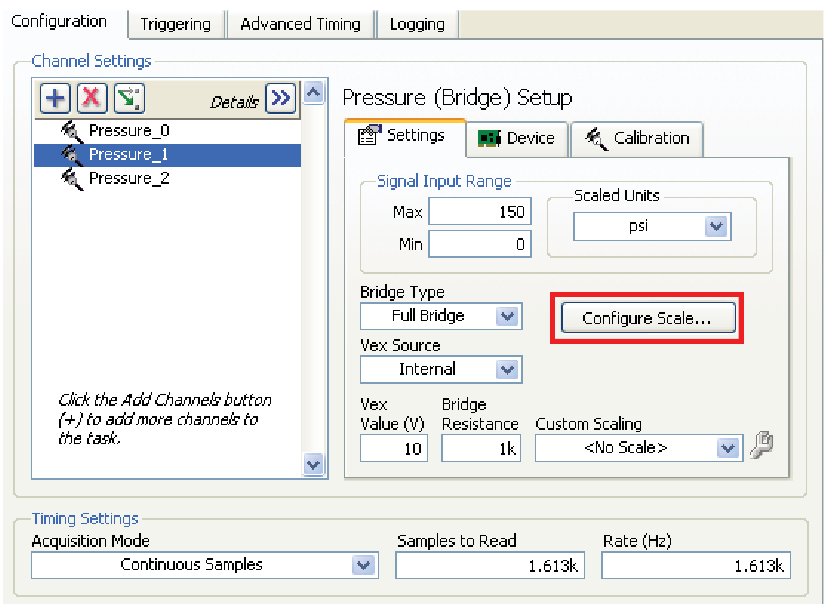

Figure B.13: Shows the location of the configure scale button for pore pressure transducer Pressure_1.

Upon clicking the “Configure Scale” button for the second pore pressure transducer, a new window will appear asking for more user input. Under scale type select “Two-Point Linear”. Under electrical, type in 0 for the “First Value” box and 0.0738 for the “Second Value” box. The 0.0738 value is the sensitivity value that comes from the calibration sheet provided by the pore pressure transducer manufactureer divided by 10. Under physical, type in 0 for the “First Value” box and 1 for the “Second Value” box. Make sure the units under the electrical section is mV/V and units under the physical section are psi. Then click the “OK” button. Figure B.14 shows the exact user input for the second pore pressure transducer.

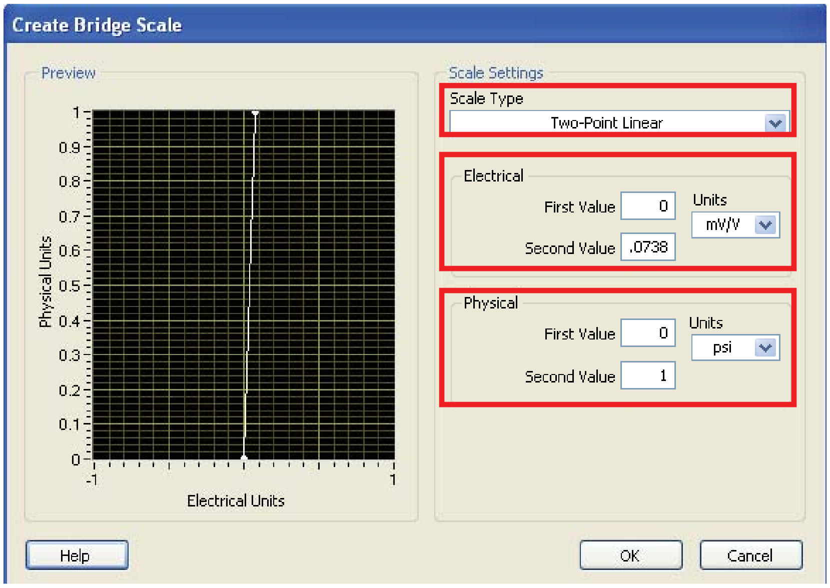

Figure B.14: Shows the user inputs for the second pore pressure transducer (Pressure_1).

Finally repeat this same procedure for the third pore pressure transducer(Pressure_2). Highlight the third pore pressure transducer (Pressure_2) and click on the “Configure Scale” button which can be seen in Figure B.15.

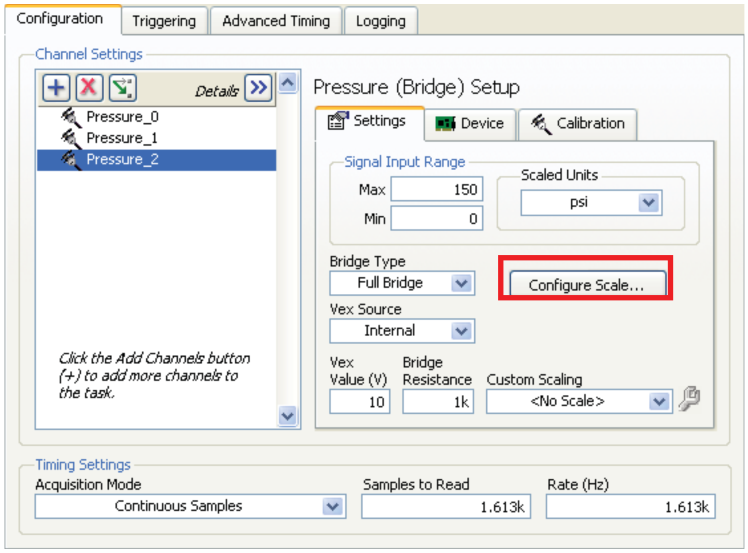

Figure B.15: Shows the location of the configure scale button for pore pressure transducer Pressure_2.

Upon clicking the "Configure Scale" button for the third pore pressure transducer, a new window will appear asking for more user input. Under scale type select "Two-Point Linear". Under electrical, type in 0 for the "First Value" box and 0.0674 for the "Second Value" box. The 0.0674 value is the sensitivity value that comes from the calibration sheet provided by the pore pressure transducer manufactureer divided by 10. Under physical, type in 0 for the "First Value" box and 1 for the "Second Value" box. Make sure the units under the electrical section is mV/V and units under the physical section are psi. Then click the "OK" button. Figure B.16 shows the exact user input for the third pore pressure transducer.

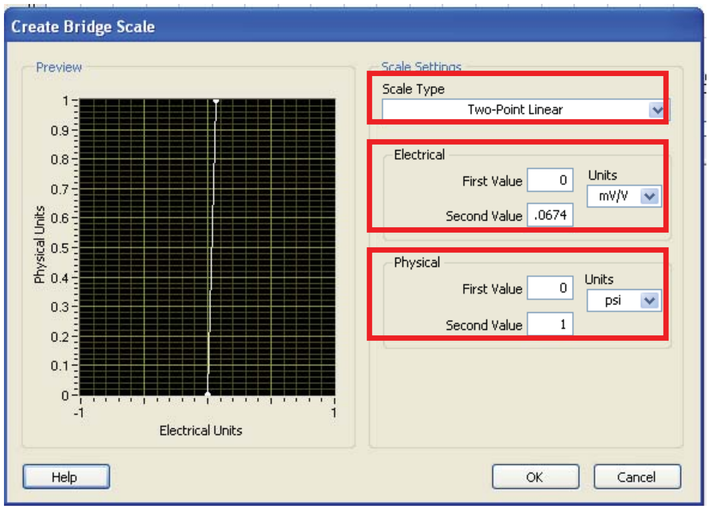

Figure B.16: Shows the user inputs for the third pore pressure transducer (Pressure_2).

Initial Pore Pressure Calibration

Now that all the settings are correct for all three pore pressure transducers the next step in this process is to calibrate all three pore pressure transducers at once. To make sure all three pore pressure transducers get calibrated at the same time, make sure all three channels are selected in the channel settings like in Figure B.17. Then click on the "Calibration" tab inside the DAQ Assistant window. After clicking on the "Calibration" tab the window you should be seeing should look like the figure below.

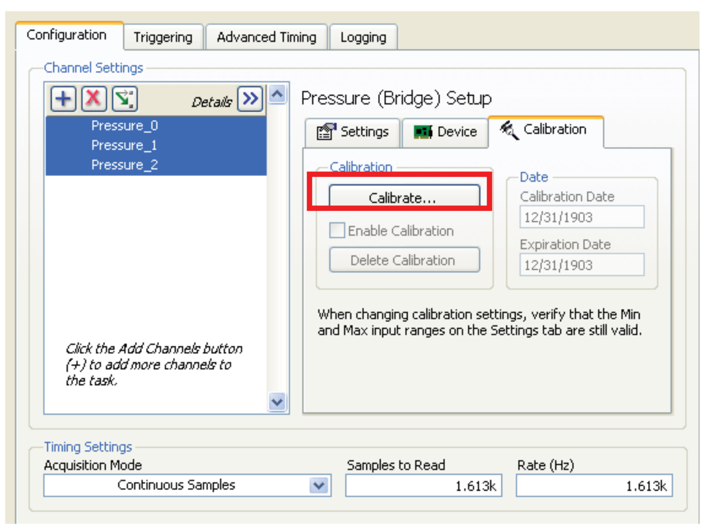

Figure B.17: This figure shows the window that should appear when the "Calibration" tab is clicked within the DAQ Assistant window.

Once this window appears click on the "Calibrate…" button which can be seen in Figure B.17. The user will be asked to type in the calibrator's name then click the "Next" button. Then the Channel Calibration Wizard Window should appear. NI LabVIEW 2012 will ask for additional user input for the number of samples to average and the sample rate at which the software will acquire data. However, it is important to note that the user should not have to input any information since the NI LabVIEW 2012 software has defaulted values for this criteria. The defaulted values for the number of samples to average and the sample rate both are 25000. Figure B.18 shows all the user input, in our case the defaulted values in the Channel Calibration Wizard window.

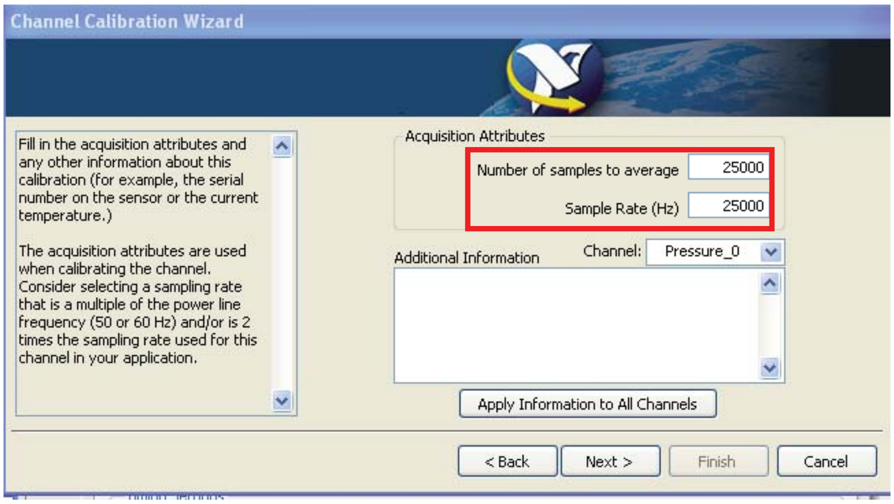

Figure B.18: This figure shows all the user input for the Channel Calibration Wizard window.

After all the user input is in the Channel Calibration Wizard window click the "Next" button to proceed in the calibration process. Now a new user panel within the Channel Calibration Wizard window will appear. There will be a table that will appear in this new user panel. There should be three columns, a Reference column, an Uncalibrated column and a Difference column. You will be able to see this table in Figure B.19. The Reference column is the only column that user input is required.

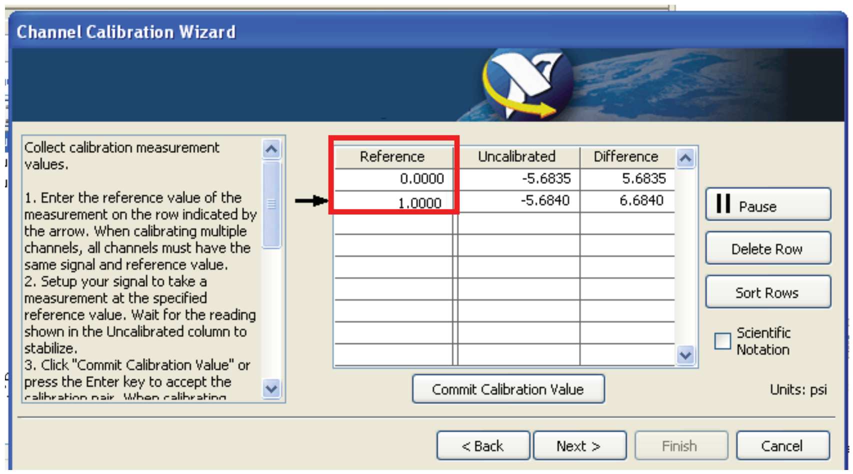

Figure B.19: Shows the values that should be inserted into the Reference Column of the Channel Calibration Wizard window.

Before proceeding any further with the calibration of these three pore pressure transducers within the NI LabVIEW software, one should find a tall narrow cylinder that is approximately 32 inches tall. This cylinder will be used to help in the calibration of these pore pressure transducers. Put a thin piece of tape along the length of the cylinder. Now make marks on this piece of tape that correspond to 0.1 psi increments starting at 0 psi and ending at 1.0 psi. To find the correct heights for different pressure heads use the following equation:

$$\sigma = \gamma H \tag{B.1}$$

Where $\sigma = pressure$, $\gamma = unit\ weight\ of\ water$, and $H = height$

Once all the pressure increments are marked on the calibration test tube, the calibration test tube should look similar to Figure B.20.

Figure B.20: Shows the bottom half of the calibration test cylinder. Also shows the incremental pressure markings along the outside of the calibration test cylinder.

Once all the pressure increments are marked on the calibration test tube, continue with the calibration process within the NI LabVIEW 2012 software. User input is only required in the Reference column of the Channel Calibration Wizard window. Once all three pore pressure are correctly wired like Figure 3 to the NI sub-connector, and the NI sub-connector is plugged into the NI 9237 Module like Figure 5 and the NI 9237 Module is inserted into the correct location of the NI chaise seen in Figure 1, place all three pore pressure transducers at the bottom of the calibration test tube where the test tube marking should indicate 0 psi. In the first row of the Reference column insert the value 0. The Reference column is the so called "theoretical" pressure values that the pore pressure transducers should be reading. The Uncalibrated column shows the raw data values that are coming from the pore pressure transducers. Once the Reference value for the 0 psi marking is inputted, click the "Commit Calibration Value" button at the bottom of the window. Now fill the calibration test tube up with room temperature water to the 1.0 psi marking. In the second row of the Reference column type in the number 1, then click the "Commit Calibration Value" button at the bottom of the window. Click the "Next" button until you see a window that shows a "Finish" button. Once you see the finish button at the bottom of the window click it. Then inside the DAQ Assistant window click the "OK" button in the bottom right hand corner. The Block Diagram should now look similar to Figure B.21.

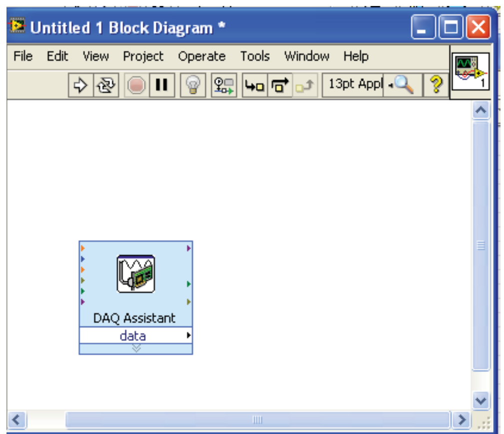

Figure B.21: Shows the DAQ Assistant function icon on the block diagram after being calibrated.

Once the DAQ Assistant function is in the Block Diagram, the next function to insert into the block diagram is the Sample Compression function. To insert the Sample Compression function, go back to the functions tool bar, click on the "Search" button and type in "Sample Compression". When the icon for the function appears, drag and drop the function anywhere in the Block Diagram window. A window will appear after inserting the Sample Compression function. The window that pops up should look like Figure 22. The only user input in this window is the reduction factor. The reduction factor should be set to 1613 and the reduction method should be mean. After these user inputs are inserted click the "OK" button. The outlined red boxes in Figure B.22 show the user where all the user inputs are located for the Sample Compression function.

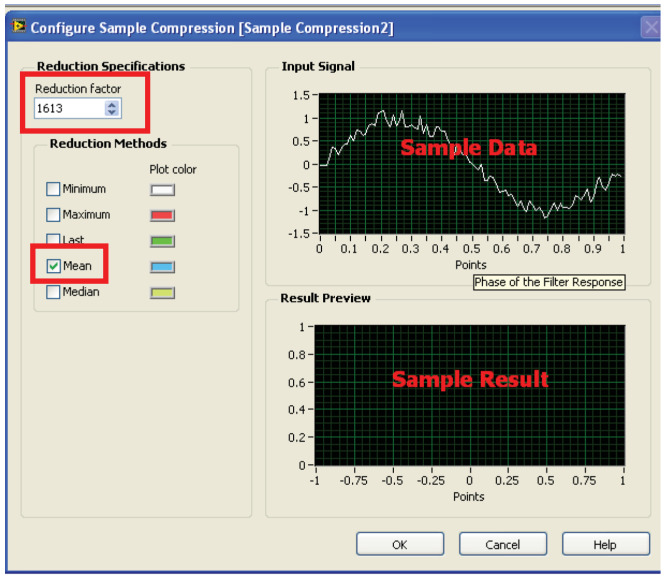

Figure B.22: Shows the window that pops up after inserting the Sample Compression function into the block diagram. The red boxes indicate where user input is required.

The next function to be inserted into the Block Diagram is the Dynamic Data Type function. To insert the Dynamic Data Type function, go back to the functions tool bar, click on the "Search" button and type in "Dynamic Data Type". When the icon for the function appears, drag and drop the function anywhere in the Block Diagram window. A window will appear after inserting the Dynamic Data Type function and should look similar to Figure B.23. Under resulting data type, select "2D array of scalars-columns are channels". Also, under Scalar Data Type select "Floating point numbers (double)". The red outlined boxes show where user inputs are required.

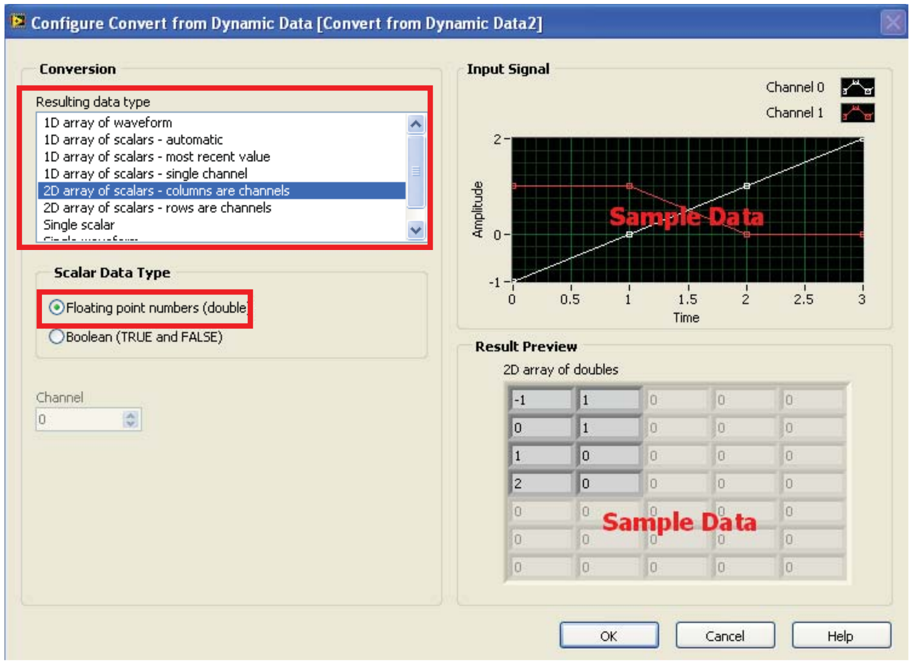

Figure B.23: Shows the window that pops up after inserting the Dynamic Data Type function into the block diagram. The red boxes indicate where user input is required.

Now insert the Insert Into Array function into the Block Diagram. Go back to the functions tool bar, click on the “Search” button and type in “Insert Into Array”. When the icon for the function appears, drag and drop the function anywhere in the Block Diagram window. Do the exact same procedure but for the Output Array. Once all the functions are in the Block Diagram enclose the functions within a while loop so continuous measurements can be taken.

Once all the functions are within the while loop in the Block Diagram, take a look at Figure B.24 to see the correct wiring connections between functions.

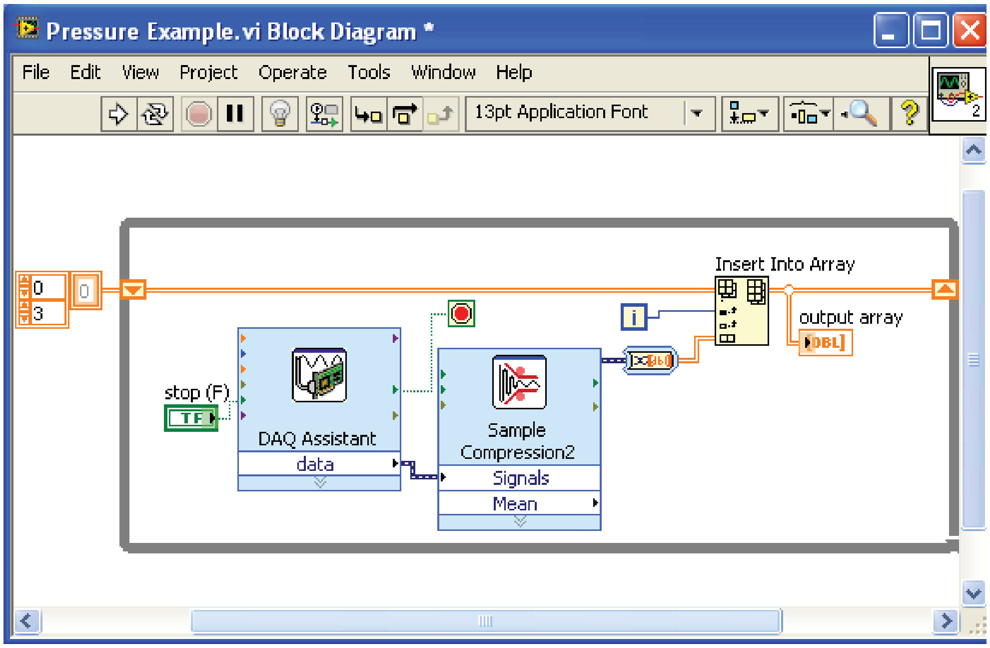

Figure B.24: Shows the correct wiring connections between functions within the Block Diagram.

Once all the connections are made similar to Figure B.24, it's time to start acquiring data from the three pore pressure transducers. By hitting the "Run" button on the Block Diagram, a table of numbers will appear which should look similar to Figure B.25. The first column shows pressure values coming from the pore pressure transducer in channel ai0, the second column shows pressure values coming from the pore pressure transducer in channel ai1, and the third column shows pressure values coming from the pore pressure transducer in channel ai2.

Pressure_0	Pressure_1	Pressure_2
0.228599	0.445427	0.876372
0.228622	0.445428	0.876805
0.228493	0.445357	0.87638
0.228309	0.445419	0.877293
0.228349	0.44499	0.877179
0.228163	0.445032	0.875683
0.228446	0.445141	0.875325
0.228648	0.445245	0.875689
0.228832	0.445143	0.875852

Figure B.25: Shows the table that will appear after hitting the “Run” button in the Block Diagram. This table will appear in the Front Panel.

Secondary Calibration

Once values are appearing in the table, it’s time to verify that these readings from the pore pressure transducers are in fact reading the correct pressure. First secure all three pore pressure transducers with a piece of tape to the bottom of the calibration test tube. Next start filling up the calibration test tube with water, to levels that correspond to the different 0.1 psi incremental markings. First start with 0.1 psi and start working your way up until you reach 1 psi. All three pore pressure transducers should be reading similar numbers at every 0.1 psi increment. If this is not the case, a secondary calibration must be performed to verify that the readings are accurate. The secondary calibration is similar to the first calibration that we performed in NI LabVIEW 2012. The first step in the secondary calibration is to make sure all the pore pressure transducers are at the same moisture content. To make sure all three pore pressure transducers are at the same moisture content, dip them into water for approximately one minute. Once the pore pressure transducers have been sitting in water for one minute, let all three pore pressure transducers air dry for 24-hours. After all three pore pressure transducers are at the same moisture content, secure them to the bottom of the calibration test tube with a piece of tape. Then fill the calibration test tube with water up to the 0.4 psi marking. Run the code in NI LabVIEW 2012 and pick a number from each column that is representative of the pressure readings for each pore pressure transducer. Formulate three tables, one for each pore pressure transducer in Microsoft Excel. All three tables should have a column for LabVIEW pressure readings and a column for theoretical pressure values. The theoretical pressure values are the markings on the side of calibration test tube. Once you have picked a representative number for each pore pressure transducer at the 0.4 psi marking on the calibration test tube, insert values into your Excel table under the LabVIEW pressure readings column. Continue the above procedure at every 0.2 psi marking starting at 0.4 psi and ending at 1.0 psi on the calibration test tube. Thus, you should have a total of 5 different LabVIEW pressure readings and 5 different theoretical pressure values for each pore pressure transducer. Now, plot LabVIEW pressure readings versus theoretical pressure values for all three pore pressure transducers. Insert a linear trendline and display the equation of the trendline on the graph. Each pore pressure transducer will have a separate linear equation.

Now, the raw values that come from LabVIEW have to run through the specific equation for that pore pressure transducer that came from the secondary calibration. Once the secondary calibration is complete, nest the three different pore pressure transducers at different pressure markings inside the calibration test tube. Run the NI LabVIEW software, grab representative pressure readings for all three pore pressure transducers and then calculate the new pressure values by using the equations from the secondary calibration. These new pressure readings should match up to the pressure markings on the calibration test tube where the pore pressure transducers are nested. The pore pressure transducers are now calibrated and ready to be used for application.

Appendix C:

Raw Data

S/D=1	# of PVC Pipes	Pore Pressure-Gauge 13(kPa)	Pore Pressure-Gauge 12(kPa)	Pore Pressure-Gauge 14(kPa)	Avg. Pore Pressure (kPa)	Normalized Pore Pressure-Gauge 13(kPa)	Normalized Pore Pressure-Gauge 12(kPa)	Normalized Pore Pressure-Gauge 14(kPa)	Normalized Avg. Pore Pressure (kPa)
Run 0	0	5.184	5.172	5.212	5.189	1	1	1	1
Run 1	3	5.071	5.092	5.183	5.115	0.97820216	0.984532096	0.994435917	0.985739979
Run2	4	4.961	4.976	5.014	4.984	0.956983025	0.962103635	0.962010744	0.96036742
Run 3	5	4.903	4.894	4.997	4.931	0.945794753	0.946249033	0.958749041	0.950282631
Run 4	6	4.712	4.641	4.771	4.708	0.908950617	0.897331787	0.915387567	0.907245632
Run 5	7	4.498	4.568	4.638	4.568	0.867669753	0.883217324	0.889869532	0.880267215
Run 6	8	4.427	4.392	4.421	4.413	0.853973765	0.849187935	0.848234843	0.850462487
Run 7	9	4.001	4.073	4.053	4.042	0.77179784	0.787509667	0.77762855	0.778969681
Run 8	10	3.682	3.831	3.761	3.758	0.710262346	0.740719258	0.721603991	0.724177801
Run 9	11	3.579	3.637	3.719	3.645	0.690393519	0.70320959	0.713545664	0.702402364
Run 10	12	3.41	3.373	3.692	3.492	0.65779321	0.652165507	0.708365311	0.672854573
Run 11	13	3.311	3.296	3.437	3.348	0.638695988	0.637277649	0.659439754	0.645169579
Run 12	14	3.077	3.059	3.268	3.135	0.593557099	0.591453983	0.627014582	0.604059609
Run 13	15	2.891	2.739	2.971	2.867	0.557677469	0.529582367	0.570030698	0.552479445
Run 14	16	2.599	2.689	2.763	2.684	0.501350309	0.519914927	0.530122794	0.517150565
Run 15	17	2.471	2.567	2.618	2.552	0.476658951	0.496326373	0.502302379	0.491778006
Run 16	18	2.072	2.121	2.225	2.139	0.399691358	0.410092807	0.426899463	0.41225591
Run 17	19	1.832	1.825	1.962	1.873	0.353395062	0.352861562	0.376438987	0.360932682
Run 18	20	1.794	1.818	1.915	1.842	0.346064815	0.351508121	0.367421335	0.355023124
Run 19	21	1.633	1.800	1.834	1.756	0.315007716	0.348027842	0.351880276	0.338322199
Run 20	22	1.625	1.641	1.799	1.688	0.313464506	0.317285383	0.345165004	0.325346865
Run 21	23	1.504	1.463	1.623	1.530	0.290123457	0.282869296	0.311396777	0.29483556
Run 22	24	1.301	1.360	1.51	1.390	0.250964506	0.26295437	0.28971604	0.267921377
Run 23	25	1.267	1.289	1.4	1.319	0.244405864	0.249226605	0.268610898	0.254110997
Run 24	26	1.225	1.243	1.273	1.247	0.236304012	0.24033256	0.244244052	0.240300617
Run 25	27	1.2	1.212	1.244	1.219	0.231481481	0.234338747	0.238679969	0.234840699

S/D=1	Slats		PVC Side By Side		PVC Pipe-Primary and Secondary-Touching		PVC Pipe-Primary and Secondary-Spacing of 0.5*Dia. of Pipe	
	Normalized Grouted Area Agc/Atotal	Area Replacement Ratio-Multiply by the inverse of Maximum Agc/Atotal	Normalized Grouted Area Agc/Atotal	Area Replacement Ratio-Multiply by the inverse of Maximum Agc/Atotal	Normalized Grouted Area Agc/Atotal	Area Replacement Ratio-Multiply by the inverse of Maximum Agc/Atotal	Normalized Grouted Area Agc/Atotal	Area Replacement Ratio-Multiply by the inverse of Maximum Agc/Atotal
Run 0	0	0	0	0	0	0	0	0
Run 1	0.111111111	0.111111111	0.087266463	0.111111111	0.043633231	0.111111111	0.034906585	0.111111111
Run2	0.148148148	0.148148148	0.116355283	0.148148148	0.058177642	0.148148148	0.046542113	0.148148148
Run 3	0.185185185	0.185185185	0.145444104	0.185185185	0.072722052	0.185185185	0.058177642	0.185185185
Run 4	0.222222222	0.222222222	0.174532925	0.222222222	0.087266463	0.222222222	0.06981317	0.222222222
Run 5	0.259259259	0.259259259	0.203621746	0.259259259	0.101810873	0.259259259	0.081448698	0.259259259
Run 6	0.296296296	0.296296296	0.232710567	0.296296296	0.116355283	0.296296296	0.093084227	0.296296296
Run 7	0.333333333	0.333333333	0.261799388	0.333333333	0.130899694	0.333333333	0.104719755	0.333333333
Run 8	0.37037037	0.37037037	0.290888209	0.37037037	0.145444104	0.37037037	0.116355283	0.37037037
Run 9	0.407407407	0.407407407	0.31997703	0.407407407	0.159988515	0.407407407	0.127990812	0.407407407
Run 10	0.444444444	0.444444444	0.34906585	0.444444444	0.174532925	0.444444444	0.13962634	0.444444444
Run 11	0.481481481	0.481481481	0.378154671	0.481481481	0.189077336	0.481481481	0.151261869	0.481481481
Run 12	0.518518519	0.518518519	0.407243492	0.518518519	0.203621746	0.518518519	0.162897397	0.518518519
Run 13	0.555555556	0.555555556	0.436332313	0.555555556	0.218166156	0.555555556	0.174532925	0.555555556
Run 14	0.592592593	0.592592593	0.465421134	0.592592593	0.232710567	0.592592593	0.186168454	0.592592593
Run 15	0.62962963	0.62962963	0.494509955	0.62962963	0.247254977	0.62962963	0.197803982	0.62962963
Run 16	0.666666667	0.666666667	0.523598776	0.666666667	0.261799388	0.666666667	0.20943951	0.666666667
Run 17	0.703703704	0.703703704	0.552687596	0.703703704	0.276343798	0.703703704	0.221075039	0.703703704
Run 18	0.740740741	0.740740741	0.581776417	0.740740741	0.290888209	0.740740741	0.232710567	0.740740741
Run 19	0.777777778	0.777777778	0.610865238	0.777777778	0.305432619	0.777777778	0.244346095	0.777777778
Run 20	0.814814815	0.814814815	0.639954059	0.814814815	0.31997703	0.814814815	0.255981624	0.814814815
Run 21	0.851851852	0.851851852	0.66904288	0.851851852	0.33452144	0.851851852	0.267617152	0.851851852
Run 22	0.888888889	0.888888889	0.698131701	0.888888889	0.34906585	0.888888889	0.27925268	0.888888889
Run 23	0.925925926	0.925925926	0.727220522	0.925925926	0.363610261	0.925925926	0.290888209	0.925925926
Run 24	0.962962963	0.962962963	0.756309343	0.962962963	0.378154671	0.962962963	0.302523737	0.962962963
Run 25	1	1	0.785398163	1	0.392699082	1	0.314159265	1

S/D=1	Qout (mL)	Time (mins)	Length Interval(m)	Flow Loss (Qout/Time/Length) (L/min/meter)	Normalized Flow Loss	Average Lugeon Value	Normalized Average Lugeon Value	Lugeon Value-Gauge 13	Lugeon Value-Gauge 12	Lugeon Value-Gauge 14
Run 0	5519	25	0.46	0.479913043	1	92.48067385	1	92.57581857	92.79061165	92.0784811
Run 1	5383	25	0.46	0.468086957	0.975357855	91.50663818	0.989467684	92.30663706	91.92595376	90.31197309
Run2	5261	25	0.46	0.457478261	0.953252401	91.79551753	0.992591357	92.21492862	91.93694953	91.24017967
Run 3	5225	25	0.46	0.454347826	0.94672948	92.1348843	0.996260953	92.66731105	92.83772499	90.92411969
Run 4	4908	25	0.46	0.426782609	0.889291538	90.65051162	0.980210328	90.57355872	91.9591917	89.45349166
Run 5	4651	25	0.46	0.404434783	0.842725131	88.53651108	0.957351492	89.91435807	88.53651108	87.20025498
Run 6	4421	25	0.46	0.384434783	0.801050915	87.10757914	0.941900351	86.83866786	87.53068821	86.95652174
Run 7	4082	25	0.46	0.354956522	0.739626744	87.80980995	0.949493622	88.7169512	87.14866726	87.57871249
Run 8	3720	25	0.46	0.323478261	0.674035151	86.07723812	0.930759201	87.85395461	84.43702972	86.00857774
Run 9	3617	25	0.46	0.314521739	0.65537235	86.28854297	0.933044055	87.87978182	86.47834455	84.5715889
Run 10	3499	25	0.46	0.30426087	0.633991665	87.13915119	0.942241742	89.22606146	90.20482347	82.41085308
Run 11	3200	25	0.46	0.27826087	0.579815184	83.11256558	0.89870199	84.04133783	84.42380751	80.96039266
Run 12	3006	25	0.46	0.261391304	0.544663888	83.38727276	0.901672418	84.95005016	85.4499197	79.98509925
Run 13	2573	25	0.46	0.22373913	0.466207646	78.03945952	0.843846139	77.39160513	81.68642951	75.30768443
Run 14	2428	25	0.46	0.211130435	0.439934771	78.67237664	0.850689916	81.23525771	78.51633871	76.41347622
Run 15	2284	25	0.46	0.198608696	0.413843088	77.824724	0.841524188	80.37583798	77.36996325	75.86275617
Run 16	1913	25	0.46	0.166347826	0.346620765	77.75685233	0.840790287	80.28369985	78.42896091	74.7630679
Run 17	1624	25	0.46	0.141217391	0.294256206	75.39636482	0.815266171	77.08372888	77.3793925	71.97624429
Run 18	1567	25	0.46	0.13626087	0.283928248	73.96102926	0.799745787	75.95366197	74.95097336	71.15450108
Run 19	1484	25	0.46	0.129043478	0.268889292	73.50112679	0.794772829	79.02233819	71.69082126	70.36176568
Run 20	1460	25	0.46	0.126956522	0.264540678	75.19636036	0.813103508	78.1270903	77.36533927	70.57060686
Run 21	1320	25	0.46	0.114782609	0.239173763	75.02131287	0.811210708	76.31822387	78.4570121	70.72249458
Run 22	1180	25	0.46	0.102608696	0.213806849	73.8015073	0.798020865	78.86909735	75.44757033	67.95277858
Run 23	1144	25	0.46	0.099478261	0.207283928	75.43851937	0.815721991	78.51480732	77.1747563	71.05590062
Run 24	1113	25	0.46	0.096782609	0.201666969	77.61235661	0.839227845	79.00621118	77.8621148	76.02718672
Run 25	1090	25	0.46	0.094782609	0.197499547	77.77566359	0.840993695	78.98550725	78.20347252	76.19180763

Figure C.1: Raw Data from S/D=1, Unit weight = 12.56 kN/m^3

S/D=1.18												Slats		PVC Side By Side		PVC Pipe-Primary and Secondary-Touching		PVC Pipe-Primary and Secondary-Spacing of 0.5*Dia. of Pipe	
	# of PVC Pipes	Pore Pressure-Gauge 13(kPa)	Pore Pressure-Gauge 12(kPa)	Pore Pressure-Gauge 14(kPa)	Avg. Pore Pressure (kPa)	Normalized Pore Pressure-Gauge 13(kPa)	Normalized Pore Pressure-Gauge 12(kPa)	Normalized Pore Pressure-Gauge 14(kPa)	Normalized Avg. Pore Pressure (kPa)			Normalized Grouted Area Agc/Atotal	Area Replacement Ratio-Multiply by the inverse of Maximum Agc/Atotal	Normalized Grouted Area Agc/Atotal	Area Replacement Ratio-Multiply by the inverse of Maximum Agc/Atotal	Normalized Grouted Area Agc/Atotal	Area Replacement Ratio-Multiply by the inverse of Maximum Agc/Atotal	Normalized Grouted Area Agc/Atotal	Area Replacement Ratio-Multiply by the inverse of Maximum Agc/Atotal
Run 0	0	5.183	5.233	5.212	5.209	1	1	1	1			0	0	0	0	0	0	0	0
Run 1	3	5.173	5.21	5.189	5.191	0.998070615	0.995604816	0.995587107	0.996416688			0.111111111	0.130434783	0.087266463	0.130434783	0.043633231	0.130434783	0.034906585	0.130434783
Run2	4	5.108	5.118	5.103	5.110	0.985529616	0.978024078	0.979086723	0.980867673			0.148148148	0.173913043	0.116355283	0.173913043	0.058177642	0.173913043	0.046542113	0.173913043
Run 3	5	5.068	5.074	5.062	5.068	0.977812078	0.969615899	0.971220261	0.972869209			0.185185185	0.217391304	0.145444104	0.217391304	0.072722052	0.217391304	0.058177642	0.217391304
Run 4	6	4.881	4.893	4.823	4.866	0.941732587	0.935027709	0.925364543	0.934028666			0.222222222	0.260869565	0.174532925	0.260869565	0.087266463	0.260869565	0.06981317	0.260869565
Run 5	7	4.564	4.602	4.658	4.608	0.880571098	0.879419071	0.89370683	0.884566163			0.259259259	0.304347826	0.203621746	0.304347826	0.101810873	0.304347826	0.081448698	0.304347826
Run 6	8	4.498	4.528	4.504	4.510	0.86783716	0.865278043	0.864159632	0.865753775			0.296296296	0.347826087	0.232710567	0.347826087	0.116355283	0.347826087	0.093084227	0.347826087
Run 7	9	4.164	4.173	4.199	4.179	0.803395717	0.797439327	0.805640829	0.802149987			0.333333333	0.391304348	0.261799388	0.391304348	0.130899694	0.391304348	0.104719755	0.391304348
Run 8	10	3.923	3.932	3.915	3.923	0.75689755	0.751385439	0.75115119	0.753135398			0.37037037	0.434782609	0.290888209	0.434782609	0.145444104	0.434782609	0.116355283	0.434782609
Run 9	11	3.724	3.705	3.763	3.731	0.718502798	0.708006879	0.721987721	0.716150499			0.407407407	0.47826087	0.31997703	0.47826087	0.159988515	0.47826087	0.127990812	0.47826087
Run 10	12	3.599	3.607	3.611	3.606	0.694385491	0.689279572	0.692824252	0.692155106			0.444444444	0.52173913	0.34906585	0.52173913	0.174532925	0.52173913	0.13962634	0.52173913
Run 11	13	3.501	3.523	3.581	3.535	0.675477523	0.673227594	0.687068304	0.678589711			0.481481481	0.565217391	0.378154671	0.565217391	0.189077336	0.565217391	0.151261869	0.565217391
Run 12	14	3.232	3.264	3.31	3.269	0.623577079	0.623733996	0.635072909	0.627463527			0.518518519	0.608695652	0.407243492	0.608695652	0.203621746	0.608695652	0.162897397	0.608695652
Run 13	15	3.042	3.109	3.057	3.069	0.586918773	0.594114275	0.586531082	0.589198874			0.555555556	0.652173913	0.436332313	0.652173913	0.218166156	0.652173913	0.174532925	0.652173913
Run 14	16	2.854	2.913	2.823	2.863	0.550646344	0.55665966	0.541634689	0.549654466			0.592592593	0.695652174	0.465421134	0.695652174	0.232710567	0.695652174	0.186168454	0.695652174
Run 15	17	2.478	2.546	2.552	2.525	0.478101486	0.486527804	0.489639294	0.484770924			0.62962963	0.739130435	0.494509955	0.739130435	0.247254977	0.739130435	0.197803982	0.739130435
Run 16	18	2.135	2.162	2.069	2.122	0.411923596	0.413147334	0.396968534	0.40734579			0.666666667	0.782608696	0.523598776	0.782608696	0.261799388	0.782608696	0.20943951	0.782608696
Run 17	19	1.863	1.85	1.856	1.856	0.359444337	0.353525702	0.356101305	0.356347581			0.703703704	0.826086957	0.552687596	0.826086957	0.276343798	0.826086957	0.221075039	0.826086957
Run 18	20	1.744	1.735	1.75	1.743	0.336484661	0.33154978	0.335763622	0.334591758			0.740740741	0.869565217	0.581776417	0.869565217	0.290888209	0.869565217	0.232710567	0.869565217
Run 19	21	1.63	1.634	1.655	1.640	0.314489678	0.312249188	0.317536454	0.314755567			0.777777778	0.913043478	0.610865238	0.913043478	0.305432619	0.913043478	0.244346095	0.913043478
Run 20	22	1.591	1.603	1.617	1.604	0.306965078	0.306325244	0.310245587	0.307844894			0.814814815	0.956521739	0.639954059	0.956521739	0.31997703	0.956521739	0.255981624	0.956521739
Run 21	23	1.549	1.571	1.556	1.559	0.298861663	0.300210204	0.298541827	0.299206552			0.851851852	1	0.66904288	1	0.33452144	1	0.267617152	1

	Qout (mL)	Time (mins)	Length Interval (m)	Flow Loss (Qout/Time/Length) (L/min/meter)	Normalized Flow Loss	Lugeon Value	Normalized Average Lugeon Value	Lugeon Value-Gauge 13	Lugeon Value-Gauge 12	Lugeon Value-Gauge 14
Run 0	5579	25	0.46	0.485130435	1	93.12716306	1	93.60031541	92.70598792	93.0795155
Run 1	5571	25	0.46	0.484434783	0.998566051	93.328047	1.002157093	93.646778	92.98172411	93.35802324
Run2	5541	25	0.46	0.481826087	0.993188744	94.2969705	1.012561399	94.32773825	94.14343239	94.42016205
Run 3	5444	25	0.46	0.473391304	0.975802115	93.40791325	1.003014697	93.40791325	93.29745848	93.51862986
Run 4	5116	25	0.46	0.444869565	0.917010217	91.43034155	0.98177521	91.14311928	90.91959232	92.23918002
Run 5	4710	25	0.46	0.409565217	0.844237319	88.88134058	0.954408334	89.73821591	88.99722238	87.92726865
Run 6	4693	25	0.46	0.408086957	0.841190177	90.48491275	0.971627501	90.72631314	90.12521125	90.60545216
Run 7	4300	25	0.46	0.373913043	0.770747446	89.48142393	0.960852033	89.79660026	89.60293398	89.04811705
Run 8	3846	25	0.46	0.334434783	0.689370855	85.24251044	0.915334556	85.24975341	85.05462426	85.42295469
Run 9	3781	25	0.46	0.328782609	0.677720022	88.12971999	0.946337428	88.28748891	88.74024526	87.37247109
Run 10	3516	25	0.46	0.30573913	0.63022047	84.79406409	0.910519136	84.95113377	84.76271983	84.66882598
Run 11	3418	25	0.46	0.297217391	0.612654598	84.07846996	0.902835083	84.89499894	84.36485703	82.99843376
Run 12	3178	25	0.46	0.276347826	0.569636136	84.54451135	0.907839438	85.50365906	84.66538789	83.48876921
Run 13	2979	25	0.46	0.259043478	0.533966661	84.39731047	0.906258794	85.15564703	83.32051408	84.73780774
Run 14	2711	25	0.46	0.23573913	0.485929378	82.33031331	0.884063367	82.59955516	80.92658099	83.50659952
Run 15	2348	25	0.46	0.204173913	0.420863954	80.85028236	0.868170786	82.39463803	80.1939957	80.00545182
Run 16	1926	25	0.46	0.167478261	0.345223158	78.92472237	0.847494112	78.44415029	77.46450549	80.94647698
Run 17	1689	25	0.46	0.146869565	0.302742427	79.11809942	0.849570596	78.83497865	79.38895417	79.13230885
Run 18	1600	25	0.46	0.139130435	0.286789747	79.82239517	0.857133328	79.77662545	80.19045232	79.50310559
Run 19	1508	25	0.46	0.131130435	0.270299337	79.97383703	0.858759511	80.4481195	80.25118408	79.23289111
Run 20	1475	25	0.46	0.12826087	0.264384298	79.97975654	0.858823075	80.61651135	80.01301907	79.32026566
Run 21	1462	25	0.46	0.127130435	0.262054132	81.56358091	0.87583019	82.0725854	80.92325575	81.70336426

Figure C.2: Raw Data from S/D=1.18, Unit weight= 12.56 kN/m^3

S/D=1.45										Slats		PVC Side By Side	
	# of PVC Pipes	Pore Pressure-Gauge 13(kPa)	Pore Pressure-Gauge 12(kPa)	Pore Pressure-Gauge 14(kPa)	Avg. Pore Pressure (kPa)	Normalized Pore Pressure-Gauge 13(kPa)	Normalized Pore Pressure-Gauge 12(kPa)	Normalized Pore Pressure-Gauge 14(kPa)	Normalized Avg. Pore Pressure (kPa)	Normalized Grouted Area Agc/Atotal	Area Replacement Ratio-Multiply by the inverse of Maximum Agc/Atotal	Normalized Grouted Area Agc/Atotal	Area Replacement Ratio-Multiply by the inverse of Maximum Agc/Atotal
Run 0	0	5.224	5.231	5.218	5.224	1	1	1	1	0	0	0	0
Run 1	3	5.158	5.213	5.201	5.191	0.987366003	0.996558975	0.996742047	0.993555797	0.111111111	0.157894737	0.087266463	0.157894737
Run2	4	5.093	5.135	5.171	5.133	0.97492343	0.981647868	0.990992718	0.982517706	0.148148148	0.210526316	0.116355283	0.210526316
Run 3	5	5.121	5.121	5.139	5.127	0.980283308	0.978971516	0.9848601	0.981369234	0.185185185	0.263157895	0.145444104	0.263157895
Run 4	6	4.835	4.823	4.803	4.820	0.925535988	0.922003441	0.920467612	0.922669559	0.222222222	0.315789474	0.174532925	0.315789474
Run 5	7	4.631	4.595	4.608	4.611	0.886485452	0.878417129	0.883096972	0.882664455	0.259259259	0.368421053	0.203621746	0.368421053
Run 6	8	4.523	4.498	4.527	4.516	0.865811639	0.859873829	0.867573783	0.864416512	0.296296296	0.421052632	0.232710567	0.421052632
Run 7	9	4.209	4.269	4.302	4.260	0.805704441	0.816096349	0.824453814	0.815415045	0.333333333	0.473684211	0.261799388	0.473684211
Run 8	10	3.984	4.097	4.003	4.028	0.762633997	0.783215446	0.767152166	0.771007465	0.37037037	0.526315789	0.290888209	0.526315789
Run 9	11	3.706	3.723	3.794	3.741	0.70941807	0.711718601	0.727098505	0.716072226	0.407407407	0.578947368	0.31997703	0.578947368
Run 10	12	3.673	3.698	3.71	3.694	0.703101072	0.7069394	0.711000383	0.707012059	0.444444444	0.631578947	0.34906585	0.631578947
Run 11	13	3.407	3.472	3.506	3.462	0.652182236	0.663735423	0.671904944	0.662604479	0.481481481	0.684210526	0.378154671	0.684210526
Run 12	14	3.354	3.393	3.362	3.370	0.642036753	0.648633149	0.644308164	0.644994577	0.518518519	0.736842105	0.407243492	0.736842105
Run 13	15	3.176	3.197	3.174	3.182	0.607963247	0.611164213	0.608279034	0.609136732	0.555555556	0.789473684	0.436332313	0.789473684
Run 14	16	2.85	2.813	2.888	2.850	0.545558959	0.537755687	0.553468762	0.545587954	0.592592593	0.842105263	0.465421134	0.842105263
Run 15	17	2.547	2.51	2.582	2.546	0.487557427	0.479831772	0.494825604	0.487398711	0.62962963	0.894736842	0.494509955	0.894736842
Run 16	18	2.026	2.001	2.033	2.020	0.387825421	0.382527241	0.389612878	0.386652204	0.666666667	0.947368421	0.523598776	0.947368421
Run 17	19	1.893	1.824	1.856	1.858	0.362366003	0.348690499	0.355691836	0.355579659	0.703703704	1	0.552687596	1

	PVC Pipe-Primary and Secondary-Touching		PVC Pipe-Primary and Secondary-Spacing of 0.5*Dia. of Pipe											
	Normalized Grouted Area Agc/Atotal	Area Replacement Ratio-Multiply by the inverse of Maximum Agc/Atotal	Normalized Grouted Area Agc/Atotal	Area Replacement Ratio-Multiply by the inverse of Maximum Agc/Atotal	Qout (mL)	Time (mins)	Length Interval(m)	Flow Loss (Qout/Time/Length) (L/min/meter)	Normalized Flow Loss	Lugeon Value	Normalized Average Lugeon Value	Lugeon Value-Gauge 13	Lugeon Value-Gauge 12	Lugeon Value-Gauge 14
Run 0	0	0	0	0	5595	25	0.46	0.486521739	1	93.2391221	1	93.13203276	93.00740568	93.2391221
Run 1	0.043633231	0.157894737	0.034906585	0.157894737	5553	25	0.46	0.482869565	0.992493298	92.8416776	0.995737363	93.61565824	92.62796187	92.8416776
Run2	0.058177642	0.210526316	0.046542113	0.210526316	5499	25	0.46	0.478173913	0.982841823	92.47223227	0.991775021	93.8884573	93.12052834	92.47223227
Run 3	0.072722052	0.263157895	0.058177642	0.263157895	5468	25	0.46	0.475478261	0.977301162	92.5234989	0.992324861	92.84871331	92.84871331	92.5234989
Run 4	0.087266463	0.315789474	0.06981317	0.315789474	5089	25	0.46	0.442521739	0.909562109	92.13444496	0.988152214	91.52466166	91.75238215	92.13444496
Run 5	0.101810873	0.368421053	0.081448698	0.368421053	4800	25	0.46	0.417391304	0.857908847	90.57971014	0.97147751	90.12984331	90.83597483	90.57971014
Run 6	0.116355283	0.421052632	0.093084227	0.421052632	4650	25	0.46	0.404347826	0.831099196	89.31915752	0.957957942	89.39814859	89.89502581	89.31915752
Run 7	0.130899694	0.473684211	0.104719755	0.473684211	4321	25	0.46	0.37573913	0.772296693	87.3405696	0.936737366	89.270404	88.0157251	87.3405696
Run 8	0.145444104	0.526315789	0.116355283	0.526315789	4156	25	0.46	0.361391304	0.742806077	90.280116	0.968264329	90.71066876	88.20876357	90.280116
Run 9	0.159988515	0.578947368	0.127990812	0.578947368	3796	25	0.46	0.330086957	0.678462913	87.00236071	0.933110037	89.06825594	88.66155158	87.00236071
Run 10	0.174532925	0.631578947	0.13962634	0.631578947	3544	25	0.46	0.308173913	0.633422699	83.06574476	0.890889392	83.90250832	83.33529287	83.06574476
Run 11	0.189077336	0.684210526	0.151261869	0.684210526	3377	25	0.46	0.293652174	0.60357462	83.75703762	0.898303585	86.19083473	84.57723903	83.75703762
Run 12	0.203621746	0.736842105	0.162897397	0.736842105	3228	25	0.46	0.280695652	0.5769437	83.49067584	0.895446825	83.68981878	82.72786684	83.49067584
Run 13	0.218166156	0.789473684	0.174532925	0.789473684	3017	25	0.46	0.262347826	0.539231457	82.65526972	0.886487001	82.6032198	82.06062749	82.65526972
Run 14	0.232710567	0.842105263	0.186168454	0.842105263	2688	25	0.46	0.23373913	0.480428954	80.93460195	0.868032647	82.01372998	83.09247438	80.93460195
Run 15	0.247254977	0.894736842	0.197803982	0.894736842	2442	25	0.46	0.212347826	0.436461126	82.24160577	0.882050409	83.37174169	84.60072752	82.24160577
Run 16	0.261799388	0.947368421	0.20943951	0.947368421	1920	25	0.46	0.166956522	0.343163539	82.12322761	0.88078079	82.40697026	83.4365426	82.12322761
Run 17	0.276343798	1	0.221075039	1	1771	25	0.46	0.154	0.316532618	82.97413793	0.889906898	81.35235077	84.42982456	82.97413793

Figure C.3: Raw Data from S/D=1.45, Unit weight= 12.56 kN/m^3

S/D=1.62									
	# of PVC Pipes	Pore Pressure-Gauge 13(kPa)	Pore Pressure-Gauge 12(kPa)	Pore Pressure-Gauge 14(kPa)	Avg. Pore Pressure (kPa)	Normalized Pore Pressure-Gauge 13(kPa)	Normalized Pore Pressure-Gauge 12(kPa)	Normalized Pore Pressure-Gauge 14(kPa)	Normalized Avg. Pore Pressure (kPa)
Run 0	0	5.213	5.231	5.198	5.214	1	1	1	1
Run 1	3	5.208	5.233	5.244	5.228	0.999040859	1.000382336	1.008849558	1.002749009
Run2	4	5.19	5.201	5.172	5.188	0.995587953	0.994264959	0.994998076	0.994949495
Run 3	5	5.181	5.178	5.132	5.164	0.9938615	0.989868094	0.987302809	0.990346503
Run 4	6	4.941	4.912	4.877	4.910	0.947822751	0.939017396	0.938245479	0.941695435
Run 5	7	4.612	4.557	4.631	4.600	0.884711299	0.871152743	0.890919584	0.882240123
Run 6	8	4.593	4.584	4.65	4.609	0.881066564	0.87631428	0.894574836	0.883966245
Run 7	9	4.392	4.461	4.511	4.455	0.842509112	0.852800612	0.867833782	0.854366449
Run 8	10	4.098	4.169	4.297	4.188	0.786111644	0.796979545	0.826664102	0.803222094
Run 9	11	4.02	3.981	4.009	4.003	0.77114905	0.761039954	0.771258176	0.767804629
Run 10	12	3.736	3.798	3.867	3.800	0.716669864	0.726056203	0.743939977	0.728870988
Run 11	13	3.718	3.723	3.713	3.718	0.713216958	0.711718601	0.714313197	0.713080169
Run 12	14	3.573	3.621	3.601	3.598	0.68540188	0.692219461	0.692766449	0.690129139
Run 13	15	3.471	3.498	3.404	3.458	0.665835411	0.668705792	0.654867257	0.663150492
Run 14	16	3.141	3.129	3.113	3.128	0.602532131	0.598164787	0.598884186	0.599859353
Run 15	17	3.075	3.101	3.086	3.087	0.589871475	0.592812082	0.593689881	0.592123769

	Slats		PVC Side By Side		PVC Pipe-Primary and Secondary-Touching		PVC Pipe-Primary and Secondary-Spacing of 0.5*Dia. of Pipe	
	Normalized Grouted Area Agc/Atotal	Area Replacement Ratio-Multiply by the inverse of Maximum Agc/Atotal	Normalized Grouted Area Agc/Atotal	Area Replacement Ratio-Multiply by the inverse of Maximum Agc/Atotal	Normalized Grouted Area Agc/Atotal	Area Replacement Ratio-Multiply by the inverse of Maximum Agc/Atotal	Normalized Grouted Area Agc/Atotal	Area Replacement Ratio-Multiply by the inverse of Maximum Agc/Atotal
Run 0	0	0	0	0	0	0	0	0
Run 1	0.111111111	0.176470588	0.087266463	0.176470588	0.043633231	0.176470588	0.034906585	0.176470588
Run2	0.148148148	0.235294118	0.116355283	0.235294118	0.058177642	0.235294118	0.046542113	0.235294118
Run 3	0.185185185	0.294117647	0.145444104	0.294117647	0.072722052	0.294117647	0.058177642	0.294117647
Run 4	0.222222222	0.352941176	0.174532925	0.352941176	0.087266463	0.352941176	0.06981317	0.352941176
Run 5	0.259259259	0.411764706	0.203621746	0.411764706	0.101810873	0.411764706	0.081448698	0.411764706
Run 6	0.296296296	0.470588235	0.232710567	0.470588235	0.116355283	0.470588235	0.093084227	0.470588235
Run 7	0.333333333	0.529411765	0.261799388	0.529411765	0.130899694	0.529411765	0.104719755	0.529411765
Run 8	0.37037037	0.588235294	0.290888209	0.588235294	0.145444104	0.588235294	0.116355283	0.588235294
Run 9	0.407407407	0.647058824	0.31997703	0.647058824	0.159988515	0.647058824	0.127990812	0.647058824
Run 10	0.444444444	0.705882353	0.34906585	0.705882353	0.174532925	0.705882353	0.13962634	0.705882353
Run 11	0.481481481	0.764705882	0.378154671	0.764705882	0.189077336	0.764705882	0.151261869	0.764705882
Run 12	0.518518519	0.823529412	0.407243492	0.823529412	0.203621746	0.823529412	0.162897397	0.823529412
Run 13	0.555555556	0.882352941	0.436332313	0.882352941	0.218166157	0.882352941	0.174532925	0.882352941
Run 14	0.592592593	0.941176471	0.465421134	0.941176471	0.232710567	0.941176471	0.186168454	0.941176471
Run 15	0.62962963	1	0.494509955	1	0.247254977	1	0.197803982	1

	Qout (mL)	Time (mins)	Length Interval(m)	Flow Loss (Qout/Time/Length) (L/min/meter)	Normalized Flow Loss	Lugeon Value	Normalized Average Lugeon Value	Lugeon Value-Gauge 13	Lugeon Value-Gauge 12	Lugeon Value-Gauge 14
Run 0	5622	25	0.46	0.488869565	1	93.76094461	1	93.7789306	93.45623499	94.04955083
Run 1	5625	25	0.46	0.489130435	1.000533618	93.5537969	0.997790682	93.9190543	93.47036782	93.27430106
Run2	5593	25	0.46	0.486347826	0.994841693	93.75078573	0.999891651	93.70863701	93.51044532	94.03476916
Run 3	5559	25	0.46	0.483391304	0.988794023	93.61396379	0.998432388	93.30077289	93.35482896	94.19160256
Run 4	5195	25	0.46	0.45173913	0.924048381	92.00389622	0.981260338	91.42666068	91.96643535	92.62643642
Run 5	4875	25	0.46	0.423913043	0.867129136	92.15500945	0.982872025	91.91523059	93.02458711	91.53812211
Run 6	4830	25	0.46	0.42	0.859124867	91.12605771	0.97189782	91.44350098	91.62303665	90.32258065
Run 7	4660	25	0.46	0.405217391	0.828886517	90.96469425	0.970176811	92.26261186	90.83555062	89.82872784
Run 8	4328	25	0.46	0.376347826	0.7698328	89.86337777	0.958430807	91.83695122	90.27292542	87.58385527
Run 9	4093	25	0.46	0.355913043	0.728032729	88.90417406	0.948200495	88.53558295	89.40292476	88.77850922
Run 10	3890	25	0.46	0.33826087	0.691924582	89.00821057	0.949310088	90.54091798	89.06289351	87.47371853
Run 11	3845	25	0.46	0.334347826	0.683920313	89.92679561	0.959107185	89.92679561	89.80602366	90.04789283
Run 12	3644	25	0.46	0.316869565	0.648167912	88.06009223	0.939198006	88.6844571	87.50885535	87.99488065
Run 13	3467	25	0.46	0.301478261	0.616684454	87.19124483	0.929931382	86.85631255	86.18589505	88.56588157
Run 14	3093	25	0.46	0.268956522	0.550160085	85.99270651	0.917148466	85.62767327	85.9560632	86.39785472
Run 15	3064	25	0.46	0.266434783	0.545001779	86.29932497	0.920418681	86.64545776	85.91898826	86.33661134

Figure C.4: Raw Data from S/D=1.62, Unit weight=12.56 kN/m^3

S/D=2.17									
	# of PVC Pipes	Pore Pressure-Gauge 13(kPa)	Pore Pressure-Gauge 12(kPa)	Pore Pressure-Gauge 14(kPa)	Avg. Pore Pressure (kPa)	Normalized Pore Pressure-Gauge 13(kPa)	Normalized Pore Pressure-Gauge 12(kPa)	Normalized Pore Pressure-Gauge 14(kPa)	Normalized Avg. Pore Pressure (kPa)
Run 0	0	5.17	5.165	5.243	5.193	1	1	1	1
Run 1	3	5.168	5.152	5.271	5.197	0.999613153	0.997483059	1.005340454	1.00083451
Run2	4	5.097	5.163	5.243	5.168	0.985880077	0.999612778	1	0.995185518
Run 3	5	5.053	5.086	5.096	5.078	0.977369439	0.984704743	0.971962617	0.977981769
Run 4	6	4.831	4.982	5.018	4.944	0.9344294	0.964569216	0.957085638	0.95204776
Run 5	7	4.742	4.897	4.892	4.844	0.9172147	0.948112294	0.933053595	0.932789832
Run 6	8	4.665	4.699	4.717	4.694	0.902321083	0.909777348	0.899675758	0.90390294
Run 7	9	4.613	4.593	4.654	4.620	0.892263056	0.889254598	0.887659737	0.889716267
Run 8	10	4.481	4.432	4.418	4.444	0.866731141	0.858083253	0.842647339	0.85575812
Run 9	11	4.255	4.211	4.213	4.226	0.823017408	0.815295257	0.803547587	0.813904224
Run 10	12	4.004	4.018	3.896	3.973	0.774468085	0.777928364	0.743086019	0.76505328
Run 11	13	3.792	3.824	3.81	3.809	0.733462282	0.740367861	0.726683197	0.733470279

	Slats		PVC Side By Side		PVC Pipe-Primary and Secondary-Touching		PVC Pipe-Primary and Secondary-Spacing of 0.5*Dia. of Pipe	
	Normalized Grouted Area Agc/Atotal	Area Replacement Ratio-Multiply by the inverse of Maximum Agc/Atotal	Normalized Grouted Area Agc/Atotal	Area Replacement Ratio-Multiply by the inverse of Maximum Agc/Atotal	Normalized Grouted Area Agc/Atotal	Area Replacement Ratio-Multiply by the inverse of Maximum Agc/Atotal	Normalized Grouted Area Agc/Atotal	Area Replacement Ratio-Multiply by the inverse of Maximum Agc/Atotal
Run 0	0	0	0	0	0	0	0	0
Run 1	0.111111111	0.230769231	0.087266463	0.230769231	0.043633231	0.230769231	0.034906585	0.230769231
Run2	0.148148148	0.307692308	0.116355283	0.307692308	0.058177642	0.307692308	0.046542113	0.307692308
Run 3	0.185185185	0.384615385	0.145444104	0.384615385	0.072722052	0.384615385	0.058177642	0.384615385
Run 4	0.222222222	0.461538462	0.174532925	0.461538462	0.087266463	0.461538462	0.06981317	0.461538462
Run 5	0.259259259	0.538461538	0.203621746	0.538461538	0.101810873	0.538461538	0.081448698	0.538461538
Run 6	0.296296296	0.615384615	0.232710567	0.615384615	0.116355283	0.615384615	0.093084227	0.615384615
Run 7	0.333333333	0.692307692	0.261799388	0.692307692	0.130899694	0.692307692	0.104719755	0.692307692
Run 8	0.37037037	0.769230769	0.290888209	0.769230769	0.145444104	0.769230769	0.116355283	0.769230769
Run 9	0.407407407	0.846153846	0.31997703	0.846153846	0.159988515	0.846153846	0.127990812	0.846153846
Run 10	0.444444444	0.923076923	0.34906585	0.923076923	0.174532925	0.923076923	0.13962634	0.923076923
Run 11	0.481481481	1	0.378154671	1	0.189077336	1	0.151261869	1

	Qout (mL)	Time (mins)	Length Interval(m)	Flow Loss (Qout/Time/Length) (L/min/meter)	Normalized Flow Loss	Lugeon Value	Normalized Average Lugeon Value	Lugeon Value-Gauge 13	Lugeon Value-Gauge 12	Lugeon Value-Gauge 14
Run 0	5639	25	0.46	0.490347826	1	94.43083055	1	94.84484064	94.93665558	93.52428497
Run 1	5641	25	0.46	0.490521739	1.000354673	94.38555688	0.999520563	94.9151972	95.20996489	93.06047033
Run2	5609	25	0.46	0.48773913	0.994679908	94.38285437	0.999491944	95.69141268	94.46816394	93.02672715
Run 3	5465	25	0.46	0.475217391	0.969143465	93.57743183	0.990962711	94.04658447	93.43637265	93.25302027
Run 4	5259	25	0.46	0.457304348	0.932612165	92.50307083	0.979585484	94.66039077	91.79131831	91.13279152
Run 5	5120	25	0.46	0.445217391	0.907962405	91.9174299	0.973383686	93.88810445	90.91635518	91.00927868
Run 6	4998	25	0.46	0.434608696	0.886327363	92.59470826	0.980555902	93.16370754	92.48961389	92.13667493
Run 7	4836	25	0.46	0.420521739	0.857598865	91.02202146	0.963901524	91.16014289	91.55709539	90.35705611
Run 8	4602	25	0.46	0.400173913	0.816102146	90.05489004	0.953659832	89.3046001	90.29194789	90.57806995
Run 9	4444	25	0.46	0.386434783	0.788082993	91.43499865	0.968274854	90.81898534	91.76793698	91.7243728
Run 10	4088	25	0.46	0.355478261	0.724951232	89.48101885	0.947582673	88.78078443	88.47144372	91.24185341
Run 11	3951	25	0.46	0.343565217	0.700656145	90.20616595	0.955261808	90.60264172	89.84446061	90.17459774

Figure C.5: Raw Data from S/D=2.17, Unit weight=12.56 kN/m^3

S/D=1									
	# of PVC Pipes	Pore Pressure-Gauge 13(kPa)	Pore Pressure-Gauge 12(kPa)	Pore Pressure-Gauge 14(kPa)	Avg. Pore Pressure (kPa)	Normalized Pore Pressure-Gauge 13(kPa)	Normalized Pore Pressure-Gauge 12(kPa)	Normalized Pore Pressure-Gauge 14(kPa)	Normalized Avearge Pore Pressure (kPa)
Run 0	0	5.263	5.287	5.330	5.293	1	1	1	1
Run 1	3	5.162	5.182	5.153	5.166	0.980809424	0.980139966	0.966791745	0.975881612
Run2	4	4.934	4.999	5.001	4.978	0.937488125	0.945526764	0.938273921	0.940428212
Run 3	5	4.662	4.676	4.732	4.690	0.885806574	0.884433516	0.887804878	0.886020151
Run 4	6	4.445	4.420	4.505	4.457	0.844575337	0.836012862	0.84521576	0.841939547
Run 5	7	4.228	4.217	4.228	4.224	0.8033441	0.797616796	0.793245779	0.798047859
Run 6	8	4.077	4.068	4.145	4.097	0.77465324	0.769434462	0.777673546	0.773929471
Run 7	9	3.962	3.989	4.047	3.999	0.752802584	0.754492151	0.759287054	0.755541562
Run 8	10	3.671	3.812	3.696	3.726	0.697510925	0.721013807	0.693433396	0.703967254
Run 9	11	3.528	3.503	3.583	3.538	0.67034011	0.662568564	0.672232645	0.668387909
Run 10	12	3.235	3.352	3.509	3.365	0.61466844	0.634007944	0.658348968	0.635768262
Run 11	13	3.098	3.255	3.304	3.219	0.588637659	0.615661055	0.61988743	0.608123426
Run 12	14	2.953	2.917	2.926	2.932	0.561086833	0.55173066	0.548968105	0.553904282
Run 13	15	2.822	2.801	2.806	2.810	0.536196086	0.529790051	0.526454034	0.530793451
Run 14	16	2.587	2.564	2.501	2.551	0.491544746	0.484963117	0.469230769	0.48186398
Run 15	17	2.497	2.486	2.399	2.461	0.474444233	0.470209949	0.450093809	0.464861461
Run 16	18	2.195	2.203	2.213	2.204	0.417062512	0.416682429	0.415196998	0.416309824
Run 17	19	1.987	1.923	1.964	1.958	0.377541326	0.363722338	0.3684803	0.369899244
Run 18	20	1.756	1.994	2.067	1.939	0.33365001	0.377151504	0.387804878	0.366309824
Run 19	21	1.602	1.725	1.802	1.710	0.304389132	0.326271988	0.338086304	0.322984887
Run 20	22	1.558	1.606	1.758	1.641	0.296028881	0.303763949	0.329831144	0.309949622
Run 21	23	1.466	1.409	1.559	1.478	0.278548356	0.266502743	0.29249531	0.279219144
Run 22	24	1.250	1.381	1.450	1.360	0.237507125	0.261206733	0.272045028	0.256989924
Run 23	25	1.238	1.257	1.313	1.269	0.235227057	0.237752979	0.246341463	0.239798489
Run 24	26	1.201	1.211	1.225	1.212	0.228196846	0.229052393	0.229831144	0.229030227
Run 25	27	1.173	1.168	1.190	1.177	0.222876686	0.220919236	0.22326454	0.222355164

	Slats		PVC Side By Side		PVC Pipe-Primary and Secondary-Touching		PVC Pipe-Primary and Secondary-Spacing of 0.5*Dia. of Pipe	
	Normalized Grouted Area Agc/Atotal	Area Replacement Ratio-Multiply by the inverse of Maximum Agc/Atotal	Normalized Grouted Area Agc/Atotal	Area Replacement Ratio-Multiply by the inverse of Maximum Agc/Atotal	Normalized Grouted Area Agc/Atotal	Area Replacement Ratio-Multiply by the inverse of Maximum Agc/Atotal	Normalized Grouted Area Agc/Atotal	Area Replacement Ratio-Multiply by the inverse of Maximum Agc/Atotal
Run 0	0	0	0	0	0	0	0	0
Run 1	0.111111111	0.111111111	0.087266463	0.111111111	0.043633231	0.111111111	0.034906585	0.111111111
Run2	0.148148148	0.148148148	0.116355283	0.148148148	0.058177642	0.148148148	0.046542113	0.148148148
Run 3	0.185185185	0.185185185	0.145444104	0.185185185	0.072722052	0.185185185	0.058177642	0.185185185
Run 4	0.222222222	0.222222222	0.174532925	0.222222222	0.087266463	0.222222222	0.06981317	0.222222222
Run 5	0.259259259	0.259259259	0.203621746	0.259259259	0.101810873	0.259259259	0.081448698	0.259259259
Run 6	0.296296296	0.296296296	0.232710567	0.296296296	0.116355283	0.296296296	0.093084227	0.296296296
Run 7	0.333333333	0.333333333	0.261799388	0.333333333	0.130899694	0.333333333	0.104719755	0.333333333
Run 8	0.37037037	0.37037037	0.290888209	0.37037037	0.145444104	0.37037037	0.116355283	0.37037037
Run 9	0.407407407	0.407407407	0.31997703	0.407407407	0.159988515	0.407407407	0.127990812	0.407407407
Run 10	0.444444444	0.444444444	0.34906585	0.444444444	0.174532925	0.444444444	0.13962634	0.444444444
Run 11	0.481481481	0.481481481	0.378154671	0.481481481	0.189077336	0.481481481	0.151261869	0.481481481
Run 12	0.518518519	0.518518519	0.407243492	0.518518519	0.203621746	0.518518519	0.162897397	0.518518519
Run 13	0.555555556	0.555555556	0.436332313	0.555555556	0.218166156	0.555555556	0.174532925	0.555555556
Run 14	0.592592593	0.592592593	0.465421134	0.592592593	0.232710567	0.592592593	0.186168454	0.592592593
Run 15	0.62962963	0.62962963	0.494509955	0.62962963	0.247254977	0.62962963	0.197803982	0.62962963
Run 16	0.666666667	0.666666667	0.523598776	0.666666667	0.261799388	0.666666667	0.20943951	0.666666667
Run 17	0.703703704	0.703703704	0.552687596	0.703703704	0.276343798	0.703703704	0.221075039	0.703703704
Run 18	0.740740741	0.740740741	0.581776417	0.740740741	0.290888209	0.740740741	0.232710567	0.740740741
Run 19	0.777777778	0.777777778	0.610865238	0.777777778	0.305432619	0.777777778	0.244346095	0.777777778
Run 20	0.814814815	0.814814815	0.639954059	0.814814815	0.31997703	0.814814815	0.255981624	0.814814815
Run 21	0.851851852	0.851851852	0.66904288	0.851851852	0.33452144	0.851851852	0.267617152	0.851851852
Run 22	0.888888889	0.888888889	0.698131701	0.888888889	0.34906585	0.888888889	0.27925268	0.888888889
Run 23	0.925925926	0.925925926	0.727220522	0.925925926	0.363610261	0.925925926	0.290888209	0.925925926
Run 24	0.962962963	0.962962963	0.756309343	0.962962963	0.378154671	0.962962963	0.302523737	0.962962963
Run 25	1	1	0.785398163	1	0.392699082	1	0.314159265	1

	Qout (mL)	Time (mins)	Length Interval (m)	Flow Loss (Qout/Time/Length) (L/min/meter)	Normalized Flow Loss	Average Lugeon Value	Normalized Average Lugeon Value	Lugeon Value-Gauge 13	Lugeon Value-Gauge 12	Lugeon Value-Gauge 14
Run 0	5700	25	0.46	0.495652174	1	93.63706056	1	94.17673835	93.74922904	92.99290317
Run 1	5552	25	0.46	0.482782609	0.974035088	93.45988424	0.99810784	93.52627057	93.16530465	93.68961939
Run2	5205	25	0.46	0.452608696	0.913157895	90.92179503	0.971002234	91.73260958	90.5398471	90.5036384
Run 3	4892	25	0.46	0.425391304	0.858245614	90.70177065	0.968652477	91.24652603	90.97333284	89.89672535
Run 4	4606	25	0.46	0.400521739	0.808070175	89.87024812	0.959772205	90.10612804	90.61577808	88.90604642
Run 5	4343	25	0.46	0.377652174	0.761929825	89.39923631	0.95474202	89.32170622	89.55470095	89.32170622
Run 6	4145	25	0.46	0.360434783	0.727192982	87.98245304	0.939611437	88.40686353	88.60245394	86.95652174
Run 7	4059	25	0.46	0.352956522	0.712105263	88.25383941	0.942509717	89.08544214	88.48245719	87.21436168
Run 8	3750	25	0.46	0.326086957	0.657894737	87.5087995	0.934553039	88.82782798	85.54222364	88.2269904
Run 9	3547	25	0.46	0.308434783	0.622280702	87.17772261	0.931017293	87.424825	88.04875324	86.08283076
Run 10	3338	25	0.46	0.29026087	0.585614035	86.25025839	0.921112409	89.72515288	86.59333818	82.71897109
Run 11	3182	25	0.46	0.276695652	0.558245614	85.95702149	0.917980776	89.31428411	85.00634475	83.74565744
Run 12	2851	25	0.46	0.247913043	0.500175439	84.55424402	0.902999769	83.95294395	84.98904473	84.72762935
Run 13	2663	25	0.46	0.231565217	0.467192982	82.41732734	0.880178498	82.05712877	82.67233752	82.52502402
Run 14	2350	25	0.46	0.204347826	0.412280702	80.11545717	0.855595602	78.99026907	79.69884013	81.70644786
Run 15	2250	25	0.46	0.195652174	0.394736842	79.5118561	0.849149425	78.35489544	78.70159852	81.55572068
Run 16	2012	25	0.46	0.174956522	0.352982456	79.39336942	0.847884042	79.70684362	79.41739525	79.05852767
Run 17	1793	25	0.46	0.155913043	0.314561404	79.62872496	0.850397529	78.46655434	81.07802573	79.38546002
Run 18	1751	25	0.46	0.15226087	0.307192982	78.52546135	0.83861519	86.70892344	76.35951332	73.66273322
Run 19	1482	25	0.46	0.128869565	0.26	75.37701222	0.804991226	80.44292461	74.70699433	71.51474207
Run 20	1458	25	0.46	0.126782609	0.255789474	77.27505609	0.825261447	81.37523023	78.94309383	72.11752486
Run 21	1323	25	0.46	0.115043478	0.232105263	77.8372654	0.831265579	78.47440536	81.64902644	73.79312268
Run 22	1197	25	0.46	0.104086957	0.21	76.51577299	0.817152659	83.26956522	75.37071435	71.78410795
Run 23	1104	25	0.46	0.096	0.193684211	75.6302521	0.80769571	77.54442649	76.37231504	73.11500381
Run 24	1039	25	0.46	0.090347826	0.182280702	74.52391484	0.795880545	75.22716577	74.60596704	73.75332742
Run 25	997	25	0.46	0.086695652	0.174912281	73.65815818	0.786634669	73.90933689	74.2257296	72.85348922

Figure C.6: Raw Data from S/D=1, Unit weight=13.03 kN/m^3

S/D=1.18

	# of PVC Pipes	Pore Pressure-Gauge 13(kPa)	Pore Pressure-Gauge 12(kPa)	Pore Pressure-Gauge 14(kPa)	Avg. Pore Pressure (kPa)	Normalized Pore Pressure-Gauge 13(kPa)	Normalized Pore Pressure-Gauge 12(kPa)	Normalized Pore Pressure-Gauge 14(kPa)	Normalized Avearge Pore Pressure (kPa)
Run 0	0	5.233	5.251	5.283	5.256	1	1	1	1
Run 1	3	5.142	5.155	5.201	5.166	0.982610357	0.981717768	0.984478516	0.98293905
Run2	4	5.001	5.056	5.076	5.044	0.955665966	0.962864216	0.960817717	0.959789434
Run 3	5	4.894	4.932	4.952	4.926	0.935218804	0.939249667	0.937346205	0.937274053
Run 4	6	4.682	4.708	4.794	4.728	0.894706669	0.896591125	0.907438955	0.899600431
Run 5	7	4.493	4.431	4.459	4.461	0.858589719	0.843839269	0.844028014	0.848798123
Run 6	8	4.218	4.199	4.280	4.232	0.806038601	0.799657208	0.810145751	0.805289529
Run 7	9	3.955	3.902	3.987	3.948	0.755780623	0.743096553	0.754684838	0.751189193
Run 8	10	3.921	3.877	3.898	3.899	0.749283394	0.738335555	0.737838349	0.741802499
Run 9	11	3.563	3.594	3.605	3.587	0.680871393	0.684441059	0.682377437	0.682564851
Run 10	12	3.397	3.491	3.522	3.470	0.649149627	0.664825747	0.666666667	0.660239741
Run 11	13	3.324	3.409	3.553	3.429	0.635199694	0.649209674	0.672534545	0.652375214
Run 12	14	3.001	3.052	3.084	3.046	0.573476018	0.581222624	0.583759228	0.57950149
Run 13	15	2.914	2.887	2.956	2.919	0.556850755	0.549800038	0.55953057	0.55540052
Run 14	16	2.823	2.755	2.801	2.793	0.539461112	0.524661969	0.530191179	0.531426397
Run 15	17	2.412	2.431	2.390	2.411	0.460921078	0.462959436	0.452394473	0.458742944
Run 16	18	2.086	2.147	2.048	2.094	0.398624116	0.4088745	0.387658527	0.398363671
Run 17	19	1.851	1.886	1.825	1.854	0.353716797	0.359169682	0.345447662	0.352762098
Run 18	20	1.763	1.748	1.713	1.741	0.33690044	0.332888974	0.324247587	0.331324919
Run 19	21	1.585	1.546	1.567	1.566	0.302885534	0.29442011	0.296611774	0.297964102
Run 20	22	1.527	1.463	1.532	1.507	0.291802026	0.278613597	0.28998675	0.286801548
Run 21	23	1.486	1.407	1.457	1.450	0.283967132	0.267948962	0.275790271	0.275892687

	Slats		PVC Side By Side		PVC Pipe-Primary and Secondary-Touching		PVC Pipe-Primary and Secondary-Spacing of 0.5*Dia. of Pipe	
	Normalized Grouted Area Agc/Atotal	Area Replacement Ratio-Multiply by the inverse of Maximum Agc/Atotal	Normalized Grouted Area Agc/Atotal	Area Replacement Ratio-Multiply by the inverse of Maximum Agc/Atotal	Normalized Grouted Area Agc/Atotal	Area Replacement Ratio-Multiply by the inverse of Maximum Agc/Atotal	Normalized Grouted Area Agc/Atotal	Area Replacement Ratio-Multiply by the inverse of Maximum Agc/Atotal
Run 0	0	0	0	0	0	0	0	0
Run 1	0.111111111	0.130434783	0.087266463	0.130434783	0.043633231	0.130434783	0.034906585	0.130434783
Run2	0.148148148	0.173913043	0.116355283	0.173913043	0.058177642	0.173913043	0.046542113	0.173913043
Run 3	0.185185185	0.217391304	0.145444104	0.217391304	0.072722052	0.217391304	0.058177642	0.217391304
Run 4	0.222222222	0.260869565	0.174532925	0.260869565	0.087266463	0.260869565	0.06981317	0.260869565
Run 5	0.259259259	0.304347826	0.203621746	0.304347826	0.101810873	0.304347826	0.081448698	0.304347826
Run 6	0.296296296	0.347826087	0.232710567	0.347826087	0.116355283	0.347826087	0.093084227	0.347826087
Run 7	0.333333333	0.391304348	0.261799388	0.391304348	0.130899694	0.391304348	0.104719755	0.391304348
Run 8	0.37037037	0.434782609	0.290888209	0.434782609	0.145444104	0.434782609	0.116355283	0.434782609
Run 9	0.407407407	0.47826087	0.31997703	0.47826087	0.159988515	0.47826087	0.127990812	0.47826087
Run 10	0.444444444	0.52173913	0.34906585	0.52173913	0.174532925	0.52173913	0.13962634	0.52173913
Run 11	0.481481481	0.565217391	0.378154671	0.565217391	0.189077336	0.565217391	0.151261869	0.565217391
Run 12	0.518518519	0.608695652	0.407243492	0.608695652	0.203621746	0.608695652	0.162897397	0.608695652
Run 13	0.555555556	0.652173913	0.436332313	0.652173913	0.218166156	0.652173913	0.174532925	0.652173913
Run 14	0.592592593	0.695652174	0.465421134	0.695652174	0.232710567	0.695652174	0.186168454	0.695652174
Run 15	0.62962963	0.739130435	0.494509955	0.739130435	0.247254977	0.739130435	0.197803982	0.739130435
Run 16	0.666666667	0.782608696	0.523598776	0.782608696	0.261799388	0.782608696	0.20943951	0.782608696
Run 17	0.703703704	0.826086957	0.552687596	0.826086957	0.276343798	0.826086957	0.221075039	0.826086957
Run 18	0.740740741	0.869565217	0.581776417	0.869565217	0.290888209	0.869565217	0.232710567	0.869565217
Run 19	0.777777778	0.913043478	0.610865238	0.913043478	0.305432619	0.913043478	0.244346095	0.913043478
Run 20	0.814814815	0.956521739	0.639954059	0.956521739	0.31997703	0.956521739	0.255981624	0.956521739
Run 21	0.851851852	1	0.66904288	1	0.33452144	1	0.267617152	1

	Qout (mL)	Time (mins)	Length Interval (m)	Flow Loss (Qout/Time/Length) (L/min/meter)	Normalized Flow Loss	Lugeon Value	Normalized Average Lugeon Value	Lugeon Value-Gauge 13	Lugeon Value-Gauge 12	Lugeon Value-Gauge 14
Run 0	5691	25	0.46	0.494869565	1	94.15923737	1	94.5670868	94.24291853	93.67207367
Run 1	5559	25	0.46	0.483391304	0.976805482	93.57168106	0.993759972	94.00842169	93.77134905	92.94199276
Run2	5322	25	0.46	0.462782609	0.93516078	91.74306655	0.974339524	92.53801414	91.53137039	91.17072669
Run 3	5283	25	0.46	0.459391304	0.928307855	93.25848647	0.990433749	93.86826815	93.14503332	92.76884175
Run 4	5035	25	0.46	0.437826087	0.884730276	92.60281027	0.983470266	93.51262002	92.99619519	91.32792803
Run 5	4637	25	0.46	0.403217391	0.814795291	90.38722065	0.959940025	89.74346568	90.99918558	90.42776212
Run 6	4347	25	0.46	0.378	0.763837638	89.31243601	0.948525482	89.61593172	90.02143367	88.31775701
Run 7	4111	25	0.46	0.357478261	0.722368652	90.54667195	0.961633446	90.38641236	91.61411094	89.66096335
Run 8	4053	25	0.46	0.352434783	0.712177122	90.39879855	0.960062986	89.88390273	90.90399345	90.41425926
Run 9	3751	25	0.46	0.326173913	0.659110877	90.92378174	0.965638468	91.54474124	90.75512327	90.47820057
Run 10	3475	25	0.46	0.302173913	0.610613249	87.08181932	0.924835648	88.9531684	86.55798139	85.79611387
Run 11	3410	25	0.46	0.296521739	0.599191706	86.48310494	0.918477118	89.20629938	86.98202967	83.45672365
Run 12	2951	25	0.46	0.256608696	0.518538043	84.25370329	0.894800188	85.50772931	84.07886489	83.20645125
Run 13	2688	25	0.46	0.23373913	0.472324723	80.07507038	0.850421824	80.21246755	80.9626361	79.07277755
Run 14	2501	25	0.46	0.217478261	0.439465823	77.86547113	0.826955202	77.03799535	78.93947763	77.64307778
Run 15	2245	25	0.46	0.195217391	0.394482516	80.96946964	0.859920619	80.93590021	80.30332839	81.68091686
Run 16	1874	25	0.46	0.162956522	0.329291864	77.83307837	0.826611181	78.11913794	75.89963751	79.56861413
Run 17	1704	25	0.46	0.148173913	0.299420137	79.92120445	0.84878772	80.05073638	78.56517128	81.19118523
Run 18	1605	25	0.46	0.139565217	0.282024249	80.14847859	0.851201442	79.16348122	79.84280171	81.47414909
Run 19	1470	25	0.46	0.127826087	0.258302583	81.62585374	0.866891619	80.64737347	82.68181563	81.57376321
Run 20	1348	25	0.46	0.117217391	0.236865226	77.76474434	0.825885452	76.76319011	80.12125175	76.51265751
Run 21	1301	25	0.46	0.113130435	0.228606572	78.02098951	0.828606855	76.1308444	80.40542628	77.64614604

Figure C.7: Raw Data from S/D=1.18, Unit weight=13.03 kN/m^3

S/D=1.45

	# of PVC Pipes	Pore Pressure-Gauge 13(kPa)	Pore Pressure-Gauge 12(kPa)	Pore Pressure-Gauge 14(kPa)	Avg. Pore Pressure (kPa)	Normalized Pore Pressure-Gauge 13(kPa)	Normalized Pore Pressure-Gauge 12(kPa)	Normalized Pore Pressure-Gauge 14(kPa)	Normalized Avearge Pore Pressure (kPa)
Run 0	0	5.159	5.168	5.197	5.175	1	1	1	1
Run 1	3	5.108	5.132	5.154	5.131	0.990114363	0.993034056	0.991725996	0.99162587
Run2	4	5.071	5.1	5.108	5.093	0.982942431	0.986842105	0.982874735	0.984217985
Run 3	5	4.935	4.997	5.052	4.995	0.956580733	0.966911765	0.972099288	0.965215151
Run 4	6	4.783	4.803	4.773	4.786	0.927117658	0.929373065	0.91841447	0.924954909
Run 5	7	4.51	4.498	4.551	4.520	0.874200426	0.870356037	0.875697518	0.873421799
Run 6	8	4.432	4.391	4.497	4.440	0.859081217	0.849651703	0.865306908	0.858026282
Run 7	9	4.157	4.184	4.286	4.209	0.805776313	0.809597523	0.824706561	0.813385725
Run 8	10	3.986	4.016	4.055	4.019	0.772630355	0.777089783	0.780257841	0.776668384
Run 9	11	3.818	3.854	3.883	3.852	0.740065904	0.745743034	0.747161824	0.744331358
Run 10	12	3.572	3.699	3.694	3.655	0.692382245	0.715750774	0.710794689	0.706325689
Run 11	13	3.291	3.31	3.307	3.303	0.637914324	0.640479876	0.636328651	0.638237568
Run 12	14	3.178	3.187	3.162	3.176	0.616010855	0.616679567	0.608427939	0.613694924
Run 13	15	2.898	2.865	2.907	2.890	0.561736771	0.554373065	0.55936117	0.55849008
Run 14	16	2.697	2.676	2.741	2.705	0.522775732	0.517801858	0.527419665	0.522674568
Run 15	17	2.501	2.451	2.46	2.471	0.484783873	0.474264706	0.47335001	0.477454264
Run 16	18	2.086	2.177	2.101	2.121	0.404341927	0.42124613	0.404271695	0.40994589
Run 17	19	2.004	1.852	1.874	1.910	0.388447374	0.358359133	0.36059265	0.369105901

	Slats		PVC Side By Side		PVC Pipe-Primary and Secondary-Touching		PVC Pipe-Primary and Secondary-Spacing of 0.5*Dia. of Pipe	
	Normalized Grouted Area Agc/Atotal	Area Replacement Ratio-Multiply by the inverse of Maximum Agc/Atotal	Normalized Grouted Area Agc/Atotal	Area Replacement Ratio-Multiply by the inverse of Maximum Agc/Atotal	Normalized Grouted Area Agc/Atotal	Area Replacement Ratio-Multiply by the inverse of Maximum Agc/Atotal	Normalized Grouted Area Agc/Atotal	Area Replacement Ratio-Multiply by the inverse of Maximum Agc/Atotal
Run 0	0	0	0	0	0	0	0	0
Run 1	0.111111111	0.157894737	0.087266463	0.157894737	0.043633231	0.157894737	0.034906585	0.157894737
Run2	0.148148148	0.210526316	0.116355283	0.210526316	0.058177642	0.210526316	0.046542113	0.210526316
Run 3	0.185185185	0.263157895	0.145444104	0.263157895	0.072722052	0.263157895	0.058177642	0.263157895
Run 4	0.222222222	0.315789474	0.174532925	0.315789474	0.087266463	0.315789474	0.06981317	0.315789474
Run 5	0.259259259	0.368421053	0.203621746	0.368421053	0.101810873	0.368421053	0.081448698	0.368421053
Run 6	0.296296296	0.421052632	0.232710567	0.421052632	0.116355283	0.421052632	0.093084227	0.421052632
Run 7	0.333333333	0.473684211	0.261799388	0.473684211	0.130899694	0.473684211	0.104719755	0.473684211
Run 8	0.37037037	0.526315789	0.290888209	0.526315789	0.145444104	0.526315789	0.116355283	0.526315789
Run 9	0.407407407	0.578947368	0.31997703	0.578947368	0.159988515	0.578947368	0.127990812	0.578947368
Run 10	0.444444444	0.631578947	0.34906585	0.631578947	0.174532925	0.631578947	0.13962634	0.631578947
Run 11	0.481481481	0.684210526	0.378154671	0.684210526	0.189077336	0.684210526	0.151261869	0.684210526
Run 12	0.518518519	0.736842105	0.407243492	0.736842105	0.203621746	0.736842105	0.162897397	0.736842105
Run 13	0.555555556	0.789473684	0.436332313	0.789473684	0.218166156	0.789473684	0.174532925	0.789473684
Run 14	0.592592593	0.842105263	0.465421134	0.842105263	0.232710567	0.842105263	0.186168454	0.842105263
Run 15	0.62962963	0.894736842	0.494509955	0.894736842	0.247254977	0.894736842	0.197803982	0.894736842
Run 16	0.666666667	0.947368421	0.523598776	0.947368421	0.261799388	0.947368421	0.20943951	0.947368421
Run 17	0.703703704	1	0.552687596	1	0.276343798	1	0.221075039	1

	Qout (mL)	Time (mins)	Length Interval (m)	Flow Loss (Qout/Time/Length) (L/min/meter)	Normalized Flow Loss	Lugeon Value	Normalized Average Lugeon Value	Lugeon Value-Gauge 13	Lugeon Value-Gauge 12	Lugeon Value-Gauge 14
Run 0	5504	25	0.46	0.478608696	1	92.49072964	1	92.77160218	92.61004173	92.09326451
Run 1	5470	25	0.46	0.475652174	0.993822674	92.69562958	1.002215356	93.11906302	92.68358806	92.28796545
Run2	5399	25	0.46	0.469478261	0.980922965	92.18108401	0.996652144	92.58100195	92.05456095	91.9103878
Run 3	5342	25	0.46	0.464521739	0.97056686	93.00355161	1.005544577	94.12801198	92.9601239	91.94808771
Run 4	5030	25	0.46	0.437391304	0.913880814	91.38337719	0.988027422	91.44706342	91.06627199	91.63865584
Run 5	4677	25	0.46	0.406695652	0.84974564	89.98355015	0.97289264	90.17641955	90.41699693	89.36401937
Run 6	4467	25	0.46	0.388434783	0.81159157	87.4853114	0.945881947	87.64322712	88.46157654	86.37642486
Run 7	4305	25	0.46	0.374347826	0.78215843	88.93984939	0.961608258	90.05239983	89.47127775	87.34200329
Run 8	4054	25	0.46	0.352521739	0.736555233	87.71379426	0.948352279	88.43997469	87.77931751	86.93507747
Run 9	3903	25	0.46	0.339391304	0.70912064	88.11544033	0.952694834	88.89243173	88.06209246	87.40440493
Run 10	3594	25	0.46	0.312521739	0.652979651	85.50526378	0.924473881	87.49208822	84.48816954	84.60252819
Run 11	3291	25	0.46	0.286173913	0.597928779	86.64934791	0.936843598	86.95652174	86.45737554	86.53580679
Run 12	3050	25	0.46	0.265217391	0.554142442	83.51550057	0.902960771	83.45418229	83.21850998	83.87646784
Run 13	2704	25	0.46	0.235130435	0.49127907	81.36001204	0.879655857	81.13541573	82.06995978	80.88422249
Run 14	2511	25	0.46	0.218347826	0.456213663	80.73003183	0.872844577	80.95952024	81.5948528	79.65991466
Run 15	2324	25	0.46	0.202086957	0.422238372	81.7945048	0.884353547	80.80246162	82.45081865	82.14916932
Run 16	1880	25	0.46	0.163478261	0.341569767	77.06391933	0.833206956	78.36925257	75.09336742	77.80973863
Run 17	1746	25	0.46	0.151826087	0.317223837	79.49009788	0.859438543	75.76152044	81.97952859	81.01712218

Figure C.8: Raw Data from S/D=1.45, Unit weight=13.03 kN/m^3

S/D=1.62									
	# of PVC Pipes	Pore Pressure-Gauge 13(kPa)	Pore Pressure-Gauge 12(kPa)	Pore Pressure-Gauge 14(kPa)	Avg. Pore Pressure (kPa)	Normalized Pore Pressure-Gauge 13(kPa)	Normalized Pore Pressure-Gauge 12(kPa)	Normalized Pore Pressure-Gauge 14(kPa)	Normalized Avearge Pore Pressure (kPa)
Run 0	0	5.23	5.263	5.284	5.259	1	1	1	1
Run 1	3	5.158	5.17	5.218	5.182	0.98623327	0.98232947	0.987509463	0.985358433
Run2	4	5.087	5.148	5.169	5.135	0.972657744	0.978149344	0.978236185	0.976357989
Run 3	5	5.043	5.091	5.12	5.085	0.964244742	0.96731902	0.968962907	0.966850479
Run 4	6	4.886	4.888	4.843	4.872	0.934225621	0.928747862	0.9165405	0.926475249
Run 5	7	4.697	4.642	4.692	4.677	0.898087954	0.88200646	0.887963664	0.889332573
Run 6	8	4.582	4.563	4.634	4.593	0.876099426	0.86699601	0.876987131	0.873359954
Run 7	9	4.384	4.407	4.532	4.441	0.838240918	0.837355121	0.857683573	0.844457121
Run 8	10	4.145	4.198	4.286	4.210	0.792543021	0.797643929	0.811127933	0.800469037
Run 9	11	3.984	3.946	3.989	3.973	0.761759082	0.749762493	0.754920515	0.755466819
Run 10	12	3.561	3.501	3.484	3.515	0.680879541	0.665209956	0.659348978	0.668441402
Run 11	13	3.395	3.324	3.314	3.344	0.649139579	0.631578947	0.627176382	0.635925715
Run 12	14	3.362	3.291	3.32	3.324	0.642829828	0.625308759	0.628311885	0.63212271
Run 13	15	3.258	3.207	3.198	3.221	0.622944551	0.60934828	0.605223316	0.612473854
Run 14	16	2.932	2.895	2.903	2.910	0.560611855	0.550066502	0.549394398	0.553337136
Run 15	17	2.706	2.714	2.787	2.736	0.517399618	0.51567547	0.527441332	0.520187615

	Slats		PVC Side By Side		PVC Pipe-Primary and Secondary-Touching		PVC Pipe-Primary and Secondary-Spacing of 0.5*Dia. of Pipe	
	Normalized Grouted Area Agc/Atotal	Area Replacement Ratio-Multiply by the inverse of Maximum Agc/Atotal	Normalized Grouted Area Agc/Atotal	Area Replacement Ratio-Multiply by the inverse of Maximum Agc/Atotal	Normalized Grouted Area Agc/Atotal	Area Replacement Ratio-Multiply by the inverse of Maximum Agc/Atotal	Normalized Grouted Area Agc/Atotal	Area Replacement Ratio-Multiply by the inverse of Maximum Agc/Atotal
Run 0	0	0	0	0	0	0	0	0
Run 1	0.111111111	0.176470588	0.087266463	0.176470588	0.043633231	0.176470588	0.034906585	0.176470588
Run2	0.148148148	0.235294118	0.116355283	0.235294118	0.058177642	0.235294118	0.046542113	0.235294118
Run 3	0.185185185	0.294117647	0.145444104	0.294117647	0.072722052	0.294117647	0.058177642	0.294117647
Run 4	0.222222222	0.352941176	0.174532925	0.352941176	0.087266463	0.352941176	0.06981317	0.352941176
Run 5	0.259259259	0.411764706	0.203621746	0.411764706	0.101810873	0.411764706	0.081448698	0.411764706
Run 6	0.296296296	0.470588235	0.232710567	0.470588235	0.116355283	0.470588235	0.093084227	0.470588235
Run 7	0.333333333	0.529411765	0.261799388	0.529411765	0.130899694	0.529411765	0.104719755	0.529411765
Run 8	0.37037037	0.588235294	0.290888209	0.588235294	0.145444104	0.588235294	0.116355283	0.588235294
Run 9	0.407407407	0.647058824	0.31997703	0.647058824	0.159988515	0.647058824	0.127990812	0.647058824
Run 10	0.444444444	0.705882353	0.34906585	0.705882353	0.174532925	0.705882353	0.13962634	0.705882353
Run 11	0.481481481	0.764705882	0.378154671	0.764705882	0.189077336	0.764705882	0.151261869	0.764705882
Run 12	0.518518519	0.823529412	0.407243492	0.823529412	0.203621746	0.823529412	0.162897397	0.823529412
Run 13	0.555555556	0.882352941	0.436332313	0.882352941	0.218166157	0.882352941	0.174532925	0.882352941
Run 14	0.592592593	0.941176471	0.465421134	0.941176471	0.232710567	0.941176471	0.186168454	0.941176471
Run 15	0.62962963	1	0.494509955	1	0.247254977	1	0.197803982	1

	Qout (mL)	Time (mins)	Length Interval (m)	Flow Loss (Qout/Time/Length) (L/min/meter)	Normalized Flow Loss	Lugeon Value	Normalized Average Lugeon Value	Lugeon Value-Gauge 13	Lugeon Value-Gauge 12	Lugeon Value-Gauge 14
Run 0	5625	25	0.46	0.489130435	1	93.00825913	1	93.52398371	92.93757074	92.56821249
Run 1	5549	25	0.46	0.482521739	0.986488889	93.11496317	1.001147253	93.54822395	93.33109074	92.47254487
Run2	5480	25	0.46	0.476521739	0.974222222	92.80480508	0.997812516	93.67441304	92.56444039	92.18838056
Run 3	5361	25	0.46	0.466173913	0.953066667	91.68229573	0.985743595	92.43980033	91.56824063	91.04959239
Run 4	5177	25	0.46	0.450173913	0.920355556	92.39390703	0.99339465	92.13547136	92.09777272	92.95352324
Run 5	4947	25	0.46	0.430173913	0.879466667	91.97646206	0.988906393	91.58482287	92.66995111	91.68241966
Run 6	4771	25	0.46	0.414869565	0.848177778	90.32648927	0.971166326	90.54333593	90.92035179	89.5273123
Run 7	4595	25	0.46	0.399565217	0.816888889	89.97190214	0.967353899	91.14170105	90.66603526	88.16531716
Run 8	4250	25	0.46	0.369565217	0.755555556	87.78966285	0.943891044	89.15928043	88.03363921	86.22613565
Run 9	4012	25	0.46	0.348869565	0.713244444	87.81010954	0.944110882	87.56766195	88.41093898	87.45790053
Run 10	3499	25	0.46	0.30426087	0.622044444	86.55249466	0.930589342	85.44253568	86.90684649	87.33090401
Run 11	3389	25	0.46	0.294695652	0.602488889	88.11790656	0.947420233	86.80284306	88.65693507	88.92445751
Run 12	3256	25	0.46	0.283130435	0.578844444	85.16908697	0.915715311	84.21488245	86.03173345	85.28025144
Run 13	3132	25	0.46	0.272347826	0.5568	84.55381127	0.909100031	83.59356233	84.92292675	85.16192185
Run 14	2869	25	0.46	0.249478261	0.510044444	85.73136112	0.921760733	85.08808352	86.17556507	85.93808504
Run 15	2596	25	0.46	0.22573913	0.461511111	82.51704536	0.887201267	83.42170378	83.1758034	80.99717633

Figure C.9: Raw Data from S/D=1.62, Unit weight=13.03 kN/m^3

S/D=2.17									
	# of PVC Pipes	Pore Pressure-Gauge 13(kPa)	Pore Pressure-Gauge 12(kPa)	Pore Pressure-Gauge 14(kPa)	Avg. Pore Pressure (kPa)	Normalized Pore Pressure-Gauge 13(kPa)	Normalized Pore Pressure-Gauge 12(kPa)	Normalized Pore Pressure-Gauge 14(kPa)	Normalized Avearge Pore Pressure (kPa)
Run 0	0	5.185	5.209	5.24	5.211	1	1	1	1
Run 1	3	5.164	5.178	5.234	5.192	0.995949855	0.994048762	0.998854962	0.996290137
Run 2	4	5.098	5.171	5.208	5.159	0.983220829	0.992704934	0.99389313	0.989957784
Run 3	5	5.072	5.103	5.142	5.106	0.978206365	0.979650605	0.98129771	0.979723679
Run 4	6	4.961	5.002	4.987	4.983	0.956798457	0.960261087	0.951717557	0.9562492
Run 5	7	4.69	4.714	4.713	4.706	0.904532305	0.904972164	0.899427481	0.90296789
Run 6	8	4.527	4.61	4.621	4.586	0.873095468	0.885006719	0.881870229	0.880005117
Run 7	9	4.323	4.428	4.564	4.438	0.833751205	0.850067191	0.870992366	0.851669438
Run 8	10	3.967	4.035	4.297	4.100	0.76509161	0.774620849	0.820038168	0.786682871
Run 9	11	4.008	4.007	4.026	4.014	0.772999036	0.769245537	0.768320611	0.770180376
Run 10	12	3.613	3.524	3.413	3.517	0.696817743	0.676521405	0.651335878	0.674811309
Run 11	13	3.436	3.383	3.305	3.375	0.66268081	0.64945287	0.630725191	0.647563004

	Slats		PVC Side By Side		PVC Pipe-Primary and Secondary-Touching		PVC Pipe-Primary and Secondary-Spacing of 0.5*Dia. of Pipe	
	Normalized Grouted Area Agc/Atotal	Area Replacement Ratio-Multiply by the inverse of Maximum Agc/Atotal	Normalized Grouted Area Agc/Atotal	Area Replacement Ratio-Multiply by the inverse of Maximum Agc/Atotal	Normalized Grouted Area Agc/Atotal	Area Replacement Ratio-Multiply by the inverse of Maximum Agc/Atotal	Normalized Grouted Area Agc/Atotal	Area Replacement Ratio-Multiply by the inverse of Maximum Agc/Atotal
Run 0	0	0	0	0	0	0	0	0
Run 1	0.111111111	0.230769231	0.087266463	0.230769231	0.043633231	0.230769231	0.034906585	0.230769231
Run 2	0.148148148	0.307692308	0.116355283	0.307692308	0.058177642	0.307692308	0.046542113	0.307692308
Run 3	0.185185185	0.384615385	0.145444104	0.384615385	0.072722052	0.384615385	0.058177642	0.384615385
Run 4	0.222222222	0.461538462	0.174532925	0.461538462	0.087266463	0.461538462	0.06981317	0.461538462
Run 5	0.259259259	0.538461538	0.203621746	0.538461538	0.101810873	0.538461538	0.081448698	0.538461538
Run 6	0.296296296	0.615384615	0.232710567	0.615384615	0.116355283	0.615384615	0.093084227	0.615384615
Run 7	0.333333333	0.692307692	0.261799388	0.692307692	0.130899694	0.692307692	0.104719755	0.692307692
Run 8	0.37037037	0.769230769	0.290888209	0.769230769	0.145444104	0.769230769	0.116355283	0.769230769
Run 9	0.407407407	0.846153846	0.31997703	0.846153846	0.159988515	0.846153846	0.127990812	0.846153846
Run 10	0.444444444	0.923076923	0.34906585	0.923076923	0.174532925	0.923076923	0.13962634	0.923076923
Run 11	0.481481481	1	0.378154671	1	0.189077336	1	0.151261869	1

	Qout (mL)	Time (mins)	Length Interval (m)	Flow Loss (Qout/Time/Length) (L/min/meter)	Normalized Flow Loss	Lugeon Value	Normalized Average Lugeon Value	Lugeon Value-Gauge 13	Lugeon Value-Gauge 12	Lugeon Value-Gauge 14
Run 0	5663	25	0.46	0.492434783	1	94.49305026	1	94.97295711	94.53537773	93.97610355
Run 1	5637	25	0.46	0.490173913	0.995408794	94.40945937	0.999115375	94.92136194	94.66471863	93.65187487
Run 2	5609	25	0.46	0.48773913	0.990464418	94.54140927	1.000511773	95.6726423	94.32201323	93.65190677
Run 3	5522	25	0.46	0.480173913	0.975101536	94.04725071	0.995282197	94.67151282	94.09639683	93.38271354
Run 4	5355	25	0.46	0.465652174	0.945611867	93.44190781	0.988875981	93.86256277	93.0931975	93.37320512
Run 5	5051	25	0.46	0.439217391	0.891930072	93.33797364	0.987776068	93.6497636	93.17297227	93.19274163
Run 6	4867	25	0.46	0.423217391	0.85943846	92.28464704	0.976628935	93.48738487	91.80420636	91.58567221
Run 7	4650	25	0.46	0.404347826	0.821119548	91.10352822	0.964129404	93.53407959	91.31613055	88.59505392
Run 8	4240	25	0.46	0.368695652	0.74871976	89.93308046	0.951742802	92.9406736	91.37438716	85.80303751
Run 9	4150	25	0.46	0.360869565	0.732827123	89.91019813	0.951500643	90.03731667	90.05978668	89.63476533
Run 10	3647	25	0.46	0.317130435	0.644004944	90.17927055	0.95434818	87.7748228	89.99161032	92.91838113
Run 11	3493	25	0.46	0.30373913	0.616810878	90.00566884	0.95251099	88.39904844	89.78395815	91.9029139

Figure C.10: Raw Data from S/D=2.17, Unit weight=13.03 kN/m^3

S/D=1									
	# of PVC Pipes	Pore Pressure-Gauge 13(kPa)	Pore Pressure-Gauge 12(kPa)	Pore Pressure-Gauge 14(kPa)	Avg. Pore Pressure (kPa)	Normalized Pore Pressure-Gauge 13(kPa)	Normalized Pore Pressure-Gauge 12(kPa)	Normalized Pore Pressure-Gauge 14(kPa)	Normalized Average Pore Pressure (kPa)
Run 0	0	5.209	5.265	5.318	5.264	1	1	1	1
Run 1	3	5.128	5.140	5.192	5.153	0.98444999	0.97625831	0.976306882	0.978976697
Run2	4	4.915	5.003	4.934	4.951	0.943559224	0.950237417	0.927792403	0.94047619
Run 3	5	4.783	4.853	4.887	4.841	0.918218468	0.921747388	0.918954494	0.919642857
Run 4	6	4.576	4.518	4.595	4.563	0.878479555	0.858119658	0.864046634	0.866831307
Run 5	7	4.298	4.352	4.359	4.336	0.825110386	0.826590693	0.819669049	0.82377153
Run 6	8	4.174	4.097	4.180	4.150	0.801305433	0.778157645	0.786009778	0.788437183
Run 7	9	3.682	3.749	3.812	3.748	0.706853523	0.712060779	0.716810831	0.711942756
Run 8	10	3.506	3.610	3.626	3.581	0.673065848	0.685660019	0.681835276	0.680217832
Run 9	11	3.254	3.313	3.375	3.314	0.62468804	0.629249763	0.634637082	0.629559271
Run 10	12	3.099	3.167	3.243	3.170	0.594931849	0.601519468	0.60981572	0.602140324
Run 11	13	2.953	2.968	3.089	3.003	0.566903436	0.563722697	0.580857465	0.570542047
Run 12	14	2.778	2.805	2.906	2.830	0.533307737	0.532763533	0.546446032	0.537550659
Run 13	15	2.655	2.743	2.862	2.753	0.509694759	0.520987654	0.538172245	0.523049645
Run 14	16	2.481	2.599	2.577	2.552	0.476291035	0.493637227	0.484580669	0.484865755
Run 15	17	2.207	2.181	2.278	2.222	0.423689768	0.414245014	0.428356525	0.422112462
Run 16	18	2.117	2.158	2.193	2.156	0.406411979	0.409876543	0.412373073	0.409574468
Run 17	19	1.864	1.837	1.916	1.872	0.357842196	0.348907882	0.360285822	0.355686424
Run 18	20	1.666	1.728	1.823	1.739	0.319831062	0.328205128	0.342798044	0.330357143
Run 19	21	1.558	1.635	1.680	1.624	0.299097715	0.310541311	0.315908236	0.308573961
Run 20	22	1.420	1.459	1.524	1.468	0.272605107	0.27711301	0.2865739	0.278812057
Run 21	23	1.355	1.387	1.391	1.378	0.260126704	0.263437797	0.261564498	0.261714792
Run 22	24	1.261	1.374	1.419	1.351	0.242081014	0.260968661	0.266829635	0.256712259
Run 23	25	1.227	1.270	1.302	1.266	0.235553849	0.241215575	0.244828883	0.240564843
Run 24	26	1.150	1.204	1.221	1.192	0.220771741	0.228679962	0.229597593	0.226380446
Run 25	27	1.093	1.116	1.143	1.117	0.209829142	0.211965812	0.214930425	0.212259372

	Slats		PVC Side By Side		PVC Pipe-Primary and Secondary-Touching		PVC Pipe-Primary and Secondary-Spacing of 0.5*Dia. of Pipe	
	Normalized Grouted Area Agc/Atotal	Area Replacement Ratio-Multiply by the inverse of Maximum Agc/Atotal	Normalized Grouted Area Agc/Atotal	Area Replacement Ratio-Multiply by the inverse of Maximum Agc/Atotal	Normalized Grouted Area Agc/Atotal	Area Replacement Ratio-Multiply by the inverse of Maximum Agc/Atotal	Normalized Grouted Area Agc/Atotal	Area Replacement Ratio-Multiply by the inverse of Maximum Agc/Atotal
Run 0	0	0	0	0	0	0	0	0
Run 1	0.111111111	0.111111111	0.087266463	0.111111111	0.043633231	0.111111111	0.034906585	0.111111111
Run2	0.148148148	0.148148148	0.116355283	0.148148148	0.058177642	0.148148148	0.046542113	0.148148148
Run 3	0.185185185	0.185185185	0.145444104	0.185185185	0.072722052	0.185185185	0.058177642	0.185185185
Run 4	0.222222222	0.222222222	0.174532925	0.222222222	0.087266463	0.222222222	0.06981317	0.222222222
Run 5	0.259259259	0.259259259	0.203621746	0.259259259	0.101810873	0.259259259	0.081448698	0.259259259
Run 6	0.296296296	0.296296296	0.232710567	0.296296296	0.116355283	0.296296296	0.093084227	0.296296296
Run 7	0.333333333	0.333333333	0.261799388	0.333333333	0.130899694	0.333333333	0.104719755	0.333333333
Run 8	0.37037037	0.37037037	0.290888209	0.37037037	0.145444104	0.37037037	0.116355283	0.37037037
Run 9	0.407407407	0.407407407	0.31997703	0.407407407	0.159988515	0.407407407	0.127990812	0.407407407
Run 10	0.444444444	0.444444444	0.34906585	0.444444444	0.174532925	0.444444444	0.13962634	0.444444444
Run 11	0.481481481	0.481481481	0.378154671	0.481481481	0.189077336	0.481481481	0.151261869	0.481481481
Run 12	0.518518519	0.518518519	0.407243492	0.518518519	0.203621746	0.518518519	0.162897397	0.518518519
Run 13	0.555555556	0.555555556	0.436332313	0.555555556	0.218166156	0.555555556	0.174532925	0.555555556
Run 14	0.592592593	0.592592593	0.465421134	0.592592593	0.232710567	0.592592593	0.186168454	0.592592593
Run 15	0.62962963	0.62962963	0.494509955	0.62962963	0.247254977	0.62962963	0.197803982	0.62962963
Run 16	0.666666667	0.666666667	0.523598776	0.666666667	0.261799388	0.666666667	0.20943951	0.666666667
Run 17	0.703703704	0.703703704	0.552687596	0.703703704	0.276343798	0.703703704	0.221075039	0.703703704
Run 18	0.740740741	0.740740741	0.581776417	0.740740741	0.290888209	0.740740741	0.232710567	0.740740741
Run 19	0.777777778	0.777777778	0.610865238	0.777777778	0.305432619	0.777777778	0.244346095	0.777777778
Run 20	0.814814815	0.814814815	0.639954059	0.814814815	0.31997703	0.814814815	0.255981624	0.814814815
Run 21	0.851851852	0.851851852	0.66904288	0.851851852	0.33452144	0.851851852	0.267617152	0.851851852
Run 22	0.888888889	0.888888889	0.698131701	0.888888889	0.34906585	0.888888889	0.27925268	0.888888889
Run 23	0.925925926	0.925925926	0.727220522	0.925925926	0.363610261	0.925925926	0.290888209	0.925925926
Run 24	0.962962963	0.962962963	0.756309343	0.962962963	0.378154671	0.962962963	0.302523737	0.962962963
Run 25	1	1	0.785398163	1	0.392699082	1	0.314159265	1

	Qout (mL)	Time (mins)	Length Interval (m)	Flow Loss (Qout/Time/Length) (L/min/meter)	Normalized Flow Loss	Average Lugeon Value	Normalized Average Lugeon Value	Lugeon Value-Gauge 13	Lugeon Value-Gauge 12	Lugeon Value-Gauge 14
Run 0	5644	25	0.46	0.490782609	1	93.23377825	1	94.21820094	93.21607003	92.28706444
Run 1	5547	25	0.46	0.482347826	0.982813607	93.59919006	1.003919307	94.06158855	93.84198951	92.90212367
Run2	5305	25	0.46	0.461304348	0.939936215	93.18024801	0.999425849	93.85642886	92.20554624	93.49500361
Run 3	5125	25	0.46	0.445652174	0.90804394	92.05787521	0.987387586	93.17419484	91.83024395	91.19135951
Run 4	4662	25	0.46	0.405391304	0.826009922	88.84315239	0.952907348	88.59075707	89.72804434	88.22444055
Run 5	4461	25	0.46	0.387913043	0.790396882	89.45646325	0.959485553	90.25431444	89.13443095	88.99129238
Run 6	4104	25	0.46	0.356869565	0.72714387	85.98575983	0.922259737	85.49821879	87.1050928	85.37549407
Run 7	3527	25	0.46	0.306695652	0.62491141	81.83642769	0.877755136	83.2959403	81.80732253	80.45531274
Run 8	3395	25	0.46	0.295217391	0.601523742	82.44760509	0.884310457	84.20347727	81.77767072	81.41682055
Run 9	3151	25	0.46	0.274	0.558291991	82.67954134	0.886798142	84.20405655	82.70449743	81.18518519
Run 10	3095	25	0.46	0.269130435	0.54836995	84.90811908	0.910701257	86.84428357	84.97961313	82.98810817
Run 11	2796	25	0.46	0.243130435	0.495393338	80.95352989	0.868285416	82.33336769	81.91726239	78.7084606
Run 12	2538	25	0.46	0.220695652	0.449681077	77.99351591	0.836537115	79.44407926	78.67937689	75.94482181
Run 13	2511	25	0.46	0.218347826	0.444897236	79.30308454	0.85058319	82.24023581	79.60183233	76.29204266
Run 14	2263	25	0.46	0.196782609	0.400956768	77.09910227	0.826943879	79.31584389	75.71473978	76.36112095
Run 15	1986	25	0.46	0.172695652	0.351878101	77.72081556	0.833612206	78.24904947	79.18186711	75.81020728
Run 16	1902	25	0.46	0.165391304	0.336995039	76.71210777	0.822793082	78.1253209	76.64101221	75.41783144
Run 17	1639	25	0.46	0.142521739	0.290396882	76.11985355	0.816440725	76.46016048	77.58396251	74.3850413
Run 18	1621	25	0.46	0.140956522	0.287207654	81.05607921	0.869385331	84.60775615	81.57206119	77.32118581
Run 19	1476	25	0.46	0.128347826	0.261516655	79.01569429	0.847500721	82.3798627	78.50019944	76.39751553
Run 20	1266	25	0.46	0.110086957	0.224309001	75.00814662	0.804516861	77.52602572	75.45370564	72.23553578
Run 21	1181	25	0.46	0.102695652	0.20924876	74.54317845	0.79952974	75.79014921	74.0415661	73.82865002
Run 22	1158	25	0.46	0.100695652	0.205173636	74.51577615	0.79923583	79.85380823	73.28650085	70.96240463
Run 23	1087	25	0.46	0.094521739	0.192593905	74.64206828	0.800590405	77.03483222	74.42656624	72.59734188
Run 24	1040	25	0.46	0.090434783	0.184266478	75.88932806	0.813968172	78.6389414	75.11194569	74.06616102
Run 25	958	25	0.46	0.083304348	0.169737775	74.55639722	0.799671521	76.21623772	74.64547296	72.88219407

Figure C.11: Raw Data from S/D=1, Unit weight=13.35 kN/m^3

S/D=1.18									
	# of PVC Pipes	Pore Pressure-Gauge 13(kPa)	Pore Pressure-Gauge 12(kPa)	Pore Pressure-Gauge 14(kPa)	Avg. Pore Pressure (kPa)	Normalized Pore Pressure-Gauge 13(kPa)	Normalized Pore Pressure-Gauge 12(kPa)	Normalized Pore Pressure-Gauge 14(kPa)	Normalized Average Pore Pressure (kPa)
Run 0	0	5.264	5.276	5.301	5.280	1	1	1	1
Run 1	3	5.087	5.163	5.206	5.152	0.96637538	0.978582259	0.982078853	0.975695979
Run2	4	4.968	5.088	5.156	5.071	0.943768997	0.964366945	0.97264667	0.960292911
Run 3	5	4.850	4.923	4.964	4.912	0.921352584	0.933093252	0.936427089	0.93030743
Run 4	6	4.652	4.721	4.742	4.705	0.883738602	0.894806672	0.894548198	0.891042232
Run 5	7	4.396	4.432	4.468	4.432	0.835106383	0.840030326	0.842859838	0.839340951
Run 6	8	4.247	4.204	4.324	4.258	0.806800912	0.79681577	0.815695152	0.806451613
Run 7	9	3.939	4.007	4.175	4.040	0.748290274	0.759476876	0.787587248	0.765166341
Run 8	10	3.733	3.867	3.847	3.816	0.709156535	0.732941622	0.72571213	0.722618522
Run 9	11	3.487	3.561	3.598	3.549	0.662424012	0.674943139	0.67873986	0.672053532
Run 10	12	3.284	3.383	3.413	3.360	0.623860182	0.641205459	0.643840785	0.636323464
Run 11	13	3.109	3.196	3.299	3.201	0.590615502	0.605761941	0.622335408	0.606274856
Run 12	14	2.983	3.011	3.184	3.059	0.566679331	0.570697498	0.600641388	0.579382615
Run 13	15	2.504	2.557	2.626	2.562	0.475683891	0.48464746	0.495378231	0.485259769
Run 14	16	2.416	2.394	2.481	2.430	0.458966565	0.453752843	0.468024901	0.460261347
Run 15	17	2.216	2.009	2.085	2.103	0.420972644	0.380780895	0.393322015	0.398333439
Run 16	18	1.996	1.969	2.026	1.997	0.379179331	0.373199393	0.382192039	0.378195821
Run 17	19	1.685	1.750	1.712	1.716	0.320098784	0.331690675	0.322957932	0.324916356
Run 18	20	1.660	1.705	1.664	1.676	0.315349544	0.323161486	0.313903037	0.317467332
Run 19	21	1.517	1.467	1.539	1.508	0.288183891	0.278051554	0.290322581	0.285524904
Run 20	22	1.423	1.452	1.480	1.452	0.270326748	0.275208491	0.279192605	0.274919513
Run 21	23	1.468	1.380	1.422	1.423	0.27887538	0.261561789	0.268251273	0.26955369

	Slats		PVC Side By Side		PVC Pipe-Primary and Secondary-Touching		PVC Pipe-Primary and Secondary-Spacing of 0.5*Dia. of Pipe	
	Normalized Grouted Area Agc/Atotal	Area Replacement Ratio-Multiply by the inverse of Maximum Agc/Atotal	Normalized Grouted Area Agc/Atotal	Area Replacement Ratio-Multiply by the inverse of Maximum Agc/Atotal	Normalized Grouted Area Agc/Atotal	Area Replacement Ratio-Multiply by the inverse of Maximum Agc/Atotal	Normalized Grouted Area Agc/Atotal	Area Replacement Ratio-Multiply by the inverse of Maximum Agc/Atotal
Run 0	0	0	0	0	0	0	0	0
Run 1	0.111111111	0.130434783	0.087266463	0.130434783	0.043633231	0.130434783	0.034906585	0.130434783
Run2	0.148148148	0.173913043	0.116355283	0.173913043	0.058177642	0.173913043	0.046542113	0.173913043
Run 3	0.185185185	0.217391304	0.145444104	0.217391304	0.072722052	0.217391304	0.058177642	0.217391304
Run 4	0.222222222	0.260869565	0.174532925	0.260869565	0.087266463	0.260869565	0.06981317	0.260869565
Run 5	0.259259259	0.304347826	0.203621746	0.304347826	0.101810873	0.304347826	0.081448698	0.304347826
Run 6	0.296296296	0.347826087	0.232710567	0.347826087	0.116355283	0.347826087	0.093084227	0.347826087
Run 7	0.333333333	0.391304348	0.261799388	0.391304348	0.130899694	0.391304348	0.104719755	0.391304348
Run 8	0.37037037	0.434782609	0.290888209	0.434782609	0.145444104	0.434782609	0.116355283	0.434782609
Run 9	0.407407407	0.47826087	0.31997703	0.47826087	0.159988515	0.47826087	0.127990812	0.47826087
Run 10	0.444444444	0.52173913	0.34906585	0.52173913	0.174532925	0.52173913	0.13962634	0.52173913
Run 11	0.481481481	0.565217391	0.378154671	0.565217391	0.189077336	0.565217391	0.151261869	0.565217391
Run 12	0.518518519	0.608695652	0.407243492	0.608695652	0.203621746	0.608695652	0.162897397	0.608695652
Run 13	0.555555556	0.652173913	0.436332313	0.652173913	0.218166156	0.652173913	0.174532925	0.652173913
Run 14	0.592592593	0.695652174	0.465421134	0.695652174	0.232710567	0.695652174	0.186168454	0.695652174
Run 15	0.62962963	0.739130435	0.494509955	0.739130435	0.247254977	0.739130435	0.197803982	0.739130435
Run 16	0.666666667	0.782608696	0.523598776	0.782608696	0.261799388	0.782608696	0.20943951	0.782608696
Run 17	0.703703704	0.826086957	0.552687596	0.826086957	0.276343798	0.826086957	0.221075039	0.826086957
Run 18	0.740740741	0.869565217	0.581776417	0.869565217	0.290888209	0.869565217	0.232710567	0.869565217
Run 19	0.777777778	0.913043478	0.610865238	0.913043478	0.305432619	0.913043478	0.244346095	0.913043478
Run 20	0.814814815	0.956521739	0.639954059	0.956521739	0.31997703	0.956521739	0.255981624	0.956521739
Run 21	0.851851852	1	0.66904288	1	0.33452144	1	0.267617152	1

	Qout (mL)	Time (mins)	Length Interval (m)	Flow Loss (Qout/Time/Length) (L/min/meter)	Normalized Flow Loss	Average Lugeon Value	Normalized Average Lugeon Value	Lugeon Value-Gauge 13	Lugeon Value-Gauge 12	Lugeon Value-Gauge 14
Run 0	5617	25	0.46	0.488434783	1	92.50074792	1	92.78776265	92.5767215	92.14012122
Run 1	5592	25	0.46	0.48626087	0.995549226	94.38293276	1.02034778	95.58892659	94.18184574	93.40393192
Run2	5499	25	0.46	0.478173913	0.978992345	94.30198127	1.019472636	96.25078765	93.9807219	92.74125544
Run 3	5153	25	0.46	0.448086957	0.917393626	91.21672454	0.986118778	92.3890632	91.01908522	90.26731598
Run 4	5017	25	0.46	0.43626087	0.893181414	92.72282031	1.002400763	93.7792067	92.40857224	91.99933985
Run 5	4566	25	0.46	0.397043478	0.812889443	89.58562235	0.968485384	90.31926257	89.58562235	88.86380445
Run 6	4340	25	0.46	0.377391304	0.772654442	88.62418106	0.958091508	88.86067915	89.76957763	87.278285
Run 7	4050	25	0.46	0.352173913	0.721025458	87.16456886	0.942312044	89.406934	87.88967134	84.35303306
Run 8	3877	25	0.46	0.337130435	0.690226099	88.35426787	0.955173551	90.3108585	87.18138991	87.63463342
Run 9	3298	25	0.46	0.286782609	0.587146163	80.81418618	0.873659814	82.24336355	80.53429056	79.70611692
Run 10	3170	25	0.46	0.275652174	0.564358198	82.03933747	0.886904585	83.93793359	81.48157668	80.76536007
Run 11	2977	25	0.46	0.258869565	0.52999822	80.86304619	0.874188026	83.2645755	80.99798661	78.46910131
Run 12	2811	25	0.46	0.244434783	0.500445077	79.89805489	0.863755772	81.94260228	81.18059867	76.76971816
Run 13	2389	25	0.46	0.20773913	0.425316005	81.07420207	0.876470773	82.96291152	81.24330482	79.10857975
Run 14	2240	25	0.46	0.194782609	0.398789389	80.14645811	0.86644119	80.62194069	81.36282736	78.50971733
Run 15	1877	25	0.46	0.163217391	0.334164145	77.59939365	0.838905581	73.65405745	81.24310169	78.28172245
Run 16	1716	25	0.46	0.149217391	0.305501157	74.72077682	0.80778565	74.75821208	75.78333738	73.65122967
Run 17	1534	25	0.46	0.133391304	0.273099519	77.74896309	0.840522535	79.16397884	76.22360248	77.91548151
Run 18	1506	25	0.46	0.130956522	0.268114652	78.12081233	0.844542494	78.88947093	76.80734413	78.69983278
Run 19	1373	25	0.46	0.119391304	0.244436532	79.18945679	0.856095313	78.70224413	81.38466554	77.57719581
Run 20	1298	25	0.46	0.112869565	0.231084209	77.75170968	0.840552227	79.31803599	77.73386034	76.26321974
Run 21	1245	25	0.46	0.10826087	0.221648567	76.06150087	0.822279847	73.74718635	78.44990548	76.13281967

Figure C.12: Raw Data from S/D=1.18, Unit weight=13.35 kN/m^3

S/D=1.45									
	# of PVC Pipes	Pore Pressure-Gauge 13(kPa)	Pore Pressure-Gauge 12(kPa)	Pore Pressure-Gauge 14(kPa)	Avg. Pore Pressure (kPa)	Normalized Pore Pressure-Gauge 13(kPa)	Normalized Pore Pressure-Gauge 12(kPa)	Normalized Pore Pressure-Gauge 14(kPa)	Normalized Average Pore Pressure (kPa)
Run 0	0	5.188	5.217	5.236	5.214	1	1	1	1
Run 1	3	5.098	5.12	5.192	5.137	0.982652274	0.981406939	0.991596639	0.985231123
Run2	4	5.021	5.075	5.134	5.077	0.967810332	0.972781292	0.980519481	0.973722908
Run 3	5	4.899	4.941	5.008	4.949	0.944294526	0.947096032	0.956455309	0.949299917
Run 4	6	4.787	4.842	4.713	4.781	0.922706245	0.928119609	0.900114591	0.916949044
Run 5	7	4.492	4.473	4.509	4.491	0.865844256	0.857389304	0.861153552	0.861453871
Run 6	8	4.321	4.218	4.426	4.322	0.832883577	0.808510638	0.845301757	0.828911195
Run 7	9	4.11	4.087	4.215	4.137	0.792212799	0.783400422	0.80500382	0.793555399
Run 8	10	3.808	3.921	3.898	3.876	0.734001542	0.751581369	0.744461421	0.743366792
Run 9	11	3.603	3.689	3.621	3.638	0.694487278	0.707111367	0.691558442	0.697717537
Run 10	12	3.361	3.433	3.467	3.420	0.647841172	0.65804102	0.662146677	0.656032223
Run 11	13	3.206	3.255	3.35	3.270	0.617964534	0.623921794	0.639801375	0.627261684
Run 12	14	3.004	3.016	3.234	3.085	0.579028527	0.578110025	0.617647059	0.59165015
Run 13	15	2.967	2.991	3.018	2.992	0.571896685	0.573317999	0.576394194	0.573876351
Run 14	16	2.793	2.852	2.832	2.826	0.538357749	0.546674334	0.540870894	0.54197302
Run 15	17	2.488	2.435	2.483	2.469	0.479568234	0.466743339	0.47421696	0.473499137
Run 16	18	2.022	2.148	2.091	2.087	0.389745567	0.41173088	0.399350649	0.400294099
Run 17	19	1.796	1.817	1.854	1.822	0.3461835	0.348284455	0.354087089	0.349530081

	Slats		PVC Side By Side		PVC Pipe-Primary and Secondary-Touching		PVC Pipe-Primary and Secondary-Spacing of 0.5*Dia. of Pipe	
	Normalized Grouted Area Agc/Atotal	Area Replacement Ratio-Multiply by the inverse of Maximum Agc/Atotal	Normalized Grouted Area Agc/Atotal	Area Replacement Ratio-Multiply by the inverse of Maximum Agc/Atotal	Normalized Grouted Area Agc/Atotal	Area Replacement Ratio-Multiply by the inverse of Maximum Agc/Atotal	Normalized Grouted Area Agc/Atotal	Area Replacement Ratio-Multiply by the inverse of Maximum Agc/Atotal
Run 0	0	0	0	0	0	0	0	0
Run 1	0.111111111	0.157894737	0.087266463	0.157894737	0.043633231	0.157894737	0.034906585	0.157894737
Run2	0.148148148	0.210526316	0.116355283	0.210526316	0.058177642	0.210526316	0.046542113	0.210526316
Run 3	0.185185185	0.263157895	0.145444104	0.263157895	0.072722052	0.263157895	0.058177642	0.263157895
Run 4	0.222222222	0.315789474	0.174532925	0.315789474	0.087266463	0.315789474	0.06981317	0.315789474
Run 5	0.259259259	0.368421053	0.203621746	0.368421053	0.101810873	0.368421053	0.081448698	0.368421053
Run 6	0.296296296	0.421052632	0.232710567	0.421052632	0.116355283	0.421052632	0.093084227	0.421052632
Run 7	0.333333333	0.473684211	0.261799388	0.473684211	0.130899694	0.473684211	0.104719755	0.473684211
Run 8	0.37037037	0.526315789	0.290888209	0.526315789	0.145444104	0.526315789	0.116355283	0.526315789
Run 9	0.407407407	0.578947368	0.31997703	0.578947368	0.159988515	0.578947368	0.127990812	0.578947368
Run 10	0.444444444	0.631578947	0.34906585	0.631578947	0.174532925	0.631578947	0.13962634	0.631578947
Run 11	0.481481481	0.684210526	0.378154671	0.684210526	0.189077336	0.684210526	0.151261869	0.684210526
Run 12	0.518518519	0.736842105	0.407243492	0.736842105	0.203621746	0.736842105	0.162897397	0.736842105
Run 13	0.555555556	0.789473684	0.436332313	0.789473684	0.218166156	0.789473684	0.174532925	0.789473684
Run 14	0.592592593	0.842105263	0.465421134	0.842105263	0.232710567	0.842105263	0.186168454	0.842105263
Run 15	0.62962963	0.894736842	0.494509955	0.894736842	0.247254977	0.894736842	0.197803982	0.894736842
Run 16	0.666666667	0.947368421	0.523598776	0.947368421	0.261799388	0.947368421	0.20943951	0.947368421
Run 17	0.703703704	1	0.552687596	1	0.276343798	1	0.221075039	1

	Qout (mL)	Time (mins)	Length Interval (m)	Flow Loss (Qout/Time/Length) (L/min/meter)	Normalized Flow Loss	Average Lugeon Value	Normalized Average Lugeon Value	Lugeon Value-Gauge 13	Lugeon Value-Gauge 12	Lugeon Value-Gauge 14
Run 0	5546	25	0.46	0.48226087	1	92.4993676	1	92.95699105	92.44026635	92.10482612
Run 1	5393	25	0.46	0.468956522	0.97241255	91.29588353	0.986989272	91.98833302	91.59307065	90.3229048
Run2	5256	25	0.46	0.457043478	0.947710061	90.0282623	0.973285165	91.02638484	90.05782823	89.0228824
Run 3	4976	25	0.46	0.432695652	0.897223224	87.42503748	0.945142002	88.32326029	87.57248577	86.40088901
Run 4	4851	25	0.46	0.421826087	0.874684457	88.23582909	0.953907377	88.11909065	87.11815096	89.50267069
Run 5	4508	25	0.46	0.392	0.812838082	87.27920439	0.943565417	87.26625111	87.63693271	86.93723664
Run 6	4332	25	0.46	0.376695652	0.781103498	87.16443938	0.942324706	87.17788757	89.306698	85.10972711
Run 7	4139	25	0.46	0.359913043	0.746303642	86.99155095	0.940455629	87.57008357	88.06289295	85.38862241
Run 8	3770	25	0.46	0.327826087	0.679769203	84.58572812	0.914446556	86.08878334	83.6077753	84.10109978
Run 9	3514	25	0.46	0.305565217	0.633609809	84.00033466	0.908117935	84.80855326	82.83144955	84.38696973
Run 10	3333	25	0.46	0.289826087	0.600973675	84.73621098	0.916073409	86.23209966	84.4235616	83.59564089
Run 11	3065	25	0.46	0.266521739	0.552650559	81.49681148	0.881052634	83.13217066	81.88071863	79.5587281
Run 12	2779	25	0.46	0.241652174	0.501081861	78.33980135	0.846922562	80.44346668	80.12339984	74.72237907
Run 13	2629	25	0.46	0.228608696	0.474035341	76.40664962	0.826023481	77.05045354	76.43219514	75.7484081
Run 14	2510	25	0.46	0.21826087	0.452578435	77.24225654	0.835057131	78.14567475	76.52905665	77.06951609
Run 15	2240	25	0.46	0.194782609	0.403894699	78.90194789	0.852999863	78.28882986	79.99285778	78.44647954
Run 16	1874	25	0.46	0.162956522	0.33790119	78.08170663	0.844132329	80.5917516	75.86430249	77.93233943
Run 17	1664	25	0.46	0.144695652	0.300036062	79.40130904	0.858398399	80.56550789	79.63437104	78.04511983

Figure C.13: Raw Data from S/D=1.45, Unit weight=13.35 kN/m^3

S/D=1.62

	# of PVC Pipes	Pore Pressure-Gauge 13(kPa)	Pore Pressure-Gauge 12(kPa)	Pore Pressure-Gauge 14(kPa)	Avg. Pore Pressure (kPa)	Normalized Pore Pressure-Gauge 13(kPa)	Normalized Pore Pressure-Gauge 12(kPa)	Normalized Pore Pressure-Gauge 14(kPa)	Normalized Average Pore Pressure (kPa)
Run 0	0	5.203	5.196	5.238	5.212	1	1	1	1
Run 1	3	5.146	5.164	5.213	5.174	0.989044782	0.993841416	0.995227186	0.992709599
Run2	4	5.111	5.128	5.184	5.141	0.982317894	0.98691301	0.989690722	0.98631451
Run 3	5	5.064	5.076	5.097	5.079	0.973284643	0.976905312	0.973081329	0.974419646
Run 4	6	4.868	4.787	4.854	4.836	0.935614069	0.921285604	0.926689576	0.927863401
Run 5	7	4.602	4.593	4.631	4.609	0.884489717	0.883949192	0.884116075	0.884184946
Run 6	8	4.336	4.461	4.534	4.444	0.833365366	0.858545035	0.865597556	0.852529258
Run 7	9	4.215	4.109	4.278	4.201	0.810109552	0.790800616	0.81672394	0.805909062
Run 8	10	3.897	4.002	3.956	3.952	0.748990967	0.770207852	0.755250095	0.75813775
Run 9	11	3.749	3.843	3.653	3.748	0.720545839	0.73960739	0.697403589	0.71912771
Run 10	12	3.532	3.496	3.517	3.515	0.678839131	0.67282525	0.671439481	0.67436209
Run 11	13	3.298	3.317	3.452	3.356	0.633865078	0.638375674	0.659030164	0.643793567
Run 12	14	3.264	3.222	3.38	3.289	0.627330386	0.620092379	0.64528446	0.630939439
Run 13	15	3.093	3.204	3.209	3.169	0.594464732	0.616628176	0.612638412	0.60791712
Run 14	16	2.899	2.918	2.913	2.910	0.557178551	0.561585835	0.556128293	0.558291232
Run 15	17	2.671	2.716	2.687	2.691	0.513357678	0.522709777	0.512982054	0.516339451

	Slats		PVC Side By Side		PVC Pipe-Primary and Secondary-Touching		PVC Pipe-Primary and Secondary-Spacing of 0.5*Dia. of Pipe	
	Normalized Grouted Area Agc/Atotal	Area Replacement Ratio-Multiply by the inverse of Maximum Agc/Atotal	Normalized Grouted Area Agc/Atotal	Area Replacement Ratio-Multiply by the inverse of Maximum Agc/Atotal	Normalized Grouted Area Agc/Atotal	Area Replacement Ratio-Multiply by the inverse of Maximum Agc/Atotal	Normalized Grouted Area Agc/Atotal	Area Replacement Ratio-Multiply by the inverse of Maximum Agc/Atotal
Run 0	0	0	0	0	0	0	0	0
Run 1	0.111111111	0.176470588	0.087266463	0.176470588	0.043633231	0.176470588	0.034906585	0.176470588
Run2	0.148148148	0.235294118	0.116355283	0.235294118	0.058177642	0.235294118	0.046542113	0.235294118
Run 3	0.185185185	0.294117647	0.145444104	0.294117647	0.072722052	0.294117647	0.058177642	0.294117647
Run 4	0.222222222	0.352941176	0.174532925	0.352941176	0.087266463	0.352941176	0.06981317	0.352941176
Run 5	0.259259259	0.411764706	0.203621746	0.411764706	0.101810873	0.411764706	0.081448698	0.411764706
Run 6	0.296296296	0.470588235	0.232710567	0.470588235	0.116355283	0.470588235	0.093084227	0.470588235
Run 7	0.333333333	0.529411765	0.261799388	0.529411765	0.130899694	0.529411765	0.104719755	0.529411765
Run 8	0.37037037	0.588235294	0.290888209	0.588235294	0.145444104	0.588235294	0.116355283	0.588235294
Run 9	0.407407407	0.647058824	0.31997703	0.647058824	0.159988515	0.647058824	0.127990812	0.647058824
Run 10	0.444444444	0.705882353	0.34906585	0.705882353	0.174532925	0.705882353	0.13962634	0.705882353
Run 11	0.481481481	0.764705882	0.378154671	0.764705882	0.189077336	0.764705882	0.151261869	0.764705882
Run 12	0.518518519	0.823529412	0.407243492	0.823529412	0.203621746	0.823529412	0.162897397	0.823529412
Run 13	0.555555556	0.882352941	0.436332313	0.882352941	0.218166157	0.882352941	0.174532925	0.882352941
Run 14	0.592592593	0.941176471	0.465421134	0.941176471	0.232710567	0.941176471	0.186168454	0.941176471
Run 15	0.62962963	1	0.494509955	1	0.247254977	1	0.197803982	1

	Qout (mL)	Time (mins)	Length Interval (m)	Flow Loss (Qout/Time/Length) (L/min/meter)	Normalized Flow Loss	Average Lugeon Value	Normalized Average Lugeon Value	Lugeon Value-Gauge 13	Lugeon Value-Gauge 12	Lugeon Value-Gauge 14
Run 0	5574	25	0.46	0.484695652	1	92.99014878	1	93.15695794	93.28245808	92.53448877
Run 1	5443	25	0.46	0.473304348	0.976498027	91.47156113	0.983669371	91.9751939	91.65459873	90.79308418
Run2	5282	25	0.46	0.459304348	0.947613922	89.34144093	0.960762426	89.86584775	89.56793054	88.60037574
Run 3	5176	25	0.46	0.450086957	0.928597058	88.61723893	0.952974483	88.87973075	88.66961318	88.30428811
Run 4	4866	25	0.46	0.423130435	0.872981701	87.4899238	0.94085153	86.92079597	88.39156774	87.1714946
Run 5	4553	25	0.46	0.395913043	0.816828131	85.90620067	0.923820445	86.0306483	86.19922566	85.49191179
Run 6	4417	25	0.46	0.384086957	0.792429135	86.43469129	0.929503742	88.58094016	86.09884701	84.7126062
Run 7	4171	25	0.46	0.362695652	0.748295658	86.34240252	0.928511285	86.04879055	88.26859386	84.78159237
Run 8	3910	25	0.46	0.34	0.701471116	86.03964572	0.92525549	87.24659995	84.95752124	85.94539939
Run 9	3724	25	0.46	0.323826087	0.668101902	86.39201964	0.929044859	86.37665696	84.26387899	88.64661565
Run 10	3412	25	0.46	0.296695652	0.612127736	84.4084359	0.907713742	84.00216653	84.8671774	84.36043565
Run 11	3287	25	0.46	0.285826087	0.589702189	85.17713925	0.915980245	86.66649089	86.17005938	82.80014107
Run 12	3151	25	0.46	0.274	0.565303193	83.3164403	0.89597061	83.94607843	85.04034761	81.06508876
Run 13	2938	25	0.46	0.255478261	0.527090061	80.62642359	0.867042635	82.59885576	79.73728492	79.61304483
Run 14	2732	25	0.46	0.237565217	0.490132759	81.63753175	0.877915917	81.94729817	81.41371398	81.55345602
Run 15	2513	25	0.46	0.218521739	0.450843201	81.1946021	0.873152728	81.81270653	80.45719408	81.32554489

Figure C.14: Raw Data from S/D=1.62, Unit weight=13.35 kN/m^3

S/D=2.17									
	# of PVC Pipes	Pore Pressure-Gauge 13(kPa)	Pore Pressure-Gauge 12(kPa)	Pore Pressure-Gauge 14(kPa)	Avg. Pore Pressure (kPa)	Normalized Pore Pressure-Gauge 13(kPa)	Normalized Pore Pressure-Gauge 12(kPa)	Normalized Pore Pressure-Gauge 14(kPa)	Normalized Average Pore Pressure (kPa)
Run 0	0	5.198	5.214	5.231	5.214	1	1	1	1
Run 1	3	5.16	5.173	5.198	5.177	0.992689496	0.992136555	0.993691455	0.992840248
Run2	4	5.142	5.184	5.165	5.164	0.989226626	0.99424626	0.98738291	0.990283194
Run 3	5	5.087	5.166	5.090	5.114	0.978645633	0.990794016	0.973045307	0.980822093
Run 4	6	4.954	4.981	5.052	4.996	0.953058869	0.95531262	0.965780921	0.95806431
Run 5	7	4.673	4.632	4.810	4.705	0.898999615	0.888377445	0.919518257	0.902320527
Run 6	8	4.468	4.568	4.603	4.546	0.85956137	0.8761028	0.879946473	0.871891581
Run 7	9	4.307	4.293	4.494	4.365	0.828587918	0.823360184	0.859109157	0.837051716
Run 8	10	4.165	4.221	4.386	4.257	0.801269719	0.809551208	0.838463009	0.81646743
Run 9	11	3.919	3.876	3.897	3.897	0.753943825	0.743383199	0.744981839	0.747426964
Run 10	12	3.591	3.518	3.503	3.537	0.690842632	0.674721903	0.669661633	0.678386499
Run 11	13	3.31	3.394	3.312	3.339	0.636783378	0.650939778	0.633148538	0.64028639

	Slats		PVC Side By Side		PVC Pipe-Primary and Secondary-Touching		PVC Pipe-Primary and Secondary-Spacing of 0.5*Dia. of Pipe	
	Normalized Grouted Area Agc/Atotal	Area Replacement Ratio-Multiply by the inverse of Maximum Agc/Atotal	Normalized Grouted Area Agc/Atotal	Area Replacement Ratio-Multiply by the inverse of Maximum Agc/Atotal	Normalized Grouted Area Agc/Atotal	Area Replacement Ratio-Multiply by the inverse of Maximum Agc/Atotal	Normalized Grouted Area Agc/Atotal	Area Replacement Ratio-Multiply by the inverse of Maximum Agc/Atotal
Run 0	0	0	0	0	0	0	0	0
Run 1	0.111111111	0.230769231	0.087266463	0.230769231	0.043633231	0.230769231	0.034906585	0.230769231
Run2	0.148148148	0.307692308	0.116355283	0.307692308	0.058177642	0.307692308	0.046542113	0.307692308
Run 3	0.185185185	0.384615385	0.145444104	0.384615385	0.072722052	0.384615385	0.058177642	0.384615385
Run 4	0.222222222	0.461538462	0.174532925	0.461538462	0.087266463	0.461538462	0.06981317	0.461538462
Run 5	0.259259259	0.538461538	0.203621746	0.538461538	0.101810873	0.538461538	0.081448698	0.538461538
Run 6	0.296296296	0.615384615	0.232710567	0.615384615	0.116355283	0.615384615	0.093084227	0.615384615
Run 7	0.333333333	0.692307692	0.261799388	0.692307692	0.130899694	0.692307692	0.104719755	0.692307692
Run 8	0.37037037	0.769230769	0.290888209	0.769230769	0.145444104	0.769230769	0.116355283	0.769230769
Run 9	0.407407407	0.846153846	0.31997703	0.846153846	0.159988515	0.846153846	0.127990812	0.846153846
Run 10	0.444444444	0.923076923	0.34906585	0.923076923	0.174532925	0.923076923	0.13962634	0.923076923
Run 11	0.481481481	1	0.378154671	1	0.189077336	1	0.151261869	1

	Qout (mL)	Time (mins)	Length Interval (m)	Flow Loss (Qout/Time/Length) (L/min/meter)	Normalized Flow Loss	Average Lugeon Value	Normalized Average Lugeon Value	Lugeon Value-Gauge 13	Lugeon Value-Gauge 12	Lugeon Value-Gauge 14
Run 0	5636	25	0.46	0.490086957	1	93.98842099	1	94.28375462	93.99442971	93.68896129
Run 1	5614	25	0.46	0.488173913	0.996096522	94.29668013	1.003279757	94.60734749	94.36959463	93.91572009
Run2	5593	25	0.46	0.486347826	0.992370476	94.18652626	1.002107762	94.58339675	93.81709608	94.16221221
Run 3	5514	25	0.46	0.479478261	0.978353442	93.75185965	0.99748308	94.25560465	92.81422007	94.20005125
Run 4	5326	25	0.46	0.463130435	0.944996451	92.70643253	0.986360145	93.48615963	92.97940871	91.67269097
Run 5	4949	25	0.46	0.430347826	0.878105039	91.46606293	0.973163098	92.09240875	92.90756176	89.46940251
Run 6	4779	25	0.46	0.415565217	0.847941803	91.40667587	0.972531243	93.00922502	90.97312115	90.28138549
Run 7	4494	25	0.46	0.390782609	0.797374024	89.53320804	0.952598279	90.73197323	91.02786133	86.95652174
Run 8	4335	25	0.46	0.376956522	0.769162527	88.54287232	0.942061494	90.50576752	89.30502766	85.94539939
Run 9	3952	25	0.46	0.343652174	0.701206529	88.17623347	0.9381606	87.68874047	88.66155158	88.1837757
Run 10	3565	25	0.46	0.31	0.632540809	87.63663777	0.932419513	86.32692843	88.11824901	88.49557522
Run 11	3429	25	0.46	0.298173913	0.60841022	89.30927907	0.950215762	90.08275319	87.85324486	90.02835539

Figure C.15: Raw Data from S/D=2.17, Unit weight=13.35 kN/m^3

S/D=1

	# of PVC Pipes	Pore Pressure-Gauge 13(kPa)	Pore Pressure-Gauge 12(kPa)	Pore Pressure-Gauge 14(kPa)	Avg. Pore Pressure (kPa)	Normalized Pore Pressure-Gauge 13(kPa)	Normalized Pore Pressure-Gauge 12(kPa)	Normalized Pore Pressure-Gauge 14(kPa)	Normalized Average Pore Pressure (kPa)
Run 0	0	5.231	5.187	5.248	5.222	1	1	1	1
Run 1	3	5.187	5.136	5.209	5.177	0.991588606	0.990167727	0.992568598	0.991446445
Run2	4	4.918	4.912	4.922	4.917	0.940164405	0.946982842	0.937881098	0.941657092
Run 3	5	4.756	4.807	4.827	4.797	0.909195183	0.926739927	0.919778963	0.918549726
Run 4	6	4.553	4.486	4.531	4.523	0.870388071	0.864854444	0.863376524	0.866207073
Run 5	7	4.265	4.333	4.294	4.297	0.815331677	0.835357625	0.818216463	0.822928635
Run 6	8	4.025	3.935	3.999	3.986	0.769451348	0.758627338	0.762004573	0.763372909
Run 7	9	3.651	3.706	3.757	3.705	0.697954502	0.714478504	0.715891768	0.709434444
Run 8	10	3.427	3.527	3.595	3.516	0.655132862	0.679969154	0.685022866	0.67336908
Run 9	11	3.218	3.342	3.401	3.320	0.615178742	0.644303065	0.648056402	0.635835567
Run 10	12	3.055	3.154	3.265	3.158	0.584018352	0.608058608	0.622141768	0.604749138
Run 11	13	2.906	2.931	3.064	2.967	0.555534315	0.565066512	0.583841463	0.568173114
Run 12	14	2.691	2.792	2.852	2.778	0.514433187	0.538268749	0.543445122	0.532043917
Run 13	15	2.474	2.548	2.659	2.560	0.472949723	0.49122807	0.506669207	0.490297459
Run 14	16	2.207	2.351	2.438	2.332	0.421907857	0.453248506	0.464557927	0.446572195
Run 15	17	2.015	1.935	1.994	1.981	0.385203594	0.373048005	0.379954268	0.379420401
Run 16	18	1.854	1.922	1.909	1.895	0.35442554	0.370541739	0.363757622	0.362887782
Run 17	19	1.805	1.800	1.887	1.831	0.345058306	0.3470214	0.359565549	0.350568109
Run 18	20	1.557	1.689	1.750	1.665	0.297648633	0.325621747	0.333460366	0.318907188
Run 19	21	1.501	1.557	1.652	1.570	0.286943223	0.300173511	0.314786585	0.300651092
Run 20	22	1.413	1.494	1.595	1.501	0.270120436	0.288027762	0.303925305	0.287373931
Run 21	23	1.374	1.368	1.508	1.417	0.262664882	0.263736264	0.287347561	0.27128814
Run 22	24	1.179	1.255	1.310	1.248	0.225387115	0.241951031	0.249618902	0.238988893
Run 23	25	1.055	1.157	1.152	1.121	0.201682279	0.223057644	0.219512195	0.214732542
Run 24	26	1.000	1.031	1.099	1.043	0.191168037	0.198766146	0.20941311	0.199795736
Run 25	27	0.988	0.976	1.023	0.996	0.18887402	0.188162714	0.194931402	0.190667688

	Slats		PVC Side By Side		PVC Pipe-Primary and Secondary-Touching		PVC Pipe-Primary and Secondary-Spacing of 0.5*Dia. of Pipe	
	Normalized Grouted Area Agc/Atotal	Area Replacement Ratio-Multiply by the inverse of Maximum Agc/Atotal	Normalized Grouted Area Agc/Atotal	Area Replacement Ratio-Multiply by the inverse of Maximum Agc/Atotal	Normalized Grouted Area Agc/Atotal	Area Replacement Ratio-Multiply by the inverse of Maximum Agc/Atotal	Normalized Grouted Area Agc/Atotal	Area Replacement Ratio-Multiply by the inverse of Maximum Agc/Atotal
Run 0	0	0	0	0	0	0	0	0
Run 1	0.111111111	0.111111111	0.087266463	0.111111111	0.043633231	0.111111111	0.034906585	0.111111111
Run2	0.148148148	0.148148148	0.116355283	0.148148148	0.058177642	0.148148148	0.046542113	0.148148148
Run 3	0.185185185	0.185185185	0.145444104	0.185185185	0.072722052	0.185185185	0.058177642	0.185185185
Run 4	0.222222222	0.222222222	0.174532925	0.222222222	0.087266463	0.222222222	0.06981317	0.222222222
Run 5	0.259259259	0.259259259	0.203621746	0.259259259	0.101810873	0.259259259	0.081448698	0.259259259
Run 6	0.296296296	0.296296296	0.232710567	0.296296296	0.116355283	0.296296296	0.093084227	0.296296296
Run 7	0.333333333	0.333333333	0.261799388	0.333333333	0.130899694	0.333333333	0.104719755	0.333333333
Run 8	0.37037037	0.37037037	0.290888209	0.37037037	0.145444104	0.37037037	0.116355283	0.37037037
Run 9	0.407407407	0.407407407	0.31997703	0.407407407	0.159988515	0.407407407	0.127990812	0.407407407
Run 10	0.444444444	0.444444444	0.34906585	0.444444444	0.174532925	0.444444444	0.13962634	0.444444444
Run 11	0.481481481	0.481481481	0.378154671	0.481481481	0.189077336	0.481481481	0.151261869	0.481481481
Run 12	0.518518519	0.518518519	0.407243492	0.518518519	0.203621746	0.518518519	0.162897397	0.518518519
Run 13	0.555555556	0.555555556	0.436332313	0.555555556	0.218166156	0.555555556	0.174532925	0.555555556
Run 14	0.592592593	0.592592593	0.465421134	0.592592593	0.232710567	0.592592593	0.186168454	0.592592593
Run 15	0.62962963	0.62962963	0.494509955	0.62962963	0.247254977	0.62962963	0.197803982	0.62962963
Run 16	0.666666667	0.666666667	0.523598776	0.666666667	0.261799388	0.666666667	0.20943951	0.666666667
Run 17	0.703703704	0.703703704	0.552687596	0.703703704	0.276343798	0.703703704	0.221075039	0.703703704
Run 18	0.740740741	0.740740741	0.581776417	0.740740741	0.290888209	0.740740741	0.232710567	0.740740741
Run 19	0.777777778	0.777777778	0.610865238	0.777777778	0.305432619	0.777777778	0.244346095	0.777777778
Run 20	0.814814815	0.814814815	0.639954059	0.814814815	0.31997703	0.814814815	0.255981624	0.814814815
Run 21	0.851851852	0.851851852	0.66904288	0.851851852	0.33452144	0.851851852	0.267617152	0.851851852
Run 22	0.888888889	0.888888889	0.698131701	0.888888889	0.34906585	0.888888889	0.27925268	0.888888889
Run 23	0.925925926	0.925925926	0.727220522	0.925925926	0.363610261	0.925925926	0.290888209	0.925925926
Run 24	0.962962963	0.962962963	0.756309343	0.962962963	0.378154671	0.962962963	0.302523737	0.962962963
Run 25	1	1	0.785398163	1	0.392699082	1	0.314159265	1

	Qout (mL)	Time (mins)	Length Interval (m)	Flow Loss (Qout/Time/Length) (L/min/meter)	Normalized Flow Loss	Average Lugeon Value	Normalized Average Lugeon Value	Lugeon Value-Gauge 13	Lugeon Value-Gauge 12	Lugeon Value-Gauge 14
Run 0	5525	25	0.46	0.480434783	1	92.00206484	1	91.84377416	92.6228615	91.54626193
Run 1	5449	25	0.46	0.473826087	0.986244344	91.51933176	0.994753019	91.34877327	92.25585805	90.96296544
Run2	5211	25	0.46	0.453130435	0.943167421	92.14962746	1.001603906	92.13713599	92.24968135	92.06225818
Run 3	5003	25	0.46	0.435043478	0.905520362	90.69704203	0.985815288	91.4725564	90.50207578	90.12709307
Run 4	4557	25	0.46	0.39626087	0.82479638	87.60372945	0.95219308	87.03291666	88.33278412	87.45549979
Run 5	4462	25	0.46	0.388	0.80760181	90.28855104	0.981375268	90.97303634	89.54534964	90.35863996
Run 6	3952	25	0.46	0.343652174	0.715294118	86.20758606	0.937017949	85.37942209	87.33219159	85.93452711
Run 7	3614	25	0.46	0.31426087	0.654117647	84.8283794	0.922026908	86.0752861	84.79786011	83.64675794
Run 8	3318	25	0.46	0.288521739	0.600542986	82.05187386	0.891848178	84.19076135	81.8037253	80.25639475
Run 9	3184	25	0.46	0.276869565	0.576289593	83.38607526	0.906350041	86.03777664	82.84547134	81.40828145
Run 10	2917	25	0.46	0.253652174	0.527963801	80.32051106	0.873029439	83.02853483	80.422376	77.68826154
Run 11	2774	25	0.46	0.241217391	0.502081448	81.30009818	0.883676886	83.00667285	82.29866643	78.72630265
Run 12	2537	25	0.46	0.220608696	0.45918552	79.40324978	0.863059432	81.98019162	79.01457581	77.35227758
Run 13	2254	25	0.46	0.196	0.407963801	76.55253222	0.832074067	79.22392886	76.92307692	73.71192178
Run 14	2163	25	0.46	0.188086957	0.391493213	80.6547841	0.87666276	85.22290735	80.00295896	77.14805436
Run 15	1859	25	0.46	0.161652174	0.336470588	81.58757095	0.88680152	80.22440393	83.54117515	81.06929484
Run 16	1697	25	0.46	0.147565217	0.307149321	77.87082712	0.846403037	79.59288964	76.77690811	77.29974719
Run 17	1601	25	0.46	0.139217391	0.289773756	76.04737325	0.826583331	77.12874865	77.34299517	73.77710191
Run 18	1415	25	0.46	0.123043478	0.256108597	73.88519511	0.803081923	79.0259976	72.84989832	70.31055901
Run 19	1295	25	0.46	0.112608696	0.23438914	71.72528385	0.779605153	75.0224488	72.32414621	68.16507001
Run 20	1200	25	0.46	0.104347826	0.21719457	69.53431325	0.75579079	73.84842611	69.84459577	65.42183454
Run 21	1200	25	0.46	0.104347826	0.21719457	73.657289	0.800604738	75.94456047	76.27765065	69.19617115
Run 22	890	25	0.46	0.077391304	0.161085973	62.0122631	0.67403121	65.64147951	61.66637797	59.07733156
Run 23	847	25	0.46	0.073652174	0.153303167	65.6826759	0.713926106	69.81248712	63.65788584	63.93417874
Run 24	785	25	0.46	0.06826087	0.142081448	65.42575358	0.711133535	68.26086957	66.20840889	62.11180124
Run 25	756	25	0.46	0.06573913	0.136832579	66.02523981	0.717649543	66.53758141	67.35566643	64.26112457

Figure C.16: Raw Data from S/D=1, Unit weight=13.82 kN/m^3

S/D=1.18	# of PVC Pipes	Pore Pressure-Gauge 13(kPa)	Pore Pressure-Gauge 12(kPa)	Pore Pressure-Gauge 14(kPa)	Avg. Pore Pressure (kPa)	Normalized Pore Pressure-Gauge 13(kPa)	Normalized Pore Pressure-Gauge 12(kPa)	Normalized Pore Pressure-Gauge 14(kPa)	Normalized Average Pore Pressure (kPa)
Run 0	0	5.174	5.187	5.265	5.209	1	1	1	1
Run 1	3	5.138	5.158	5.174	5.157	0.993042134	0.9944091	0.982716049	0.990016639
Run2	4	4.947	5.021	4.989	4.986	0.956126788	0.967996915	0.947578348	0.95718674
Run 3	5	4.802	4.887	4.901	4.863	0.928102049	0.9421631	0.930864198	0.933700243
Run 4	6	4.604	4.613	4.658	4.625	0.889833784	0.889338731	0.884710351	0.887943172
Run 5	7	4.361	4.382	4.417	4.387	0.842868187	0.844804318	0.838936372	0.8421861
Run 6	8	4.208	4.152	4.173	4.178	0.813297256	0.800462695	0.792592593	0.802060668
Run 7	9	3.699	3.799	3.766	3.755	0.714920758	0.732407943	0.715289649	0.720849866
Run 8	10	3.538	3.596	3.641	3.592	0.683803634	0.693271641	0.691547958	0.689555868
Run 9	11	3.296	3.381	3.425	3.367	0.63703131	0.651821862	0.650522317	0.646486625
Run 10	12	3.110	3.184	3.302	3.199	0.601082335	0.613842298	0.627160494	0.614104697
Run 11	13	2.985	3.003	3.105	3.031	0.576923077	0.578947368	0.58974359	0.581914757
Run 12	14	2.822	2.841	2.947	2.870	0.545419405	0.547715442	0.559734093	0.551004736
Run 13	15	2.553	2.575	2.688	2.605	0.493428682	0.496433391	0.510541311	0.500191988
Run 14	16	2.387	2.452	2.502	2.447	0.461345187	0.472720262	0.475213675	0.469793933
Run 15	17	2.043	2.118	2.121	2.094	0.39485891	0.408328514	0.402849003	0.402022271
Run 16	18	1.935	1.941	1.990	1.955	0.373985311	0.374204743	0.377967711	0.375399974
Run 17	19	1.655	1.649	1.716	1.673	0.319868574	0.31791016	0.325925926	0.321259439
Run 18	20	1.549	1.628	1.684	1.620	0.299381523	0.313861577	0.319848053	0.311084091
Run 19	21	1.495	1.520	1.628	1.548	0.288944724	0.293040293	0.309211776	0.297132983
Run 20	22	1.490	1.456	1.575	1.507	0.287978353	0.280701754	0.299145299	0.289325483
Run 21	23	1.468	1.432	1.494	1.465	0.283726324	0.276074802	0.283760684	0.281198003

	Slats		PVC Side By Side		PVC Pipe-Primary and Secondary-Touching		PVC Pipe-Primary and Secondary-Spacing of 0.5*Dia. of Pipe	
	Normalized Grouted Area Agc/Atotal	Area Replacement Ratio-Multiply by the inverse of Maximum Agc/Atotal	Normalized Grouted Area Agc/Atotal	Area Replacement Ratio-Multiply by the inverse of Maximum Agc/Atotal	Normalized Grouted Area Agc/Atotal	Area Replacement Ratio-Multiply by the inverse of Maximum Agc/Atotal	Normalized Grouted Area Agc/Atotal	Area Replacement Ratio-Multiply by the inverse of Maximum Agc/Atotal
Run 0	0	0	0	0	0	0	0	0
Run 1	0.111111111	0.130434783	0.087266463	0.130434783	0.043633231	0.130434783	0.034906585	0.130434783
Run2	0.148148148	0.173913043	0.116355283	0.173913043	0.058177642	0.173913043	0.046542113	0.173913043
Run 3	0.185185185	0.217391304	0.145444104	0.217391304	0.072722052	0.217391304	0.058177642	0.217391304
Run 4	0.222222222	0.260869565	0.174532925	0.260869565	0.087266463	0.260869565	0.06981317	0.260869565
Run 5	0.259259259	0.304347826	0.203621746	0.304347826	0.101810873	0.304347826	0.081448698	0.304347826
Run 6	0.296296296	0.347826087	0.232710567	0.347826087	0.116355283	0.347826087	0.093084227	0.347826087
Run 7	0.333333333	0.391304348	0.261799388	0.391304348	0.130899694	0.391304348	0.104719755	0.391304348
Run 8	0.37037037	0.434782609	0.290888209	0.434782609	0.145444104	0.434782609	0.116355283	0.434782609
Run 9	0.407407407	0.47826087	0.31997703	0.47826087	0.159988515	0.47826087	0.127990812	0.47826087
Run 10	0.444444444	0.52173913	0.34906585	0.52173913	0.174532925	0.52173913	0.13962634	0.52173913
Run 11	0.481481481	0.565217391	0.378154671	0.565217391	0.189077336	0.565217391	0.151261869	0.565217391
Run 12	0.518518519	0.608695652	0.407243492	0.608695652	0.203621746	0.608695652	0.162897397	0.608695652
Run 13	0.555555556	0.652173913	0.436332313	0.652173913	0.218166156	0.652173913	0.174532925	0.652173913
Run 14	0.592592593	0.695652174	0.465421134	0.695652174	0.232710567	0.695652174	0.186168454	0.695652174
Run 15	0.62962963	0.739130435	0.494509955	0.739130435	0.247254977	0.739130435	0.197803982	0.739130435
Run 16	0.666666667	0.782608696	0.523598776	0.782608696	0.261799388	0.782608696	0.20943951	0.782608696
Run 17	0.703703704	0.826086957	0.552687596	0.826086957	0.276343798	0.826086957	0.221075039	0.826086957
Run 18	0.740740741	0.869565217	0.581776417	0.869565217	0.290888209	0.869565217	0.232710567	0.869565217
Run 19	0.777777778	0.913043478	0.610865238	0.913043478	0.305432619	0.913043478	0.244346095	0.913043478
Run 20	0.814814815	0.956521739	0.639954059	0.956521739	0.31997703	0.956521739	0.255981624	0.956521739
Run 21	0.851851852	1	0.66904288	1	0.33452144	1	0.267617152	1

	Qout (mL)	Time (mins)	Length Interval (m)	Flow Loss (Qout/Time/Length) (L/min/meter)	Normalized Flow Loss	Average Lugeon Value	Normalized Average Lugeon Value	Lugeon Value-Gauge 13	Lugeon Value-Gauge 12	Lugeon Value-Gauge 14
Run 0	5541	25	0.46	0.482	1.000	92.505	1.000	93.1244853	92.8910906	91.5149263
Run 1	5402	25	0.46	0.470	0.975	91.094	0.985	91.42450962	91.07001366	90.78839011
Run2	5176	25	0.46	0.450	0.934	90.276	0.976	90.98179837	89.64089953	90.21586621
Run 3	4983	25	0.46	0.433	0.899	89.096	0.963	90.23414157	88.6646916	88.41141559
Run 4	4732	25	0.46	0.411	0.854	88.968	0.962	89.37407925	89.19970971	88.33796927
Run 5	4383	25	0.46	0.381	0.791	86.884	0.939	87.39519257	86.97636577	86.28717111
Run 6	4096	25	0.46	0.356	0.739	85.257	0.922	84.6420896	85.78369775	85.35200408
Run 7	3762	25	0.46	0.327	0.679	87.126	0.942	88.43753306	86.10961695	86.86416218
Run 8	3345	25	0.46	0.291	0.604	80.985	0.875	82.21299186	80.88697587	79.88727416
Run 9	3175	25	0.46	0.276	0.573	81.990	0.886	83.76424652	81.65837223	80.60933037
Run 10	3097	25	0.46	0.269	0.559	84.193	0.910	86.59303789	84.58051125	81.55794907
Run 11	2845	25	0.46	0.247	0.513	81.620	0.882	82.87815891	82.38138673	79.67513828
Run 12	2562	25	0.46	0.223	0.462	77.625	0.839	78.94493575	78.41696892	75.59640607
Run 13	2310	25	0.46	0.201	0.417	77.099	0.833	78.67981403	78.00759814	74.72826087
Run 14	2315	25	0.46	0.201	0.418	82.266	0.889	84.3336187	82.09802114	80.45737323
Run 15	1902	25	0.46	0.165	0.343	78.983	0.854	80.95511716	78.08843454	77.97798413
Run 16	1715	25	0.46	0.149	0.310	76.269	0.824	77.06999214	76.83175414	74.93991698
Run 17	1481	25	0.46	0.129	0.267	76.962	0.832	77.81426507	78.09739763	75.04814027
Run 18	1372	25	0.46	0.119	0.248	73.630	0.796	77.02023746	73.28276893	70.84581225
Run 19	1255	25	0.46	0.109	0.226	70.513	0.762	72.99694634	71.79633867	67.0334366
Run 20	1189	25	0.46	0.103	0.215	68.607	0.742	69.39013715	71.01051123	65.6452726
Run 21	1146	25	0.46	0.100	0.207	68.037	0.736	67.88295226	69.58950692	66.70158896

Figure C.17: Raw Data from S/D=1.18, Unit weight=13.82 kN/m^3

S/D=1.45	# of PVC Pipes	Pore Pressure-Gauge 13(kPa)	Pore Pressure-Gauge 12(kPa)	Pore Pressure-Gauge 14(kPa)	Avg. Pore Pressure (kPa)	Normalized Pore Pressure-Gauge 13(kPa)	Normalized Pore Pressure-Gauge 12(kPa)	Normalized Pore Pressure-Gauge 14(kPa)	Normalized Average Pore Pressure (kPa)
Run 0	0	5.193	5.228	5.212	5.211	1	1	1	1
Run 1	3	5.155	5.143	5.176	5.158	0.992682457	0.983741393	0.993092863	0.989829207
Run2	4	4.997	5.007	5.082	5.029	0.962256884	0.957727621	0.975057559	0.965009915
Run 3	5	4.834	4.904	4.986	4.908	0.930868477	0.938026014	0.956638526	0.941853771
Run 4	6	4.701	4.805	4.747	4.751	0.905257077	0.919089518	0.910782809	0.911725197
Run 5	7	4.447	4.422	4.592	4.487	0.85634508	0.845830145	0.881043745	0.861063136
Run 6	8	4.312	4.208	4.192	4.237	0.830348546	0.80489671	0.804297774	0.813151666
Run 7	9	3.744	3.892	3.799	3.812	0.720970537	0.744452946	0.728894858	0.73146549
Run 8	10	3.603	3.641	3.694	3.646	0.693818602	0.696442234	0.708749041	0.699673767
Run 9	11	3.372	3.407	3.465	3.415	0.649335644	0.651683244	0.664811972	0.655280496
Run 10	12	3.108	3.196	3.297	3.200	0.598497978	0.611323642	0.632578665	0.614149555
Run 11	13	3.152	3.104	3.165	3.140	0.606970922	0.59372609	0.607252494	0.602635451
Run 12	14	2.761	2.771	2.803	2.778	0.531677258	0.530030604	0.537797391	0.533167018
Run 13	15	2.494	2.587	2.647	2.576	0.480261891	0.494835501	0.507866462	0.494338898
Run 14	16	2.397	2.411	2.504	2.437	0.4615829	0.46117062	0.480429777	0.467728523
Run 15	17	2.131	2.133	2.191	2.152	0.4103601	0.407995409	0.420376055	0.412908591
Run 16	18	2.042	2.031	2.003	2.025	0.393221645	0.38848508	0.384305449	0.388665004
Run 17	19	1.811	1.754	1.767	1.777	0.348738687	0.335501148	0.339025326	0.34107337

	Slats		PVC Side By Side		PVC Pipe-Primary and Secondary-Touching		PVC Pipe-Primary and Secondary-Spacing of 0.5*Dia. of Pipe	
	Normalized Grouted Area Agc/Atotal	Area Replacement Ratio-Multiply by the inverse of Maximum Agc/Atotal	Normalized Grouted Area Agc/Atotal	Area Replacement Ratio-Multiply by the inverse of Maximum Agc/Atotal	Normalized Grouted Area Agc/Atotal	Area Replacement Ratio-Multiply by the inverse of Maximum Agc/Atotal	Normalized Grouted Area Agc/Atotal	Area Replacement Ratio-Multiply by the inverse of Maximum Agc/Atotal
Run 0	0	0	0	0	0	0	0	0
Run 1	0.111111111	0.157894737	0.087266463	0.157894737	0.043633231	0.157894737	0.034906585	0.157894737
Run2	0.148148148	0.210526316	0.116355283	0.210526316	0.058177642	0.210526316	0.046542113	0.210526316
Run 3	0.185185185	0.263157895	0.145444104	0.263157895	0.072722052	0.263157895	0.058177642	0.263157895
Run 4	0.222222222	0.315789474	0.174532925	0.315789474	0.087266463	0.315789474	0.06981317	0.315789474
Run 5	0.259259259	0.368421053	0.203621746	0.368421053	0.101810873	0.368421053	0.081448698	0.368421053
Run 6	0.296296296	0.421052632	0.232710567	0.421052632	0.116355283	0.421052632	0.093084227	0.421052632
Run 7	0.333333333	0.473684211	0.261799388	0.473684211	0.130899694	0.473684211	0.104719755	0.473684211
Run 8	0.37037037	0.526315789	0.290888209	0.526315789	0.145444104	0.526315789	0.116355283	0.526315789
Run 9	0.407407407	0.578947368	0.31997703	0.578947368	0.159988515	0.578947368	0.127990812	0.578947368
Run 10	0.444444444	0.631578947	0.34906585	0.631578947	0.174532925	0.631578947	0.13962634	0.631578947
Run 11	0.481481481	0.684210526	0.378154671	0.684210526	0.189077336	0.684210526	0.151261869	0.684210526
Run 12	0.518518519	0.736842105	0.407243492	0.736842105	0.203621746	0.736842105	0.162897397	0.736842105
Run 13	0.555555556	0.789473684	0.436332313	0.789473684	0.218166156	0.789473684	0.174532925	0.789473684
Run 14	0.592592593	0.842105263	0.465421134	0.842105263	0.232710567	0.842105263	0.186168454	0.842105263
Run 15	0.62962963	0.894736842	0.494509955	0.894736842	0.247254977	0.894736842	0.197803982	0.894736842
Run 16	0.666666667	0.947368421	0.523598776	0.947368421	0.261799388	0.947368421	0.20943951	0.947368421
Run 17	0.703703704	1	0.552687596	1	0.276343798	1	0.221075039	1

	Qout (mL)	Time (mins)	Length Interval (m)	Flow Loss (Qout/Time/Length) (L/min/meter)	Normalized Flow Loss	Average Lugeon Value	Normalized Average Lugeon Value	Lugeon Value-Gauge 13	Lugeon Value-Gauge 12	Lugeon Value-Gauge 14
Run 0	5543	25	0.46	0.482	1	92.49664172	1	92.817254	92.1958684	92.47889486
Run 1	5447	25	0.46	0.473652174	0.982680859	91.82864946	0.9927782	91.88208999	92.09647558	91.50930717
Run2	5279	25	0.46	0.459043478	0.952372362	91.28532645	0.986904224	91.86381394	91.68034317	90.32732748
Run 3	5074	25	0.46	0.441217391	0.915388779	89.89759399	0.971901167	91.27376734	89.97091992	88.49125377
Run 4	4928	25	0.46	0.428521739	0.889049251	90.19611432	0.975128531	91.15544334	89.18246392	90.27211694
Run 5	4597	25	0.46	0.39973913	0.829334296	89.08828403	0.963151552	89.88961782	90.39781331	87.05120436
Run 6	4200	25	0.46	0.365217391	0.75771243	86.19038498	0.931821776	84.69791078	86.79120516	87.1224693
Run 7	3719	25	0.46	0.323391304	0.670936316	84.84249349	0.917249447	86.37588257	83.09129094	85.12537624
Run 8	3583	25	0.46	0.311565217	0.646400866	85.45398173	0.923860371	86.47383219	85.57133134	84.3435889
Run 9	3078	25	0.46	0.267652174	0.555294967	78.38310443	0.847415679	79.3749033	78.5594875	77.24449464
Run 10	3070	25	0.46	0.266956522	0.553851705	83.41522396	0.901818946	85.89334676	83.52832345	80.96952434
Run 11	2921	25	0.46	0.254	0.526970954	80.88313343	0.874444001	80.58375635	81.82989691	80.25276461
Run 12	2616	25	0.46	0.227478261	0.471946599	81.87579875	0.885175907	82.38980836	82.09247956	81.15528393
Run 13	2448	25	0.46	0.212869565	0.441638102	82.63570078	0.893391363	85.3526725	82.28433136	80.4191784
Run 14	2147	25	0.46	0.186695652	0.387335378	76.59832556	0.828120072	77.88721409	77.43494491	74.55896652
Run 15	1852	25	0.46	0.161043478	0.3341151	74.84592328	0.809174494	75.57178708	75.50092745	73.50227214
Run 16	1697	25	0.46	0.147565217	0.306151903	72.85971892	0.787701235	72.2650428	72.65643397	73.67210054
Run 17	1453	25	0.46	0.126347826	0.262132419	71.08842428	0.768551409	69.76688354	72.03410837	71.50414606

Figure C.18: Raw Data from S/D=1.45, Unit weight=13.82 kN/m^3

S/D=1.62	# of PVC Pipes	Pore Pressure-Gauge 13(kPa)	Pore Pressure-Gauge 12(kPa)	Pore Pressure-Gauge 14(kPa)	Avg. Pore Pressure (kPa)	Normalized Pore Pressure-Gauge 13(kPa)	Normalized Pore Pressure-Gauge 12(kPa)	Normalized Pore Pressure-Gauge 14(kPa)	Normalized Average Pore Pressure (kPa)
Run 0	0	5.251	5.242	5.263	5.252	1	1	1	1
Run 1	3	5.132	5.192	5.186	5.170	0.97733765	0.990461656	0.985369561	0.9843869
Run2	4	4.996	5.087	5.157	5.080	0.951437821	0.970431133	0.979859396	0.967250571
Run 3	5	4.945	4.916	4.983	4.948	0.941725386	0.937809996	0.946798404	0.942117289
Run 4	6	4.754	4.793	4.791	4.779	0.905351362	0.91434567	0.91031731	0.910002539
Run 5	7	4.508	4.475	4.598	4.527	0.858503142	0.853681801	0.873646209	0.86195735
Run 6	8	4.352	4.371	4.41	4.378	0.828794515	0.833842045	0.837925138	0.833523737
Run 7	9	4.107	4.098	4.202	4.136	0.782136736	0.781762686	0.798403952	0.787446052
Run 8	10	3.838	3.874	3.899	3.870	0.730908398	0.739030904	0.740832225	0.736925616
Run 9	11	3.501	3.537	3.504	3.514	0.666730147	0.674742465	0.665779973	0.669078446
Run 10	12	3.276	3.3	3.328	3.301	0.623881165	0.629530713	0.63233897	0.628585936
Run 11	13	3.195	3.238	3.217	3.217	0.608455532	0.617703167	0.611248337	0.612465093
Run 12	14	3.001	3.062	3.096	3.053	0.571510189	0.584128195	0.588257648	0.581302361
Run 13	15	2.884	2.956	3.005	2.948	0.549228718	0.563906906	0.570967129	0.561373445
Run 14	16	2.797	2.843	2.901	2.847	0.532660446	0.542350248	0.551206536	0.542079208
Run 15	17	2.562	2.587	2.624	2.591	0.487907065	0.493513926	0.498574957	0.493335872

S/D=1.62	Slats		PVC Side By Side		PVC Pipe-Primary and Secondary-Touching		PVC Pipe-Primary and Secondary-Spacing of 0.5*Dia. of Pipe	
	Normalized Grouted Area Agc/Atotal	Area Replacement Ratio-Multiply by the inverse of Maximum Agc/Atotal	Normalized Grouted Area Agc/Atotal	Area Replacement Ratio-Multiply by the inverse of Maximum Agc/Atotal	Normalized Grouted Area Agc/Atotal	Area Replacement Ratio-Multiply by the inverse of Maximum Agc/Atotal	Normalized Grouted Area Agc/Atotal	Area Replacement Ratio-Multiply by the inverse of Maximum Agc/Atotal
Run 0	0	0	0	0	0	0	0	0
Run 1	0.111111111	0.176470588	0.087266463	0.176470588	0.043633231	0.176470588	0.034906585	0.176470588
Run2	0.148148148	0.235294118	0.116355283	0.235294118	0.058177642	0.235294118	0.046542113	0.235294118
Run 3	0.185185185	0.294117647	0.145444104	0.294117647	0.072722052	0.294117647	0.058177642	0.294117647
Run 4	0.222222222	0.352941176	0.174532925	0.352941176	0.087266463	0.352941176	0.06981317	0.352941176
Run 5	0.259259259	0.411764706	0.203621746	0.411764706	0.101810873	0.411764706	0.081448698	0.411764706
Run 6	0.296296296	0.470588235	0.232710567	0.470588235	0.116355283	0.470588235	0.093084227	0.470588235
Run 7	0.333333333	0.529411765	0.261799388	0.529411765	0.130899694	0.529411765	0.104719755	0.529411765
Run 8	0.37037037	0.588235294	0.290888209	0.588235294	0.145444104	0.588235294	0.116355283	0.588235294
Run 9	0.407407407	0.647058824	0.31997703	0.647058824	0.159988515	0.647058824	0.127990812	0.647058824
Run 10	0.444444444	0.705882353	0.34906585	0.705882353	0.174532925	0.705882353	0.13962634	0.705882353
Run 11	0.481481481	0.764705882	0.378154671	0.764705882	0.189077336	0.764705882	0.151261869	0.764705882
Run 12	0.518518519	0.823529412	0.407243492	0.823529412	0.203621746	0.823529412	0.162897397	0.823529412
Run 13	0.555555556	0.882352941	0.436332313	0.882352941	0.218166157	0.882352941	0.174532925	0.882352941
Run 14	0.592592593	0.941176471	0.465421134	0.941176471	0.232710567	0.941176471	0.186168454	0.941176471
Run 15	0.62962963	1	0.494509955	1	0.247254977	1	0.197803982	1

S/D=1.62	Qout (mL)	Time (mins)	Length Interval (m)	Flow Loss (Qout/Time/Length) (L/min/meter)	Normalized Flow Loss	Average Lugeon Value	Normalized Average Lugeon Value	Lugeon Value-Gauge 13	Lugeon Value-Gauge 12	Lugeon Value-Gauge 14
Run 0	5617	25	0.46	0.488434783	1	92.9997682	1	93.01747907	93.17718096	92.80539286
Run 1	5489	25	0.46	0.477304348	0.977212035	92.32192414	0.992711336	93.00552374	91.93072955	92.03708982
Run2	5328	25	0.46	0.463304348	0.948549048	91.20164327	0.980665275	92.73505761	91.07614465	89.83989681
Run 3	5110	25	0.46	0.444347826	0.909738294	89.80352184	0.965631674	89.85800325	90.38808505	89.17275258
Run 4	4919	25	0.46	0.42773913	0.875734378	89.49765597	0.962342785	89.97457519	89.2424641	89.27971831
Run 5	4656	25	0.46	0.404869565	0.828912231	89.43440804	0.961662698	89.81134987	90.47364586	88.05340696
Run 6	4324	25	0.46	0.376	0.769805946	85.89050484	0.923556117	86.39705882	86.02150538	85.26077098
Run 7	4105	25	0.46	0.356956522	0.730817162	86.31172445	0.928085372	86.91417622	87.10505655	84.94919604
Run 8	3810	25	0.46	0.331304348	0.678298024	85.60098557	0.920442999	86.32213336	85.51996588	84.97162037
Run 9	3495	25	0.46	0.303913043	0.622218266	86.48635273	0.9299631	86.80749599	85.92395914	86.73317451
Run 10	3124	25	0.46	0.271652174	0.556168773	82.28559388	0.884793537	82.92190901	82.31884058	81.62625418
Run 11	2929	25	0.46	0.254695652	0.521452733	79.17999549	0.851399923	79.71694904	78.65832371	79.17179116
Run 12	2773	25	0.46	0.241130435	0.4936799	78.98147225	0.849265259	80.35002825	78.74932553	77.88450736
Run 13	2610	25	0.46	0.226956522	0.464660851	76.97790449	0.827721466	78.69504915	76.77825499	75.52629675
Run 14	2621	25	0.46	0.227913043	0.466619192	80.05375605	0.860795221	81.48482069	80.16638884	78.56361375
Run 15	2289	25	0.46	0.199043478	0.407512907	76.82110315	0.826035426	77.69066287	76.93988336	75.85498409

Figure C.19: Raw Data from S/D=1.62, Unit weight=13.82 kN/m^3

S/D=2.17									
	# of PVC Pipes	Pore Pressure-Gauge 13(kPa)	Pore Pressure-Gauge 12(kPa)	Pore Pressure-Gauge 14(kPa)	Avg. Pore Pressure (kPa)	Normalized Pore Pressure-Gauge 13(kPa)	Normalized Pore Pressure-Gauge 12(kPa)	Normalized Pore Pressure-Gauge 14(kPa)	Normalized Average Pore Pressure (kPa)
Run 0	0	5.193	5.201	5.211	5.202	1	1	1	1
Run 1	3	5.157	5.167	5.193	5.172	0.993067591	0.993462796	0.996545769	0.994360782
Run2	4	5.133	5.156	5.154	5.148	0.988445985	0.991347818	0.9890616	0.989618712
Run 3	5	5.075	5.182	5.073	5.110	0.977277104	0.996346856	0.973517559	0.982377443
Run 4	6	4.962	4.963	4.972	4.966	0.955517042	0.954239569	0.954135483	0.954629926
Run 5	7	4.634	4.591	4.768	4.664	0.892355093	0.882714863	0.914987526	0.896699776
Run 6	8	4.408	4.498	4.563	4.490	0.84883497	0.864833686	0.875647668	0.863120795
Run 7	9	4.214	4.281	4.301	4.265	0.811476988	0.82311094	0.825369411	0.819993592
Run 8	10	3.956	4.007	4.124	4.029	0.761794724	0.770428764	0.791402802	0.774559436
Run 9	11	3.861	3.799	3.856	3.839	0.743500867	0.730436455	0.739973134	0.7379686
Run 10	12	3.502	3.563	3.609	3.558	0.674369343	0.685060565	0.692573402	0.684011535
Run 11	13	3.447	3.485	3.452	3.461	0.663778163	0.670063449	0.662444828	0.665427748

	Slats		PVC Side By Side		PVC Pipe-Primary and Secondary-Touching		PVC Pipe-Primary and Secondary-Spacing of 0.5*Dia. of Pipe	
	Normalized Grouted Area Agc/Atotal	Area Replacement Ratio-Multiply by the inverse of Maximum Agc/Atotal	Normalized Grouted Area Agc/Atotal	Area Replacement Ratio-Multiply by the inverse of Maximum Agc/Atotal	Normalized Grouted Area Agc/Atotal	Area Replacement Ratio-Multiply by the inverse of Maximum Agc/Atotal	Normalized Grouted Area Agc/Atotal	Area Replacement Ratio-Multiply by the inverse of Maximum Agc/Atotal
Run 0	0	0	0	0	0	0	0	0
Run 1	0.111111111	0.230769231	0.087266463	0.230769231	0.043633231	0.230769231	0.034906585	0.230769231
Run2	0.148148148	0.307692308	0.116355283	0.307692308	0.058177642	0.307692308	0.046542113	0.307692308
Run 3	0.185185185	0.384615385	0.145444104	0.384615385	0.072722052	0.384615385	0.058177642	0.384615385
Run 4	0.222222222	0.461538462	0.174532925	0.461538462	0.087266463	0.461538462	0.06981317	0.461538462
Run 5	0.259259259	0.538461538	0.203621746	0.538461538	0.101810873	0.538461538	0.081448698	0.538461538
Run 6	0.296296296	0.615384615	0.232710567	0.615384615	0.116355283	0.615384615	0.093084227	0.615384615
Run 7	0.333333333	0.692307692	0.261799388	0.692307692	0.130899694	0.692307692	0.104719755	0.692307692
Run 8	0.37037037	0.769230769	0.290888209	0.769230769	0.145444104	0.769230769	0.116355283	0.769230769
Run 9	0.407407407	0.846153846	0.31997703	0.846153846	0.159988515	0.846153846	0.127990812	0.846153846
Run 10	0.444444444	0.923076923	0.34906585	0.923076923	0.174532925	0.923076923	0.13962634	0.923076923
Run 11	0.481481481	1	0.378154671	1	0.189077336	1	0.151261869	1

	Qout (mL)	Time (mins)	Length Interval (m)	Flow Loss (Qout/Time/Length) (L/min/meter)	Normalized Flow Loss	Average Lugeon Value	Normalized Average Lugeon Value	Lugeon Value-Gauge 13	Lugeon Value-Gauge 12	Lugeon Value-Gauge 14
Run 0	5623	25	0.46	0.488956522	1	93.99997214	1	94.15684994	94.0120211	93.83161039
Run 1	5516	25	0.46	0.479652174	0.980971012	92.73419616	0.986534294	93.00992319	92.8299156	92.36514036
Run2	5444	25	0.46	0.473391304	0.968166459	91.96230739	0.978322709	92.2250739	91.81367423	91.84930236
Run 3	5350	25	0.46	0.465217391	0.951449404	91.04058538	0.968517153	91.66845149	89.77564479	91.70459123
Run 4	5209	25	0.46	0.452956522	0.926373822	91.21766565	0.970400986	91.28507089	91.26667776	91.10147259
Run 5	4851	25	0.46	0.421826087	0.86270674	90.43652261	0.962090951	91.02850387	91.8810906	88.47023636
Run 6	4651	25	0.46	0.404434783	0.827138538	90.08124937	0.958311448	91.75017754	89.91435807	88.63352676
Run 7	4334	25	0.46	0.376869565	0.770762938	88.35641573	0.939962148	89.43273973	88.03306826	87.62370733
Run 8	3996	25	0.46	0.347478261	0.710652677	86.24429409	0.917492762	87.83575856	86.71780905	84.25758023
Run 9	3759	25	0.46	0.326869565	0.668504357	85.15184922	0.905871005	84.65930205	86.04094899	84.76907812
Run 10	3406	25	0.46	0.296173913	0.605726481	83.24168439	0.885550096	84.5727907	83.12487035	82.06536798
Run 11	3343	25	0.46	0.290695652	0.594522497	83.98372077	0.893444103	84.33294232	83.41338656	84.21079148

Figure C.20: Raw Data from S/D=2.17, Unit weight=13.82 kN/m^3

REFERENCES

Ajalloeian, R., Habibi, V., Sharifipour, M., and Azimian, A. (2012). "Evaluation Engineeing Geology Properties of Jamishan Dam Site with Emphais on Its Groutability." *Electronic Journal of Geotechnical Engineering* 17: 2777-2793.

Akinyemi,O., Alabi, A., Ojo, A., and Adewusi, O. (2012) "Characterization of Unit weight and Porosity of Rocks Samples from Ogun State of Nigeria", *Canadian Center of Science and Education*,1(2), 98-105.

Aminfar, M. H., B. F. Azar, H. Ebadi, and H. Ahmadi. (2009). "Change of pore water pressure inside the foundation of alavian earthfill dam, iran: A comparison between observed and predicted values." *Journal of Applied Sciences (Faisalabad)* 9, (8): 1489-1495.

Anagnostopoulos, C., and Hadjispyrou, S. (2004) "Laboratory Study of an Epoxy Resin Grouted Sand." *Grouted Improvement*, 8(1), 39-45.

Arthur, H. (1977). "Teton Dam Failure." *Engineering Foundation Conference Proceedings*, New York, pg. 523.

ASTM D4253-00, 2006, "Standard Test Methods for Maximum Index Unit weight and Unit Weight of Soils Using a Vibratory Table," *Annual Book of ASTM Standards*, Vol. 4.08, ASTM International, West Conshohocken, PA.

ASTM D4254-00, 2006, "Standard Test Methods for Minimum Index Unit weight and Unit Weight of Soils and Calculation of Relative Unit weight," *Annual Book of ASTM Standards*, Vol. 4.08, ASTM International, West Conshohocken, PA.

ASTM D6913-04, 2009, "Standard Test Methods for Particle-Size Distribution of Soils Using Sieve Analysis," *Annual Book of ASTM Standards*, Vol. 4.09, ASTM

International, West Conshohocken, PA.

ASTM D854-10, 2009, "Standard Test Methods for Specific Gravity of Soil Solids by Water Pycnometer," *Annual Book of ASTM Standards*, Vol. 4.08, ASTM International, West Conshohocken, PA.

Awal, R., Nakagawa, H., Kawaike, K., and Baba Y. (2009) "Three Dimensional Transient Seepage and Slope Stability Analysis of Landslide Dam," *Annuals of Disaster Prevention Research Institute,* Kyoto University, Kyoto, Japan, 52(B), 989-696.

Beckhaus, K., Schmitz, S., and Schwarz, W. (2008). "Deep Cut-Off Walls constructed Under Dams with Trench Cutters." *Long Term Behavior of Dams.* 305-310.

Berhane, G. and Walraevens, K. (2013). "Evaluating core drilling and lugeon test for the proposed geba dam site, northern ethiopia." *Abstracts - Colloquium of African Geology (CAG)* 24: 279-281.

Bliss, J., Rushton, K. (1984). "The reliability of packer tests for estimating the hydraulic Conductivity of aquifers." *Quarterly Journal of Engineering Geology*. 17: 81-91.

Bodocsi, A. and Bowers, M.T. (1991) "Permeability of Acrylate, Urethane, and Silicate Grout Sands with Chemicals." *Journal of Geotechnical Engineering,* 117(8), 1227-1244.

Bruce D.A. (1982). "Aspects of Rock Grouting Practice on British Dams." *ASCE Geotechnical Engineering Specialty Conference on Grouting*, New Orleans, LA February 10-12, 1982, pp. 301-316.

Bruce D.A (1992). "Current Technologies in Ground Treatment and In Situ Reinforcement." *Proc. 2nd Interagency Symposium on Stabilization of Soils and Other Minerals,* Metairie, LA. November 2-5, pp. 271-295.

Cotton, E.N. and Matheson, G.M., (1990) "Numerical Simulation of Concrete Dam Foundation Seepage and Uplift Pressure Distribution", *Rock Mechanics Contributions and Challenges*, Hustrulid and Johnson, Eds., Balkema, Rotterdam.

Gurocak, Z. and Alemdag, S. (2012). "Assessment of permeability and injection depth at the Atasu dam site (Turkey) based on experimental and Numerical analyses." *Bull Eng. Geol. Environ* 71:221-229.

Hacker, Adam. (2014), *Personal Conversation,* Stantec Consulting Services, Lexington, KY, February, 2014.

Hayward Baker. (2014), *Website*, http://www.haywardbaker.com/WhatWeDo/Techniques/Default.aspx, February 15th, 2014.

Hong, W., Yea, G., and Lee, H. (2003). "Cut-off effect by rock grouting in the area of dam foundation". *ISOPE-2003:Thirteenth (2003) International Offshore and Polar Engineering Conference;Honolulu, HI; USA;25-30 May 2003* (May 25): 635-639.

Houlsby, A.C., (1976). "Routine Interpretation of Lugeon Water-Test." *Quaterly Journal of Engineering Geology,* (9):303-313.

Huff, J. (2010). "Investigation of Humboldt Geogauge for Quality Control of Compacted Subgrades." *Master's Thesis*, University of Kentucky, Lexington, KY.

KGS (2012). "Sand and Gravel Resources." *Mineral and Fuel Resources Map of Kentucky,* Kentucky Geological Survey, Lexington, KY,

<http://www.uky.edu/KGS/im/sandgravel.htm>.

Lirer, S., Flora, A., Evangelista A., Verdolotti, L., Lavorgna, M., Iannance, S. (2006) "Permeation Grouting of a Fine-Grained Pyroclastic Soil," *Ground Improvement*, 10(4), 135-145.

Liua, J., Fenga, X., Ding, X., Zhang, J., and yueb, D. (2003). "Stability Assessment of Three-Gorges Dam Foundation, China, using Physical and Numerical Modeling—Part I: Physical Model Tests," *International Journal of Rock Mechanincs and Mining Sciences,* 40(2003), 609-631.

Lugeon, M. (1933). *Barrage et Geologie.* Dunod. Paris.

Luofenga, X., Xiangbaoa, D. Yangchao. (2012). "Study of Physical Model Experimetn of Dam's Seepage Stability base on Coastal Sand," *Proceedings of the 2012 International Conference on Modern Hydraulic Engineering*, Nanjing, Jiangsu Province, China.

Nappi, M., L. Esposito, V. Piscopo, and G. Rega. (2005). "Hydraulic characterisation of some arenaceous rocks of molise (southern italy) through outcropping measurements and lugeon tests." *Engineering Geology,* 81, (1): 54-64.

Powers, P., Corwin, A., Schmall, P. and Kaeck, E. (2007). "Construction Dewatering and Groundwater Control-New Methods and Applications," *John Wiley and Sons, Inc.*, Hoboken, New Jersey, Third Edition, 410-431.

Priebe, H. J., (1991). "Vibro Replacement-Design Criteria and Quality Control," *Deep Foundation Improvements: Design, Construction, and Testing,* ASTM STP 1089, Melvin I. Esrig and Robert C, Bachus, Eds., American Society for Testing and Materials, Philadelphia.

Priebe, H. J., (1995). “The Design of Vibro Replacement.” *Ground Engineering,* 1-16.

Quinn, P. M., J.A. Cherry and B.L. Parker, (2011). “Quantification of non-Darcian flow observed during packer testing in fractured sedimentary rock.” *Water Resources Research,* 47,(9): 1-15

Quinones-Rozo, C. (2010). “Lugeon Test Interpretation, Revisted.” *Collaborative Management of Integrated Watersheds*. 405-414.

Sadeghiyeh, S. M., M. Hashemi, and R. Ajalloeian. (2013). “Comparison of permeability and groutability of ostur dam site rock mass for grout curtain design.” *Rock Mechanics and Rock Engineering*, 46, (2) (03): 341-357.

Saeidi, O., Ramezanzadeh, A., Sereshki, F., and Jalali, M. 2013.”Numerical modeling of the effects of joint hydraulic aperture, orientation and spacing on rock grouting using UDEC: A case study of Bakhtiary Dam of Iran.” *Journal of Mining & Environment,* 4(1): 15-26.

Sasaki, Kenji and Tosaka, Hiroyuki. (2012). “The study of quantification method for non-darcy effect in lugeon-test.” *Journal of Japan Society of Dam Engineers*, 22, (3): 160-171.

Uromeihy, A. and Farrokhi, R. (2012). “Evaluating groutability at the Kamal-Saleh Dam based on Lugeon tests.” *Bull Eng.Geol. Environ*, 71:215-219.

Veni, G., DuChene, H., Crawford, N., Groves, C., Huppert, G., Kastning, E., Olson, R. and Wheeler, B. (2001). “Living With Karst, A Fragile Foundation.” *AGI Environmental Awareness Series,* 4: 1-64.

Weaver, D. and Bruce, D. (2007) “Dam Foundation Grouting.” *American Society of Civil Engineers Press*, Reston, Virginia, 321-331.

Willowstick, (2012) “Willowstick Technology Used For Mapping and Modeling Groundwater Systems.” *White Paper,* Willowstick Technologies, LLC, Draper, Utah.

Zou, Y.J. and Zhou, X.W. (2012). “Study and application of key technology to simultaneous shaft drilling and grouting.” *Tunnels & Tunneling International* (04): 130-133.

VITA

Elliot Nicholas Magoto graduated from the University of Kentucky with a Bachelors of Science in Civil Engineering. He graduated on December 2012 with Magna Cum Laude honors. Elliot passed the Fundamentals of Engineering exam and was awarded the Engineer in Training certificate in the Spring of 2012.

Personal Publications:

Magoto, E.N. and Bryson, L.S.(2013), "Evaluation of the Effectiveness of a Grout Curtain using a Physical Model", *Dam Safety 2013*, The Association of State Dam Safety Officials, Providence, RI, 8-12 September, 2013.

"Evaluation of the Effectiveness of a Grout Curtain using a Physical Model", Dam Safety 2013, The Association of State Dam Safety Officials, *Poster Presentation*. Providence, RI, 8-12 September, 2013.